Posttranslational Modification and Evolution of Tetramerization Domain in Tumor Suppressor Protein p53

癌抑制タンパク質 p53 における四量体形成ドメインの翻訳後修飾および進化

Graduate School of Chemical Sciences and Engineering
Hokkaido University

Département de Biochimie et Médicine Moléculaire
Université de Montréal

Natsumi Nakagawa

2020

Table of Contents

Abbreviation

Bax	Bcl2-associated X
CBP	CREB-binding protein
CD	Circular dichroism
CID	Collision-induced dissociation
CREB	Cyclic AMP-responsive element-binding protein
DBD	DNA binding domain
DTT	Dithiothreitol
Gadd45	Growth arrest and DNA damage inducible 45
H1299	p53-null lung carcinoma cell
IPTG	Isopropyl β-D-1-thiogalactopyranoside
LB	Luria-Bertani medium
MDM2	Murine double minute 2
MEP50	Methylosome protein 50
miRNA	Micro RNA
NLS	Nuclear localization signal
NMR	Nuclear magnetic resonance
p53Tet	p53 tetramerization domain peptide
PCAF	p300/CBP-associated factor
PPM1D	Protein phosphatase magnesium-dependent 1 delta
PRMT5	Protein arginine methyltransferase 5
Puma	p53 up-regulated modulator of apoptosis
RE	Response element
SAM	*S*-adenosylmethionine
TD	Tetramerization domain
WT	wild type

1. General Introduction

1.1. Tumor suppressor protein p53

Tumor suppressor protein p53 is considered to be the most important tumor suppressor gene [1,2] and it is often called “the guardian of the genome” because of its role in maintaining genomic integrity [3]. Mutations of the *TP53* gene have been reported in many types of cancer [4] and patients with mutated *TP53* generally have a poor prognosis because many cancer forms with mutated p53 often develop resistance to therapeutic treatments, such as radiation and anticancer agents. To prevent tumorigenesis, wild type (WT) p53 induces cell cycle arrest and apoptosis in response to various cellular stresses, including genotoxic stress induced by UV, radiation, as well as oxidative stress, and starvation stress **(Figure 1)**. During the stress response in cells, p53 forms a tetrameric structure which is the active form that induces apoptosis and cell cycle arrest through transcription-independent, transcription-dependent, and miRNA processing. In transcription-dependent induction of apoptosis, the tetrameric form of p53 binds to response elements in its target genes and activates transcription, such as the pro-apoptosis genes, *Bax* and *Puma*, and the pro-cell cycle arrest genes, *CDKN1A (p21)* and *GADD45* [5]. In the transcription-independent induction of apoptosis, p53 binds to the anti-apoptotic proteins BCL2 or BCL-X and promotes apoptosis through mitochondrial outer membrane permeabilization [6]. For miRNA processing, p53 interacts with the Drosha complex to facilitate the miRNA processing [7]. For all of these functions, the homotetramer form of p53 protein which forms via tetramerization domain (TD) is essential, and this tetrameric structure is in equilibrium with the four monomers in the cell and p53 activity is defined by the stability of the tetrameric structure.

The p53 protein consists of 393 amino acid residues and there are five major domains in the following order in the sequence starting from the N-terminus: the transactivation domain (TAD; 1-42), the proline-rich domain (PRD; 61-92), the DNA-binding domain (DBD; 101-300), the tetramerization domain (TD; 326-356), and the basic domain (BD; 364-393) **(Figure 2)**. The TAD binds to diverse proteins such as CBP and p300 to modulate the transcriptional activity of p53 [8] and its interaction with MDM2 regulates the level of the p53 protein [9]. It has been suggested that the PRD mediates binding to cofactors important for efficient transcription [10]. The DBD binds directly to response elements in p53 target genes containing the general sequence, 5′-RRRCWWGYYY-3′ (R = A, G; W = A, T; Y = C, T) [11]. The affinity of the tetrameric

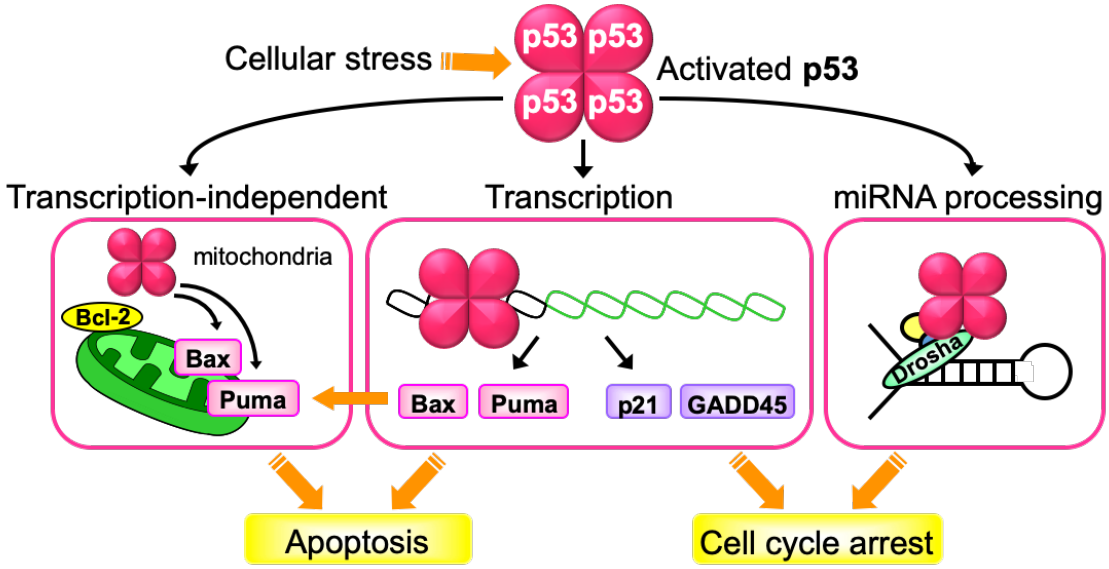

Figure 1. Functions of the tumor suppressor protein p53

In response to cellular stresses the tumor suppressor protein p53 functions as a transcription activation factor to induce apoptosis and cell cycle arrest.

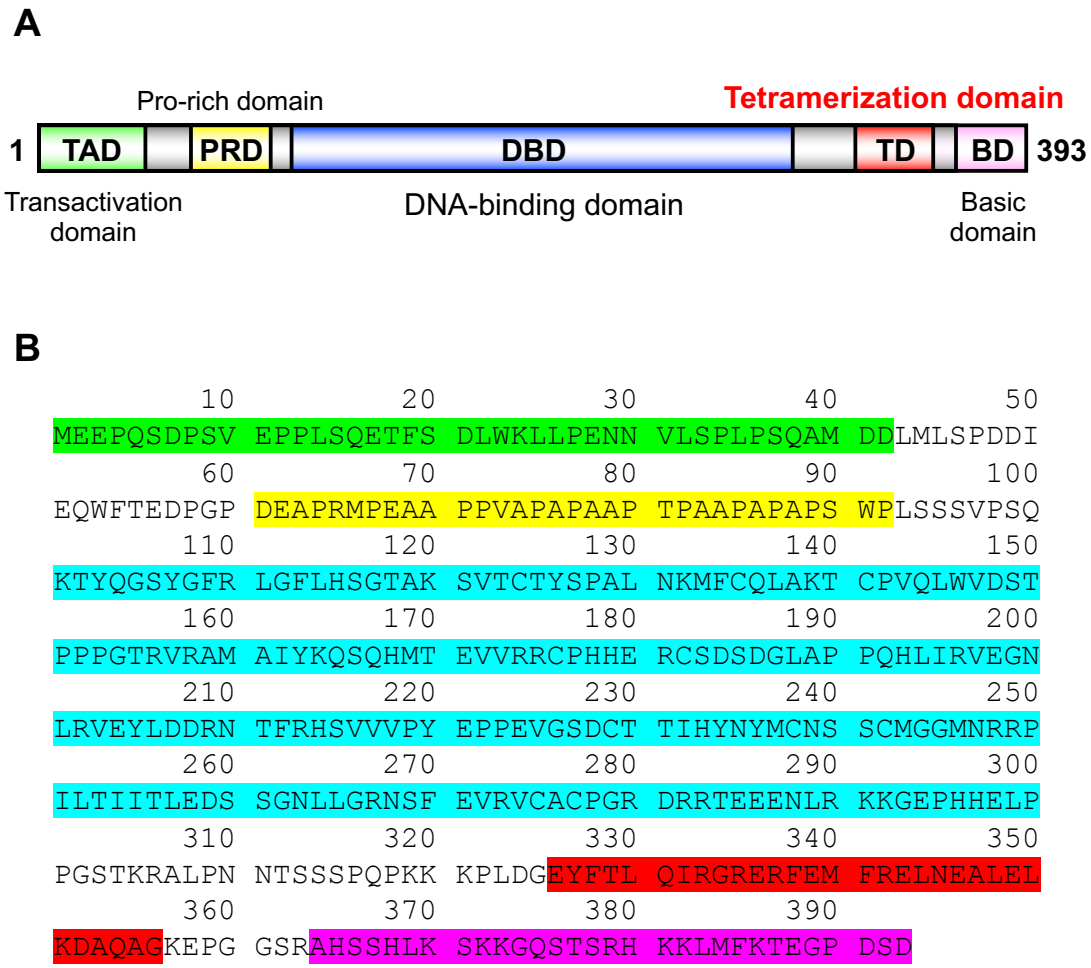

Figure 2. Domain structure and primary sequence of p53

A: p53 consists of five domains: A transactivation domain (TAD; green), a proline-rich domain (PRD; yellow), a DNA-binding domain (DBD; blue), a tetramerization domain (TD; red) and a basic domain (BD; pink). B: Primary structure of p53 with the five domains highlight in the same color as in A

form of p53 for DNA is increased up to 100-fold compared to that of the monomeric form. The TD controls the structure and function of the entire molecule whereas the BD binds to nonspecific DNA sequences to help regulate the binding of the DBD to specific target sequences [12].

1.2 Structure and stability of p53 tetramer

The structure of the p53 TD has been determined both in its crystal form by X-ray crystallography and in solution by nuclear magnetic resonance (NMR) spectroscopy **(Figure 3)** [13]. Each monomer within the tetrameric form of the TD contains a β-strand and a single helix linked by a tight turn. To generate the tetramer, two monomers form a primary dimer stabilized by an antiparallel β-sheet and the two primary dimers form a tetramer via a four-helix bundle, which is stabilized by a compact hydrophobic core that connects the four helices from each monomer. In total, nine hydrophobic side chains (F328, L330, I332, F338, M340, F341, L344, A347, and L348) contribute to the thermodynamic stability and oligomerization status of the TD [14], which is further stabilized by a series of salt bridges and hydrogen bonds that are also important for forming the tetrameric form.

As mentioned above, the stability of the tetrameric structure regulates several functions of the p53 protein. Whereas missense mutations within the DBD are found in over 90% of malignant tumors of human somatic cells, missense mutations in the TD are more common in germ line cells. The oligomeric states and the structure stability of 50 mutations known to occur in the TD in humans have been comprehensively analyzed. For this work, synthetic peptides corresponding to the p53 tetramerization domain (p53 TD; residues 319-356 of human p53) were prepared with each mutation. Analysis of the synthetic peptides by gel filtration chromatography determined that the L330P, the L330R, the R337P, and the L344P mutants of p53 TD are all monomeric at the concentrations tested and they did not form a tetramer. In contrast, the F342C, L344R, and A347T mutants of p53 TD are dimeric at the concentrations tested and again do not form the tetramer. All of the other remaining mutants form a tetramer but at lower temperatures and higher concentrations of protein than the wild-type p53 TD suggesting the dissociation constant for tetramer formation is higher for these mutants [15]. In addition, the p53 TD mutants were analyzed by circular dichroism (CD) spectroscopy to determine their thermostability in a quantitative fashion. The CD experiments indicated that

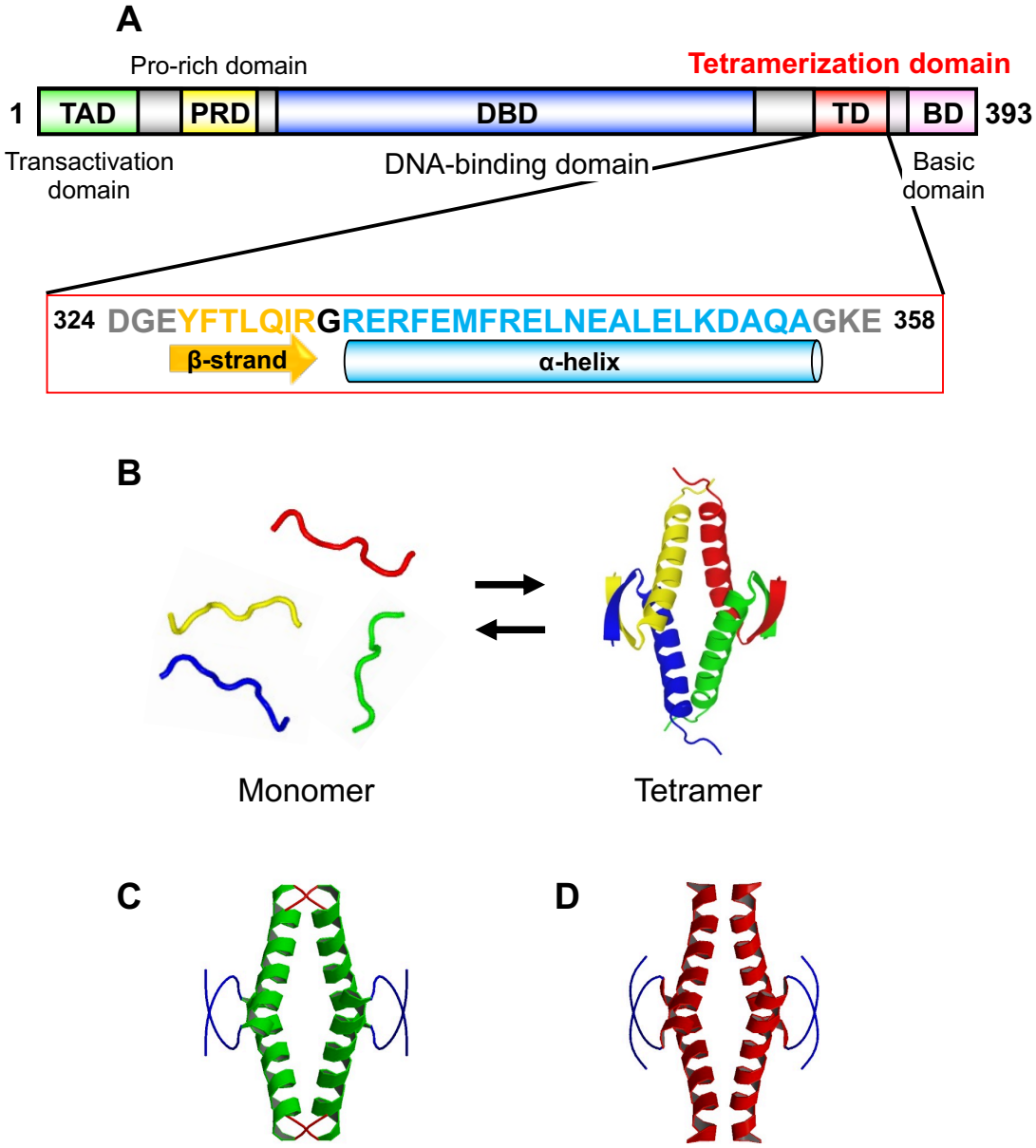

Figure 3. Structure of p53 tetramerization domain

A: The tetramerization domain of p53 is located in the C-terminal region of human p53 between residues 324 and 358. Each monomer contains a single β-strand and a single α-helix. B: In cells, p53 exists in equilibrium between the monomer and tetramer (PDB ID: 3SAK) forms. The individual monomers are colored in yellow, blue, red, and green. C: The crystal structure of p53 TD(326-356) (PDB ID: 1AIE). D: Crystal structure of p53 TD(325-356) (PDB ID: 1C26).

mutations at the residues forming the hydrophobic core of the p53 TD destabilized the tetrameric form of the structure. To correlate tetramer stability with a functional activity, the transcriptional activity of the full length p53 protein containing the individual mutations in the p53 TD were determined in H1299 cells using a reporter assay. These studies showed that the mutants that destabilized the tetrameric structure had decreased transcriptional activity, indicating that the stability of the tetrameric structure is directly correlated with the strength of the transcriptional activity [16]. Therefore, the formation of the tetrameric structure via the TD contributes to the regulation of p53 functions, because mutations in this domain decreased p53 functions, leading to tumorigenesis.

1.3. Posttranslational modification of p53

The functions of p53 are precisely regulated by a considerable variety of posttranslational modifications, including phosphorylation [17], acetylation, ubiquitylation, neddylation, and methylation. The circulating levels of p53 are maintained low in unstressed cells through regulation by MDM2, which is an ubiquitin ligase that binds with high affinity to p53 and is a ubiquitin ligase [18] **(Figure 4)**. MDM2 directly binds to the N-terminal transactivation domain (TAD) and blocks the ability of p53 to activate its target genes [19]. Moreover, MDM2 induces ubiquitination of p53, which leads to its rapid degradation via the ubiquitin-proteasome pathway [20,21]. This regulation by MDM2 prevents overexpression of the p53 protein and thus decreases the ability of p53 to promote apoptosis and cell cycle arrest. Under genotoxic stress, p53 is phosphorylated at both Ser15 and Ser37 and these phosphorylation events inhibit MDM2 to p53, and this leads to increased levels of the p53 protein accumulates and the activation of p53 targeted genes [22–24]. The activation of p53 is also regulated by dephosphorylation by PPM1D (Protein Phosphatase Magnesium-dependent 1, Delta, also known as PP2Cδ and Wip1), which is a Ser/Thr protein phosphatase. PPM1D dephosphorylates p53 specifically at Ser15 by PPM1D, which results in a negative feedback loop to prevent excessive p53 activity [25]. DNA damage activates p53 through a phosphorylation-acetylation cascade [26]. The histone acetyltransferase p300 acetylates p53 at Lys382, whereas a second histone acetyltransferase PCAF (p300/CBP-associated factor) acetylates p53 at Lys320, and these two acetylation reactions enhance the sequence-specific DNA binding of p53. The initial acetylation reaction at Lys382 by p300 requires that p53 is present in its tetrameric form, which suggests that the interaction of

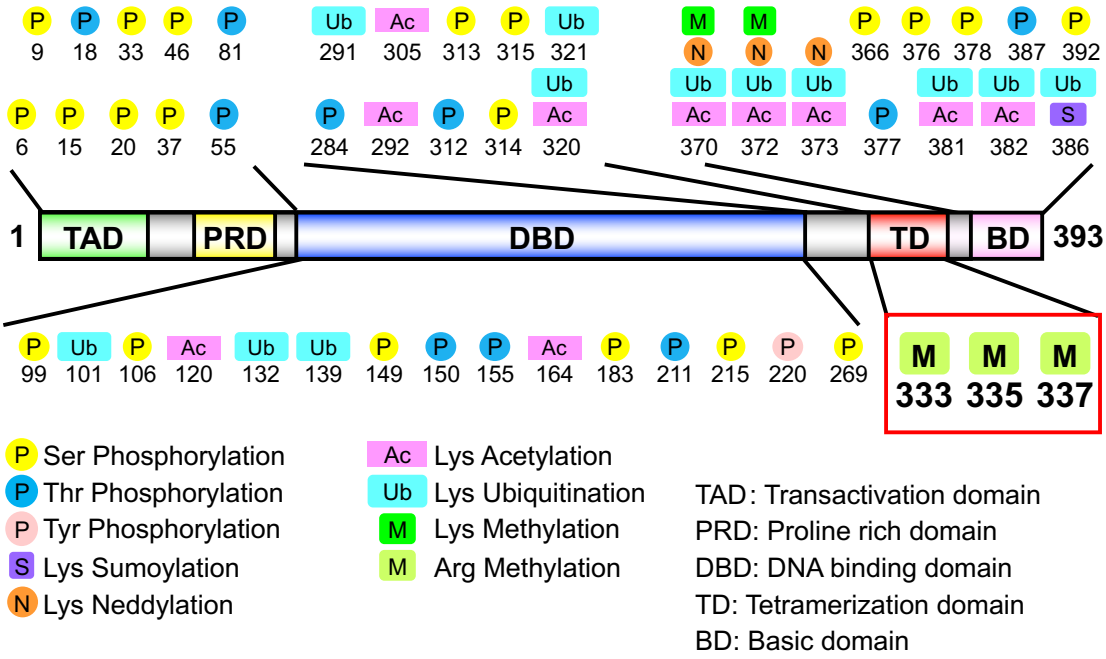

Figure 4. Posttranslational modification of p53

Over 50 posttranslational modifications are known to occur in p53. The modifications at N- and C-terminal regions are the most important for the regulation of p53 activity and protein levels. In the tetramerization domain, three nearby arginine residues (333, 335 and 337) are methylated.

p300 with p53 requires tetramer formation [27]. In addition, phosphorylation at Ser392 has been shown to enhance tetramer formation by 10-fold more in comparison to the non-phosphorylated p53 protein [28]. According to these studies, the tetramer formation is regulated by a series of posttranslational modifications, but in turn the tetramer form of p53 modulates several additional posttranslational modifications. In additional, there are posttranslational modifications with the p53 TD including methylation of Arg333, Arg335, and Arg337 by PRMT5 (Protein arginine methyltransferase 5) [29].

1.4. p53/p63/p73 protein family

In addition to p53, p63 and p73 are paralogs with similar and different structures and functions. Like p53, p63 is a potent transcription factor and it has been shown to be required for the development of epithelial cell layers. Likewise, p73 is a transcription factor that is involved in the development of the central nervous system. The structure of all three proteins includes a TAD, a PRD, a DBD, and a TD. However, their C-terminal region differ from each other: p53 contains a BD, whereas p63 and p73 have a sterile alpha motif (SAM) domain. In addition, p63 and p73 form both homo-tetramers as well as hetero-tetramers with each other to exert their functions. However, they do not form hetero-tetramers with p53 [30] **(Figure 5)**. A common ancestral p53/p63/p73-family protein was first detected in sea anemones [31] and the p53 protein is conserved from Lamprey, an early vertebrate, to mammals, including humans.

1.5. Evolution of vertebrate p53

Evolution is triggered by gene mutations, and proteins gain-of-function to adapt to environmental changes, however the evolution patterns of vertebrates is still not completely understood. To date, it has been suggested that jawless fish is the first vertebrate, which appeared around the Cambrian explosion about 540 million years ago. After that, cartilaginous fish, ray-finned fish, lobe-finned fish, Amphibia, and Reptile appeared in this order **(Figure 6)**. The mammal and bird branches evolved from reptiles. Jawless fishes, including early vertebrates such as Lamprey, do not have a jaw. Cartilaginous fish such as sharks and rays (thornback) developed a jaw. Ray-finned fish, such as salmon and tuna, developed bony fins. Lobe-finned fishes such as Coelacanth developed fleshy fins (ancestor of extremities). Amphibians such as frogs and newts developed extremities with fingers. Reptiles such as alligators and turtles developed an

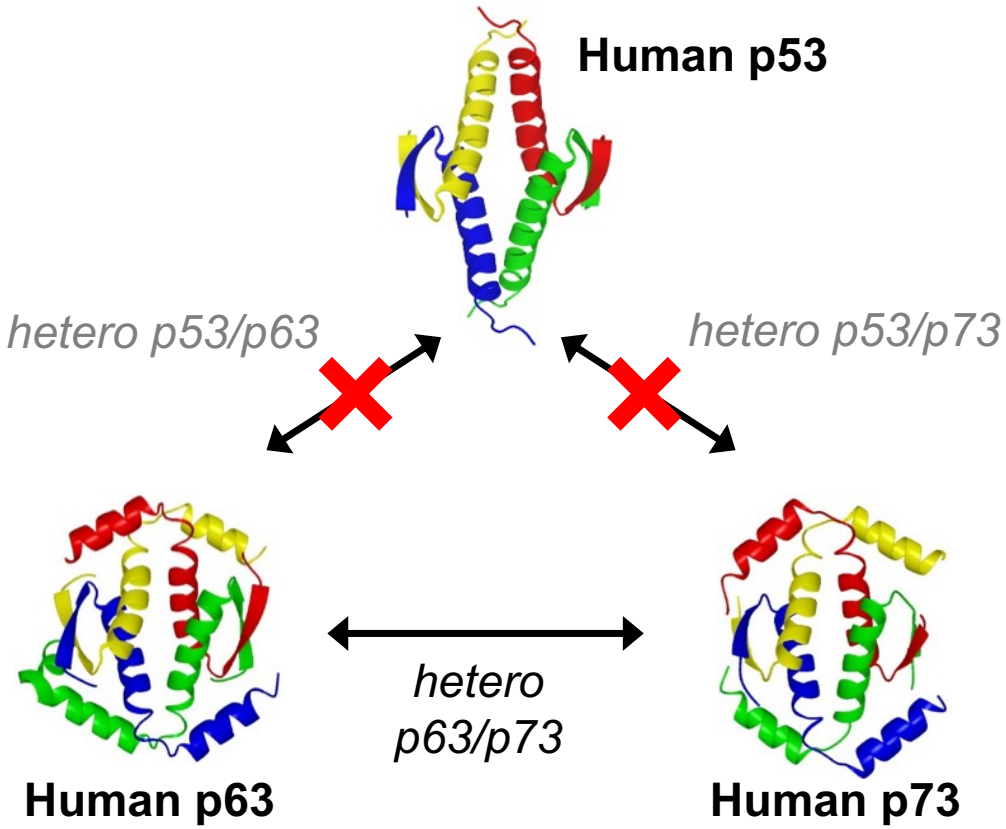

Figure 5. Hetero and homo oligomerization of Human p53/p63/p73

Human p53 doesn't form hetero tetramer with p63 and p73, whereas p63 and p73 form hetero tetramer. (PDB ID: p53, 3SAK; p63, 4A9Z; p73, 2WQI)

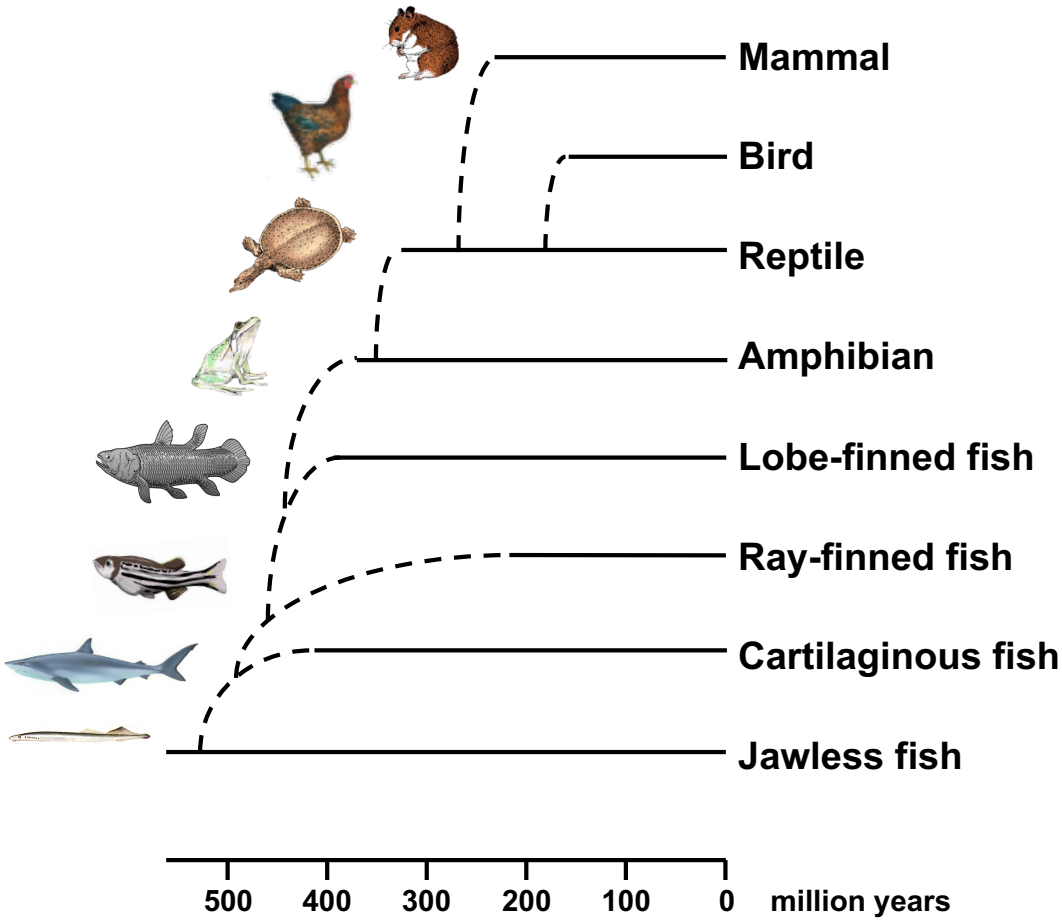

Figure 6. Evolution of vertebrate

The first vertebrate appeared 540 million years ago with the Cambrian explosion.

amnion. Mammals such as humans and cats feed their offspring on mother's milk. Birds such as chickens developed wings. In the vertebrate evolution process, there were two rounds of whole genome duplication before the separation of cartilaginous fish (2R hypothesis or Ohno's hypothesis). In addition, whole genome duplications occurred in ray-finned fish and in frogs. The whole-genome project of these species was performed later than the other species, because was difficult to map them. The divergence of vertebrates through whole-genome duplications is still not completely understood. The chromosomal structures in vertebrates are widely different. The number of chromosomes in humans is 2n = 46, in Western clawed frogs it is 2n = 20, and in Medaka it is 2n = 48, and they do not have microchromosomes. Furthermore, the number of chromosomes in chickens is 2n = 78, and in Coelacanth it is 2n = 48, and they possess many microchromosomes. The significance of having microchromosomes is again still not completely understood. Over half of the genes are conserved in vertebrates. Hence, it has been suggested that the embryogenesis plan is similar in all vertebrates. The common genes (orthologues) can be determined by frequency of the sequences of amino acids or DNA using phylogenetic analysis. So far, the structures and functions of orthologue proteins of p53-family proteins have not been analyzed much at all.

1.6. Aim of this study

The stability of the tetrameric structure of the p53 is extremely important for regulating its function. Though, p53 clearly has an important role in the evolution of vertebrates, the function of p53 in different organisms and the evolution process of the tetrameric structure are still unclear. In addition to performing phylogenetic analysis of the different sequences, a comprehensive analysis of the structure and the function is required to completely understand the evolutionary process of the p53-family proteins. The aim of this study is to understand how the stability of the tetrameric structure is regulated by posttranslational modifications and how the p53 TD regulates its activity and function. To this end, I have explored how Arg residues in the p53 TD are methylated by PRMT5 as well as how the structures of the TD of p53 have evolved in vertebrates.

2. Arg Methylation on p53 Tetramerization Domain

2.1. Abstract

The tumor suppressor protein p53 is regulated by multiple posttranslational modifications, including phosphorylation, acetylation, SUMOylation, ubiquitylation, and methylation. In the p53 tetramerization domain (p53 TD), mono- and di-methylations at arginine 333, 335, and 337 by the arginine methyltransferase PRMT5 have been reported. These methylations by PRMT5 induce p53-regulated cell cycle arrest, but not apoptosis. However, how methylation effects the stability of the p53 TD and p53 transcriptional activity is unclear. In order to determine the effect of methylation on tetramer formation and stability, we have synthesized peptides corresponding to the p53 TD (residues 324-358) that are methylated on the three arginine positions and analyzed their oligomeric state and thermostability. Furthermore, I determined the order of methylation by PRMT5 at the three arginine residues and the results suggest that there is methylation cascade. More specifically, it was revealed that methylation, especially at R337, destabilized the tetrameric structure, although all of the methylated peptides formed the tetramer. Moreover, initial methylation and di-methylation at R335 triggered the methylation cascade followed by rapid di-methylation at both R333 and R337. Although we could not determine the order between R333 and R337, it appears that methylation at R337 modulates the structural stability of the p53 TD and thus the methylation cascade can serve to regulate the functions of p53 associated with tetramer formation. Future studies to analyze how methylation alters the binding affinity of p53 to p53-regulated response elements are needed to determine how methylation of the p53 TD alters the activity of this important tumor suppressor protein.

2.2. Introduction

The tumor suppressor protein p53 carries out a wide variety of cellular functions by serving as a transcriptional activator at p53-target genes and by inducing cell cycle arrest and apoptosis to help maintain genomic integrity in response to various cellular stresses [32–35]. The p53 protein consists of 393 amino acids, which can be subdivided into five functional domains from N-terminus to C-terminus and they include the transactivation domain (TAD), the proline-rich domain (PRD), the DNA-binding domain (DBD), the tetramerization domain (Tet) and the basic domain (BD) [36]. In the cell, p53 forms a tetrameric structure via the p53Tet(326–356) and this tetrameric form is essential for executing most of its functions [26,37]. The structure of the p53Tet has been determined by both NMR spectroscopy and X-ray crystallography and it is composed of a single β-strand (residues 326–333; human p53), a turn (residue 334) and single α-helix (residues 335–356) starting at the N-terminus [13,38]. The tetrameric form of p53 is symmetrical and is comprised of a dimer of dimers. The first dimer is formed through an anti-parallel β-sheet between two monomers and a second dimer is formed by the formation of a four-helix bundle involving the helix from each monomer [39]. In the cellular context, the p53 protein is in equilibrium between the monomeric and tetrameric form, with the ratio of the tetrameric form increasing at higher protein concentrations. Importantly, the transcriptional activity of p53 is directly linked to the stability of the tetramer formation [15,16] and almost all the reported mutations in p53Tet linked with human cancer demonstrate a destabilized oligomeric structure and thus decreased transcriptional activity. In particular, the tetrameric structure is markedly destabilized by mutations in the turn and the hydrophobic core of the TD, as well as by mutations to a Pro in the α-helical region of the TD.

Given its importance in protecting the cell from cellular stresses, it is not surprising that the activity of p53 is highly regulated by posttranslational modifications linked to cellular signaling cascades. For example, it has been reported that p53 is posttranslationally modified at over 50 different positions in all five domains within its sequences and types of modifications include phosphorylation, acetylation, SUMOylation, ubiquitination and methylation [40,41]. Although the functional role of these modifications have not been clearly defined, many of them serve to regulate the transcriptional activity of p53 under different cellular stresses, In the TD, it has been reported that three arginine residues (R333, R335 and R337) can be mono- and di-

methylated by the protein arginine methyltransferase 5 (PRMT5) [29,42,43] and that this methylation decreases the transcriptional activity of p53 in cells.

PRMT5 is a member of PRMT-family of methyltransferases that have the ability to catalyze mono- and symmetrical di-methylation of the Arg side chain using S-adenosylmethionine as a methyl group donor **(Figure 7)** [44–46]. PRMT5 consists of 637 amino acids and can be subdivided into three domain, an N-terminal TIM (triosephosphate isomerase), a central catalytic domain and a C-terminal beta-barrel domain. In the cell, PRMT5 can localize to both the cytoplasm and the nucleus and it has been shown to from many complexes by interacting with proteins such as the SWI/SNF complex and MEP50. Heterodimers of PRMT5 and MEP50 can also form a tetramer, and a crystal structure of the symmetric hetero-octamer has been reported [47]. Functionally, PRMT5 substrates contain a signature RGG/RG motif that is required for the enzymatic activity [48] and PRMT5 has been shown to methylate Arg residues in several different histones proteins (H2AR3, H3R2, H3R8, and H4R3). These methylation events on histones require that PRMT5 form complexes with regulator proteins such as MEP50 and SWI/SNF [49–51] and di-methylation of histone H3 at Arg8 and histone H4 at Arg4 are involved in transcriptional repression [52–54].

Importantly, deletion of the *PRMT5* gene has been shown to be embryonic lethal [55] and in recent years the functions of PRMT5 in several different cancer types have been identified. For example, the protein level of PRMT5 is increased in lymphoid cancer cell lines [56,57] and PRMT5 activity is upregulated in cancers that harbors a mutation in Fbx4 [58]. In addition, in methylthioadenosine phosphorylase (MTAP)-deficient cancer cells, cell viability is decreased because of impaired PRMT5 activity [59] whereas in ovarian cancer the expression level of PRMT5 is high, and suppression of PRMT5 by siRNA inhibited cell growth and induced apoptosis in an E2F-1-dependent manner [60]. Given that PRMT5 has been shown to methylate p53, it is not surprising that PRMT5 plays a role in regulating p53 activity. Previous studies have shown that a defect in PRMT5 activity led to and induction of p53-dependent apoptosis, whereas overexpression of PRMT5 led to a p53-dependent cell cycle arrest [29,61–63]. However, the mechanism by which PRMT5 methylates the three arginine residues within the TD remains unclear [64–67].

Given that alterations in both p53 and PRMT5 activity are associated with a number of different cancers, it is important to clarify the mechanism by which PRMT5

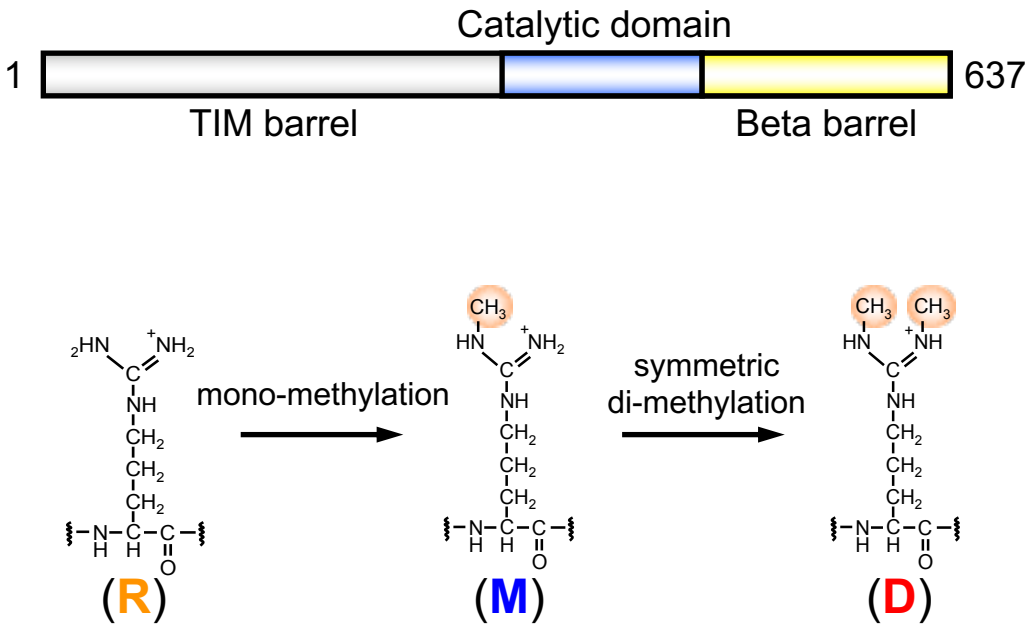

Figure 7. Domain structure of the Protein Arginine Methyltransferase 5 (PRMT5) and methylation of Arginine residues

PRMT5 contains 637 amino acids residues and three domains (Upper Panel). The catalytic domain is highly conserved with other PRMT family proteins. PRMT5 catalyzes mono-methylation and symmetrical di-methylation on the side chain of arginine residue (Lower Panel).

methylates the TD of p53 to regulate p53 activity. In this manuscript, we have used a combination of biochemical, biophysical and enzymatic studies to clarify the mechanism by which PRMT5 methylates the p53Tet as well as how methylation of Arg333, Arg335 and Arg337 alters the stability of the tetramerization domain. The results suggest that there is a specific methylation cascade that is initiated by methylation and di-methylation at Arg335 and that di-methylation at Arg337 is important for altering the stability of the TD and most likely the transcriptional activity of p53. These results provide important insights into how PRMT5 can regulate the activity of p53 through methylation events in the p53Tet.

2.3. Experimental procedures

2.3.1. Peptide synthesis

All p53Tet peptides (The sequences of the synthesized peptides are shown in **Figure 8**.) were synthesized on 433A peptide synthesizer (Applied Biosystems) using amide resins and Fmoc Solid Phase Chemistry. Following their synthesis on the resin, the peptides were cleaved from the resin by a reaction with Reagent K (TFA: H_2O: thioanisole: ethanedithiol: phenol = 82.5: 5: 5: 2.5: 5) for 5 h at room temperature. The crude peptides were purified by reverse phase high-performance liquid chromatography on a C8 column (Vydac) using a gradient of water and acetonitrile. The molecular weights of the peptides were confirmed by matrix-assisted laser desorption ionization (MALDI) mass spectrometry.

2.3.2. Circular dichroism (CD) spectrometry

CD spectra were recorded on a J-805s spectropolarimeter (JASCO) in 50 mM phosphate buffer (pH 7.5) with 100 mM NaCl at a peptide concentration of 10 μM. Continuous scans in the region between 195-260 nm were recorded using a 1 mm quartz cell, a scan rate of 50 nm/min, and a bandwidth of 0.2 nm, at 4.0ºC. The final spectra was an average of six consecutive scans over the same wavelength. The raw CD data were normalized for the peptide concentration and the number of residues in the peptide. Peptide denaturation analyses were performed by increasing the temperature from 4.0 to 96.0ºC at a constant rate of 1.0ºC/min. To monitor the changes in the α-helical content, the ellipticity at 222 nm was registered every 0.5ºC. The denaturation curves were normalized prior to analysis [14].

2.3.3. Isothermal titration calorimetry

Lyophilized peptides were dialyzed overnight at 4°C against the experimental buffer (50 mM sodium phosphate and 100 mM NaCl pH 7.5) and filtered before using. Concentration of the peptides in the syringe for the ITC experiments were 258 μM. Titrations consisted of 25 injections of 1 μl of the peptide solution into the buffer with a delay time of 280 sec between each injection. Measurements were performed between 30 and 70ºC depending on the peptide stability using a VP-ITC calorimeter (GE Healthcare). The enthalpy (ΔH) and dissociation constants (K_d) were determined by monomer-tetramer dissociation fitting as previously described [28].

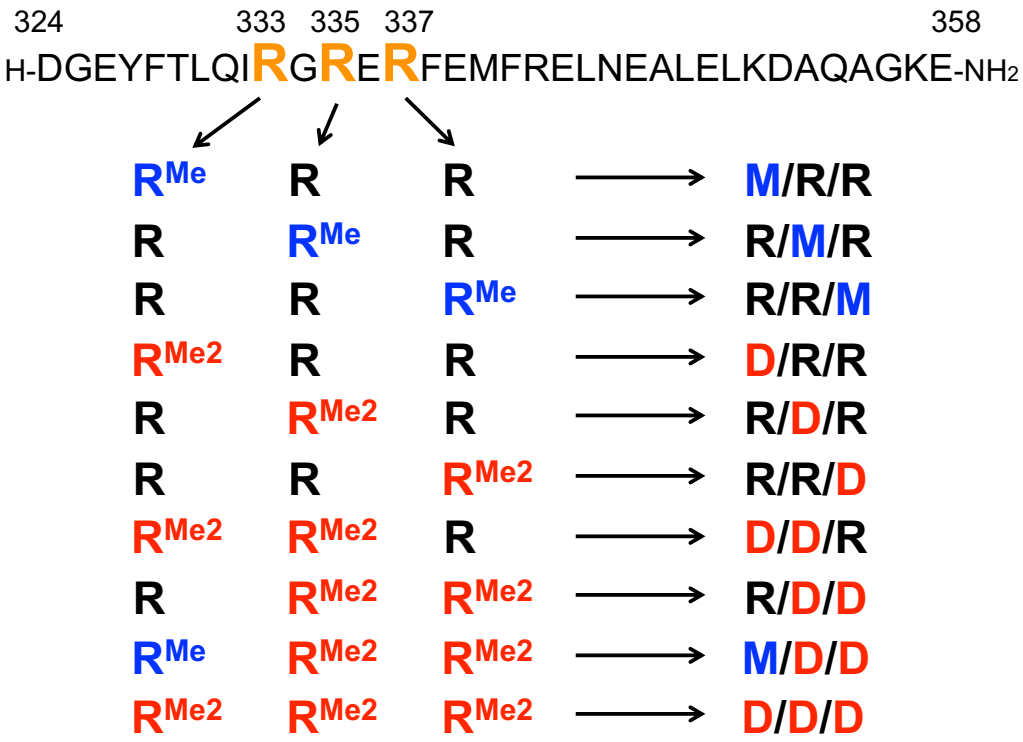

Figure 8. Sequences of the various mono- and di-methylated p53Tet

In total, 10 methylated p53Tet analogues were synthesized and the symbol M reveres to mono-methylation and the symbol D refers to di-methylation at a particular Arg residue (333, 335 and 337) in p53Tet.

2.3.4. *In vitro* methylation assay

The *in vitr*o methylation assay was performed using PRMT5/MEP50 and p53Tet peptides as an enzyme and substrate, respectively. The reaction sample (Total volume was 20 μl) included the appropriate p53Tet peptide (30 μM, 600 pmol), PRMT5/MEP50 (0.15 μM, 2.9 pmol), and S-adenosylmethionine (150 μM, 3 nmol) as a methyl-group donor, in 25 mM Tris-HCl pH 8.2. After an 11 h incubation at 37ºC, the methylation reaction was stopped by boiling the sample for 5 min. Afterward, the sample was digested with chymotrypsin (0.47 μM, 5.68 pmol) for18 h at 25ºC and the digestion was stopped by boiling the sample for 5 min.

2.3.5. nLC-MS/MS experiment

Peptide mixtures following the methylation reaction and digestion were subjected to LC-MS/MS analysis using an EASY nanoLC II system (Thermo SCIENTIFIC) attached to an LTQ-Orbitrap mass spectrometer (Thermo SCIENTIFIC). The peptides were separated on an NTCC-360 analytical column (NIKKYO 155 mm x 100 μm, C18) with an EASY-column (Thermo SCIENTIFIC 20 mm x 100 μm) precolumn. The LC separation was performed using a 45 min gradient (from 0 to 60% buffer B for 30 min, from 60 to 100% buffer B for 5 min, and held at 100% buffer B for 10 min). The two buffers used for the LC separation were 0.1% HCOOH/H_2O (buffer A) and 0.1% HCOOH/CH_3CN (buffer B). The flow rate was 300 nl/min. SEQUEST searches were performed with the MS/MS data, against a database containing sequences of each of the p53Tet peptides. The following differential modifications were allowed: mono-methylation on arginine, di-methylation on arginine, and amidation on the C-terminus. Fragment ion mass tolerance was 0.4 Da, and precursor mass tolerance is 10 ppm.

2.3.6. Gel filtration

The oligomeric states of the peptides were determined by gel filtration chromatography. For the analysis, 20 μl of peptide at 100 μM in 50 mM phosphate buffer pH 7.5 and 100 mM NaCl was injected onto a TSKgel G2000SW_{XL} (Tosoh) column. The peptides were eluted at room temperature using a flow rate of 0.1 ml/min with the same buffer and the elution was monitored by UV detection at 214 nm.

2.4. Results

2.4.1. Synthesis of p53Tet methylated analogues

A series of p53Tet peptides (residues 324-358 from human p53) systematically methylated at R333, R335, and R337 were chemically synthesized using solid-phase methods. The 10 peptides included the wild-type non-methylated peptide (p53Tet), three mono-methylated peptides at each Arg position (p53Tet M/R/R, R/M/R and R/R/M), three di-methylated peptides at each Arg position (p53Tet D/R/R, R/D/R and R/R/D), two peptides di-methylated at two positions (p53Tet D/D/R and R/D/D), a peptide mono-methylated at R333 and di-methylated at R335 and R337 (p53Tet M/D/D), and a peptide di-methylated at all three positions (p53Tet D/D/D). The calculated mass and the result of the mass spectroscopic analysis of each peptide is shown in **Table 1**.

2.4.2. Secondary structure and oligomeric state of p53Tet methylated analogues

To determine the effect that methylation of the three arginine residues had on the overall secondary structure of the tetramerization domain, circular dichroism (CD) spectroscopy studies were performed with each of the peptides. All of the methylated versions of the p53Tet peptide gave similar CD spectrum to the wild-type p53Tet peptide **(Figure 9),** which indicates that all had similar secondary structures to p53Tet and that methylation at the three Arg positions did not alter the fold of the peptide. Each of the variant methylated peptides showed the characteristic spectra of the wild-type p53Tet peptide, which includes a double minimum at 208 and 222 nm. These spectra are also indicative of the presences of the tetrameric form for the p53Tet peptide with each monomer composed of a single α-helix and a single β-strand. Some shifts at short-wavelengths were present in the spectrum with p53Tet D/D/D peptide, where all three Arg residues are di-methylated, which indicates the presence of some minor differences in this particular peptide.

To further asses the methylated peptides, we verified the oligomeric state of the methylated peptides by gel filtration chromatography **(Figure 10)**. Like the wild-type p53Tet peptide, all of the methylated variants of the p53 presented a predominant form that eluted at approximately 17 min, which corresponds to the tetrameric form of the peptide. In contrast, the predominant form of a p53Tet peptide where the three Arg residues are substituted by an Ala residue (p53Tet 3Ala) eluted at approximately 20 min, which corresponds to the monomeric form of the p53Tet peptide. Each of the methylated

Table 1. Molecular weight determination of methylated peptides

No.	Peptides	Calculated (MH^+)	Observed
1	R/R/R (WT)	4190.71	4190.50
2	M/R/R	4204.74	4205.37
3	R/M/R	4204.74	4205.59
4	R/R/M	4204.74	4205.34
5	D/R/R	4218.77	4218.46
6	R/D/R	4218.77	4217.77
7	R/R/D	4218.77	4218.66
8	D/D/R	4246.82	4247.61
9	R/D/D	4246.82	4246.60
10	M/D/D	4260.85	4260.83
11	D/D/D	4274.88	4274.93

The MH^+ (average) values were calculated using the protein prospector website at UCSF. The observed MH^+ values of the peptides were measured using MALDI-TOF MS (linear, positive mode).

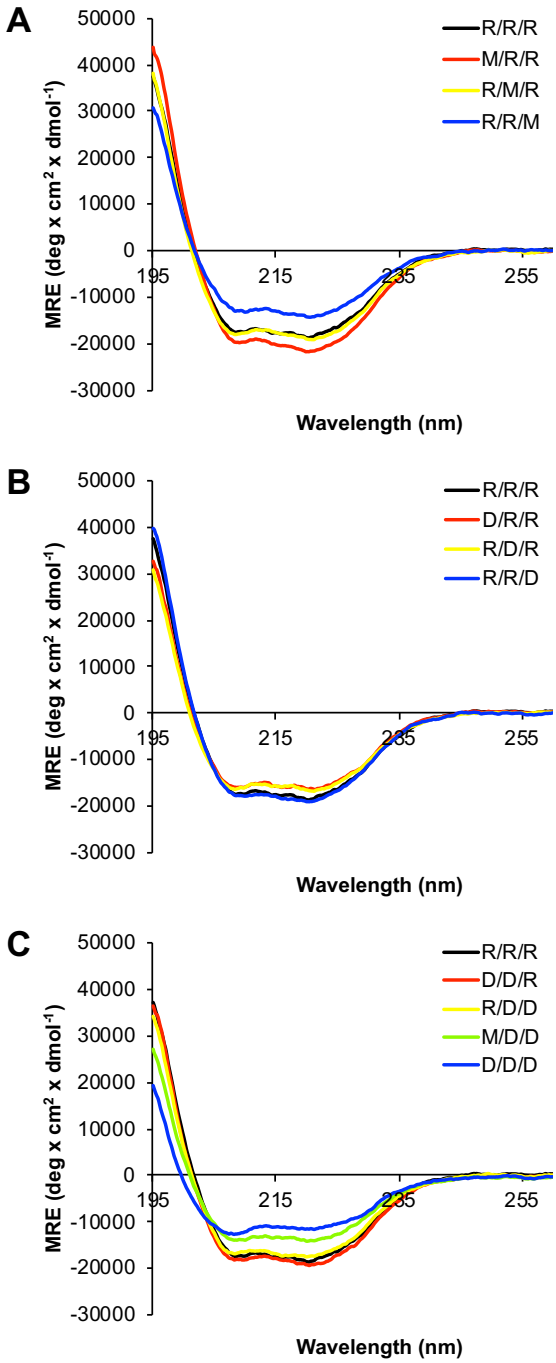

Figure 9. CD spectroscopy studies with the methylated p53Tet peptides

CD spectra of the methylated p53Tet peptides analogues were measured in 50 mM Na phosphate buffer, pH 7.5 with 100 mM NaCl, at 4℃. The concentration of each peptide was 10 μM. The mono-methylated peptides are presented in panel A, the single di-methylated peptides in panel B and the peptides containing more than one di-methylation in panel C for clarity. In all three panels, the WT p53Tet was used as a control for the percentage change of secondary structure.

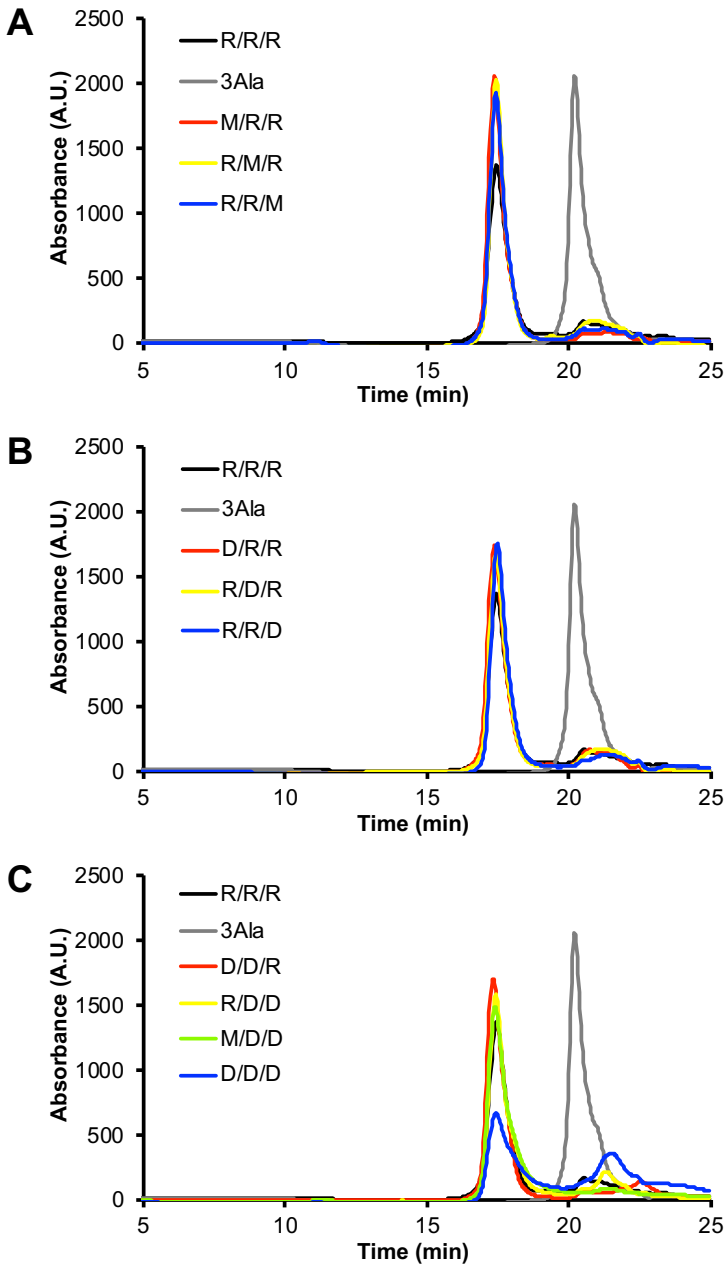

Figure 10. Gel filtration chromatography with the methylated p53Tet peptides

Gel filtration chromatography of methylated p53Tet peptides were performed in 50 mM Na phosphate buffer, pH 7.5 with 300 mM NaCl at a flow rate of 0.1 ml/min. The peptides were detected by UV absorbance at 214 nm. The injection volume of samples was 20 µl (100 µM peptide). The mono-methylated peptides are presented in panel A, the single di-methylated peptides in panel B and the peptides containing more than one di-methylation in panel C for clarity. In all three panels, the WT p53Tet was used as a control for the tetrameric form and the p53Tet 3Ala peptide was used as a control for the monomeric form.

p53Tet peptides also presented a minor form that eluted at approximately 20 min, which suggests that there is a small percentage of the monomeric form present for each peptide under the experimental conditions used. The largest percentage of the monomeric form was obtained the p53Tet D/D/D peptide, where all three Arg residues are di-methylated and this is consistent with the observed shifts at short-wavelengths in the CD spectra for this peptide.

2.4.3. Structural stability of p53Tet

Given the subtle differences displayed in the initial CD spectroscopy experiments and by gel filtration chromatography, the thermostability of the methylated peptides were determined using CD spectrometry at varying temperatures and compared with the WT p53Tet peptides. In these experiments, the ellipticity at 222 nm was monitored from 4℃ to 96℃ to generate denaturation curves **(Figure 11),** which were used to calculate the T_m, ΔT_m and $\Delta G^{37℃}$ of the peptides **(Table 2)**. Based on this analysis, the WT p53Tet peptide has a T_m of 70°C, a ΔG of 35 kcal/mol, and a K_d of 9 nM, whereas the methylated peptides have a 1.5–24°C lower T_m, a 1–10 kcal/mol smaller ΔG, and a 7–1800 nM larger K_d. This indicated that the tetrameric form of the p53Tet peptides were destabilized by methylation at all three Arg positions to some degree although the degree differed depending on whether the peptide was methylated at R333, R335 or R337. The thermodynamic stability of the peptides mono-methylated at R333 (M/R/R) and R335 (R/M/R) were similar, with the T_m being 0.3°C lower than the WT p53Tet peptide. In contrast, the peptide mono-methylated at R337 (R/R/M) presented a T_m value that was 10°C lower than p53Tet, which strongly suggests that the contribution of R337 to the stabilization of the tetrameric form is larger than that of R333 and R335.

To further determine the role of methylation at the three Arg positions, in p53Tet, we analyzed the di-methylated versions of the peptides. Peptides di-methylated at R333 (D/R/R) , R335 (R/D/R) and R337 (R/R/D) presented T_m values that were 2.6-4°C lower than there corresponding mono-methylated derivatives, which indicated that di-methylation at each of these positions is more destabilizing than their mono-methylation with di-methylation at R337 still having the most dramatic effect on the stability of the tetrameric structure. Furthermore, a peptide di-methylated at both R333 and R335 (D/D/R) presented T_m value that was only slightly lower than each of the individually di-methylated peptide at either R333 or R335. However, the p53Tet D/D/R

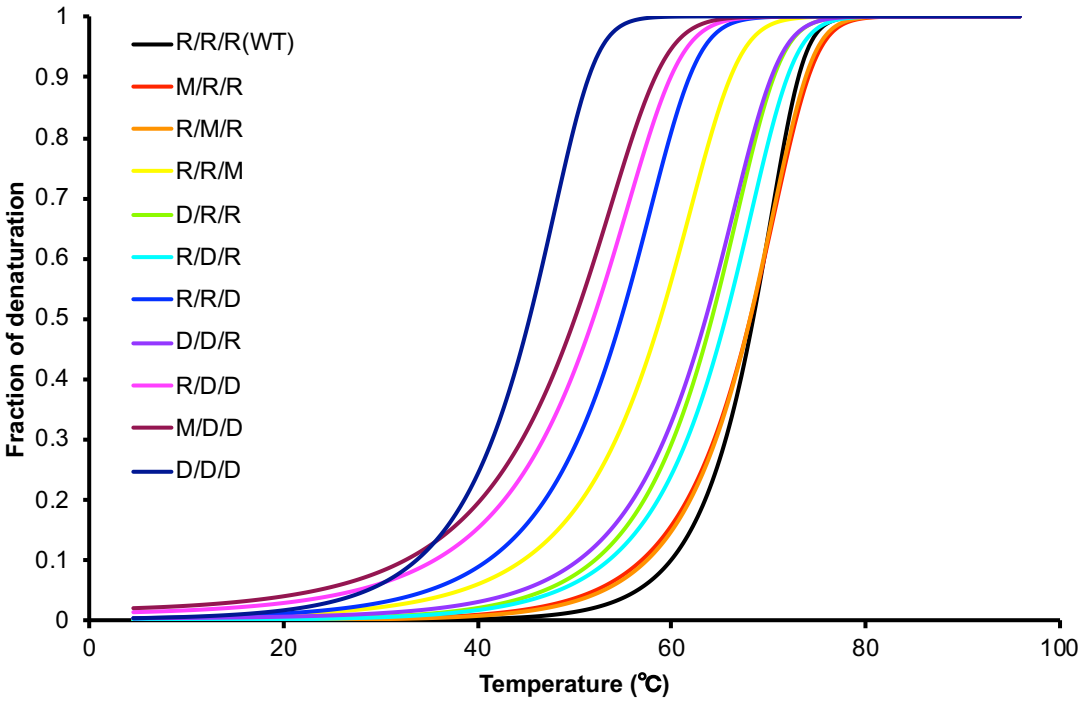

Figure 11. Thermal denaturation by CD spectroscopy of the methylated p53Tet

Thermal denaturation studies were performed using solutions containing 10 μM peptide in 50 mM Na phosphate buffer pH 7.5 with 100 mM NaCl at temperatures varying from 4℃ to 96℃. The T_m values were obtained by measuring the change in ellipticity at 222 nm for the peptides at the different temperatures.

Table 2. Thermodynamic parameters for the methylated peptides determined by CD

No.	Peptides	T_m (ºC)	ΔT_m (ºC)	ΔG_u (kcal/mol)	$\Delta\Delta G_u$ (kcal/mol)	K_d (nM)
1	R/R/R (WT)	68.5±0.3	-	37.2	-	2.4
2	M/R/R	68.2±0.4	−0.3	33.0	−4.2	23.1
3	R/M/R	68.2±0.3	−0.3	33.6	−3.6	16.1
4	R/R/M	58.9±0.4	−9.6	28.1	−9.1	314.3
5	D/R/R	64.2±0.4	−4.3	30.9	−6.3	71.2
6	R/D/R	65.6±0.4	−2.9	31.3	−5.9	55.9
7	R/R/D	54.8±0.2	−13.6	27.2	−10.0	511.3
8	D/D/R	63.6±0.2	−4.9	30.1	−7.1	111.4
9	R/D/D	52.0±0.1	−16.5	25.7	−11.5	1145.3
10	M/D/D	50.3±0.2	−18.2	25.6	−11.6	1225.3
11	D/D/D	45.4±0.2	−23.1	24.7	−12.5	2012.1

T_m: transition temperature; ΔT_m: difference of T_m value from WT p53Tet; ΔG_u: free energy of unfolding; $\Delta\Delta G_u$: difference of ΔG_u value from WT p53Tet; K_d: dissociation constant for tetramer formation

peptide is still more stable than the p53Tet R/R/M containing a single methylation at R337. Based on these results, the K_d for tetramerization increased by approximately 3-fold for the peptide di-methylated at R337 (R/R/D). Additionally, di-methylation of the R/R/D peptide at either R333 (D/R/D) or R335 (R/D/D) appeared to synergistically decrease the overall stability of the p53Tet peptide. Taken together these results further indicate that R333 and R335 make a small contribution to the stability of the p53 tetrameric form, whereas R337 makes a significant contribution to the overall stability of the p53Tet peptide. However, methylation at either R333 or R335 appears to be more dramatic in the context of an initial di-methylation at R337.

2.4.4. Thermodynamic stability of p53Tet

Given the effect that methylation at R333, R335 and R337 had on the thermal stability of the p53Tet as determined using CD spectroscopy, we next attempted to thermodynamically characterize the stability of the methylated p53Tet peptides using isothermal titration calorimetry experiments **(Table 3)**. For each peptide, ITC measurement at three different temperatures between 30–70°C were performed, depending on the thermal stability of each peptide. Based on these experiments, we were able to calculate the ΔH and K_d for the formation of the tetrameric structure. For, the WT p53Tet peptide, the experiments were performed at 55°C, 60°C, and 65°C and the ΔH was determined to be 63 kcal/mol art 60°C with a K_d of 4.1 μM. Likewise, the peptides mono-methylated at R333 (M/R/R) or R335 (R/M/R) presented ΔH values of 74 kcal/mol and 78 kcal/mol, at 60°C, respectively, indicating they were just slightly more stable than the WT p53Tet peptide. In contrast, the peptide mono-methylated at R337 (R/R/M) gave a ΔH value of 26 kcal/mol at 60°C, which indicated that it was dramatically less stable than the WT p53Tet peptide. These results are similar to what was observed with the CD spectroscopy experiments and again indicated that methylation at R337 is more important than methylation at either R333 or R335 for destabilizing the tetrameric form of the p53Tet peptide.

To further verify the role of R337, ITC experiments were also performed with several of the di-methylated peptides. As seen in the CD studies, di-methylation at either R333 or R335 resulted in small changes in the stability relative the WT p53Tet peptide giving ΔH values of 50 kcal/mol and 64 kcal/mol, at 60°C respectively. In this case, the peptide di-methylated at R335 (R/D/R) is almost identical to the WT peptide, whereas the

Table 3. Thermodynamic parameters for the methylated peptides determined by ITC

No.	Peptide	Temperature (°C)	ΔH (kcal/mol)	K_d (μM)	K
1	R/R/R (WT)	65	117.5	5.1	6.67E-17
		60	63.0	4.1	3.35E-17
		55	23.5	4.6	4.97E-17
2	M/R/R	70	106.7	18.4	3.09E-15
		65	106.0	7.4	2.02E-16
		60	73.6	4.1	3.50E-17
3	R/M/R	70	130.7	21.7	5.08E-15
		65	129.2	5.0	6.25E-17
		60	77.6	4.1	3.47E-17
4	R/R/M	60	25.8	36.1	2.36E-14
		55	25.0	22.6	5.77E-15
		50	19.8	10.4	5.65E-16
5	D/R/R	60	50.1	17.0	2.47E-15
		55	45.5	12.0	8.54E-16
		50	30.8	10.4	5.66E-16
6	R/D/R	60	63.9	11.6	7.85E-16
		55	44.4	12.2	9.07E-16
		50	31.3	9.9	4.87E-16
7	R/R/D	47.5	13.1	40.1	3.22E-14
		45	14.1	28.1	1.11E-14
		40	12.3	19.0	3.41E-15
8	D/D/R	60	160.4	3.9	2.87E-17
		55	75.7	3.9	2.96E-17
		50	38.5	3.6	2.34E-17
9	R/D/D	45	20.5	27.9	1.09E-14
		40	17.5	21.2	4.77E-15
		35	14.1	12.2	9.04E-16
10	M/D/D	47.5	20.8	22.5	5.70E-15
		45	18.3	16.1	2.09E-15
		40	17.6	10.5	5.76E-16
11	D/D/D	35	11.9	41.8	3.65E-14
		32.5	10.7	22.7	5.87E-15
		30	10.2	19.8	3.86E-15

ITC studies were performed in 50 mM Na phosphate pH 7.5 with 100 mM NaCl. The concentration of the peptides in the syringe was 258 μM.

peptide di-methylated at R333 (D/R/R) is less stable, but still considerably more stable than the peptide mono-methylated at R337 (R/R/D). Likewise, the peptide di-methylate at R337 (R/R/D) was by far the least stable as we were not able to make a measurement of its ΔH value at 60°C, but it had to perform the measurements between 40 and 47.5°C. For the R/R/D peptide, the ΔH was only 14 kcal/mol and the K_d was 28 μM at 45°C, indicating that R/R/D was remarkably destabilized. As expected, the peptide di-methylated at all three Arg positions (D/D/D) was the least stable peptide with a ΔH of 12 kcal/mol and a K_d of 42 μM at 35°C. Therefore, the ITC studies supported the CD spectroscopy studies and indicated that mono- and di-methylation at R337 drastically destabilized the oligomeric structure of the p53Tet peptide.

2.4.5. Distinct cascade for p53Tet methylation by PRMT5

Given that methylation at the three arginine residues present in the tetramerization domain of p53 (R333/R335/R337) have different roles in the overall stability of the p53Tet peptide, I was interested to determine whether there is preference for methylation of the different sites. To determine for the presence of a difference, *in vitro* methylation studies were performed with a recombinant PRMT5/MEP50 enzyme complex. The assay was performed using the WT p53Tet peptide (R/R/R) as the substrate and *S*-adenosylmethionine (SAM) as the methyl group donor for the PRMT5. During the incubation with PRMT5, samples of the peptide were taken at varying time intervals and digested with chymotrypsin prior to identification of the methylation sites by LC-MS/MS **(Figure 12)**. Under the chosen experimental conditions, mono-methylation was observed at either R333 (M/R/R) or R335 (R/M/R) **(Figure 12)**. However, the di-methylation was observed only when the initial mono-methylation occurred at R335 **(Figure 13A)**. In contrast, no additional methylation sites were observed, when the initial methylation occurred at R333. Under the experimental conditions, the methylation efficiency was about 1% based on the relative intensity of the signals in comparison to the precursor ion and methylation was not observed at R337.

In this assay, it was assumed that the PRMT5/MEP50 complex and the p53Tet peptide in its tetrameric state are required for the methylation reaction to occur. However, it is not known whether p53Tet can also be methylated in its monomeric state. To test this, a monomeric form of the p53Tet domain containing three alanine substitutions (p53Tet3Ala: L330A, I332A and L344A) was tested. When the p53Tet-3Ala peptide was

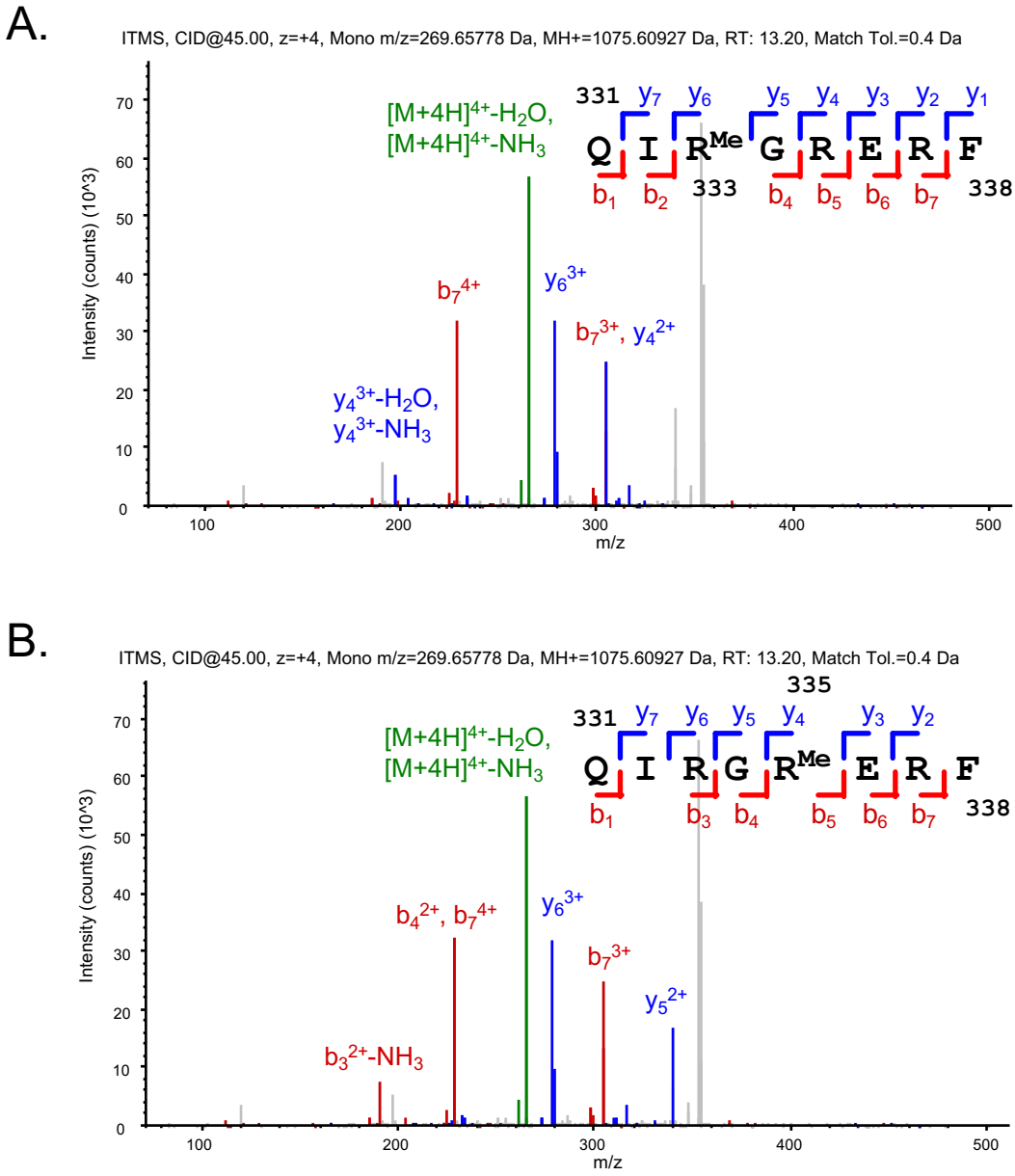

Figure 12. MS/MS spectra from PRMT5 assays with the WT p53Tet

The target fragment was cleaved by CID. The MS/MS fragment patterns are shown, b-ion: red; y-ion: blue; precursor-ion: green. A and B are the same MS/MS spectrum detecting both the mono-methylation at R333 (M/R/R) and R335 (R/M/R).

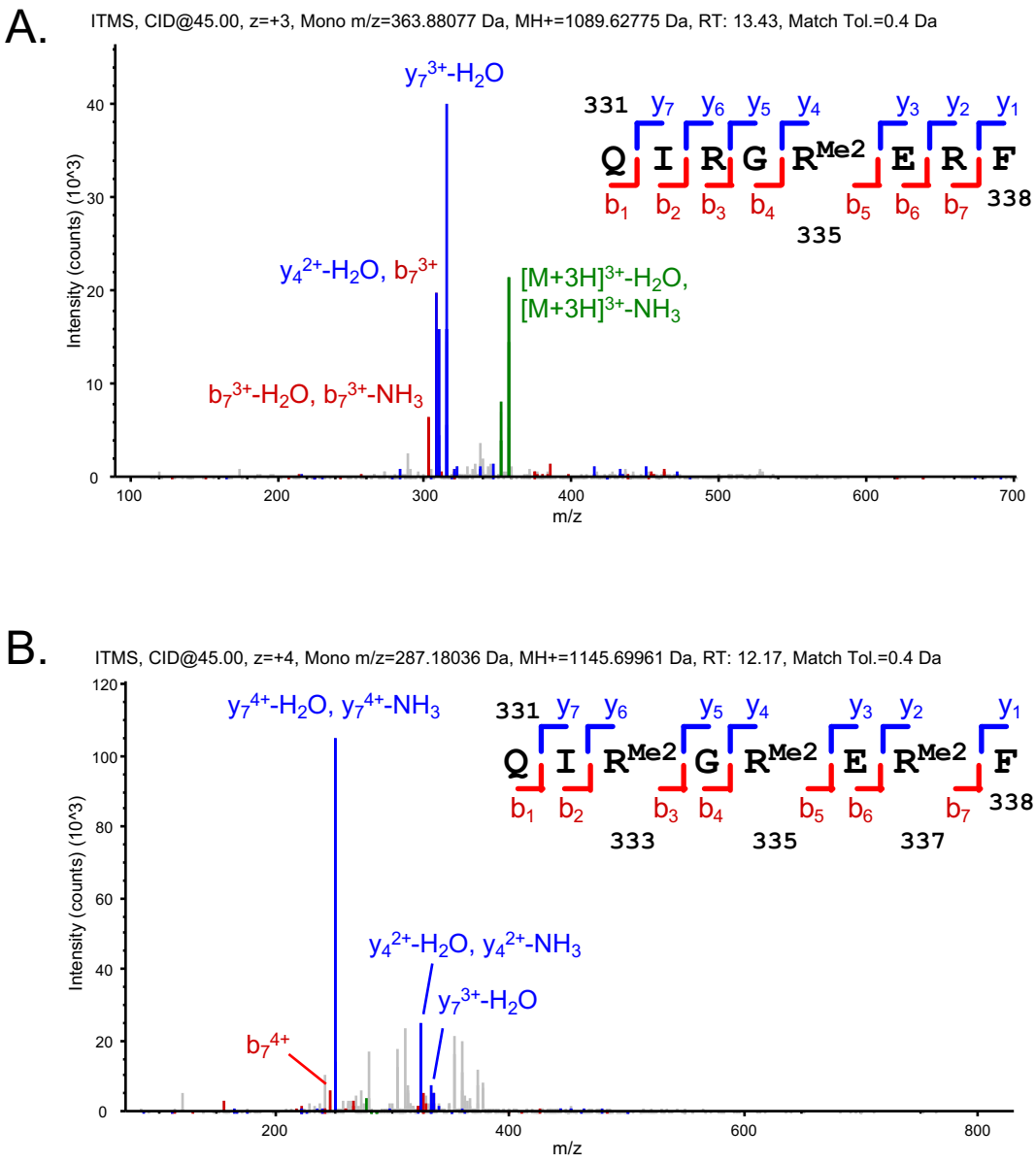

Figure 13. MS/MS spectra from PRMT5 assay with R335 methylated peptides

PRMT5 assays were performed with the p53Tet peptide either mono-methylated (A) or di-methylated (B) at R335. The target fragment was cleaved by CID. The MS/MS fragment patterns are shown, b-ion: red; y-ion: blue; precursor-ion: green.

used as the substrate, no methylated products were identified. Together, these results suggest that the p53Tet can be methylated at R333 and di-methylated at R335 by the PRMT5/MEP50 complex in its tetrameric form, but not in its monomeric form.

The presence of the R335 di-methylated product (R/D/R), suggests that there might be a distinct order for methylation of the three Arg residues in p53Tet by PRMT5. To determine whether a methylation cascade could in fact be present, additional methylation studies were performed using the three products obtained in the initial studies as the substrates for PRMT5. Under the same experimental conditions as with the WT p53Tet, no additional methylation was observed when the peptide mono-methylated at R333 (M/R/R peptide) was used as the substrate. This is consistent with what was observed in the assays with the WT p53Tet (R/R/R) where no subsequent methylations were observed following initial methylation at R333. Likewise, di-methylation at R335 was observed when the peptide mono-methylated at R335 (R/M/R) was used as the substrate **(Figure 13A)**. However, when the peptide di-methylated at R335 (R/D/R) was used as the substrate, additional di-methylation was also observed at both R333 and R337 with the final product being the peptide di-methylated at R333, R335 and R337 (D/D/D) **(Figure 13B)**. Surprisingly, no intermediate products containing a combination of mono-methylated and di-methylated peptides were observed, which strongly suggests that the rate of reaction was very rapid for converting the peptide di-methylated at R335 (R/D/R) to the peptide di-methylated at all three Arg residues (D/D/D). Moreover, this suggests that di-methylation at R335 initiates a cascade, leading to subsequent di-methylation at both R333 and R337. Due to the rapid conversion from R/D/R to the D/D/D form under the experimental conditions, it was not possible to determine the order in which the subsequent methylation/di-methylation reactions occurred.

2.5. Discussion

Posttranslational modifications (PTMs) regulate activity, localization, and interactions of many proteins. PTM cascades are important for precise signal transduction and efficient signal amplification in response to external or internal stimuli. A number of signaling pathways are driven by a PTM cascade such as the mitogen-activated protein kinase (MAPK) pathway and NF-κB signaling [68,69]. In these pathways, several proteins are involved in the PTM cascade, however there are PTM cascades where there is only one target protein, and this appears to be the case for many of the PTMs regulating p53. Previous studies have shown that p53 is regulated by both a phosphorylation-acetylation and phosphorylation-phosphorylation cascades [26,70]. In our current studies, we have identified another PTM cascade that regulates p53 which is controlled by the arginine methyltransferase PRMT5. Our results clearly show that an initial mono-methylation of R335 in the tetramerization domain of p53 by PRMT5 leads to a subsequent di-methylation at R335 as well as to di-methylation at R333 and R337 by PRMT5 **(Figure 14A)**. Importantly, we also show that the di-methylation at R337, but not at either R333 or R335, significantly destabilized the tetrameric structure of the p53Tet peptide. This suggests that di-methylation at R337 will significantly alter the ability of p53 to activity its target genes as previous studies have linked the stability of the tetrameric structure of p53 with its ability to activate p53 response elements (REs).

Given that it was shown that PRMT5 can di-methylate p53 at three Arg positions (R333, R335 and R337) within its tetramerization domain, we performed biochemical and biophysical studies to determine how either mono-methylation or di-methylation at these sites would alter the stability of the tetramer form of p53. Our CD and ITC experiments clearly demonstrated that that either mono- or di-methylation at R337 significantly altered the stability of the tetrameric form of the p53Tet peptide. In contrast, either mono- or di-methylation at R333 and R335 had only minor consequences. These results are consistent with the location of these three Arg residues in the structure of the p53Tet that have been determined by both NMR spectroscopy and X-ray crystallography [13]. In all of these previously determined structures of the tetramerization domain of p53, R333 and R335 are on the surface of the protein, but there is an apparent salt bridge between the positively charged sides chain of R337 from one monomer to the negatively charged side chain of D352 on an adjacent monomer **(Figure 14B)**. The presence of these four salt bridges across the four monomers suggested that

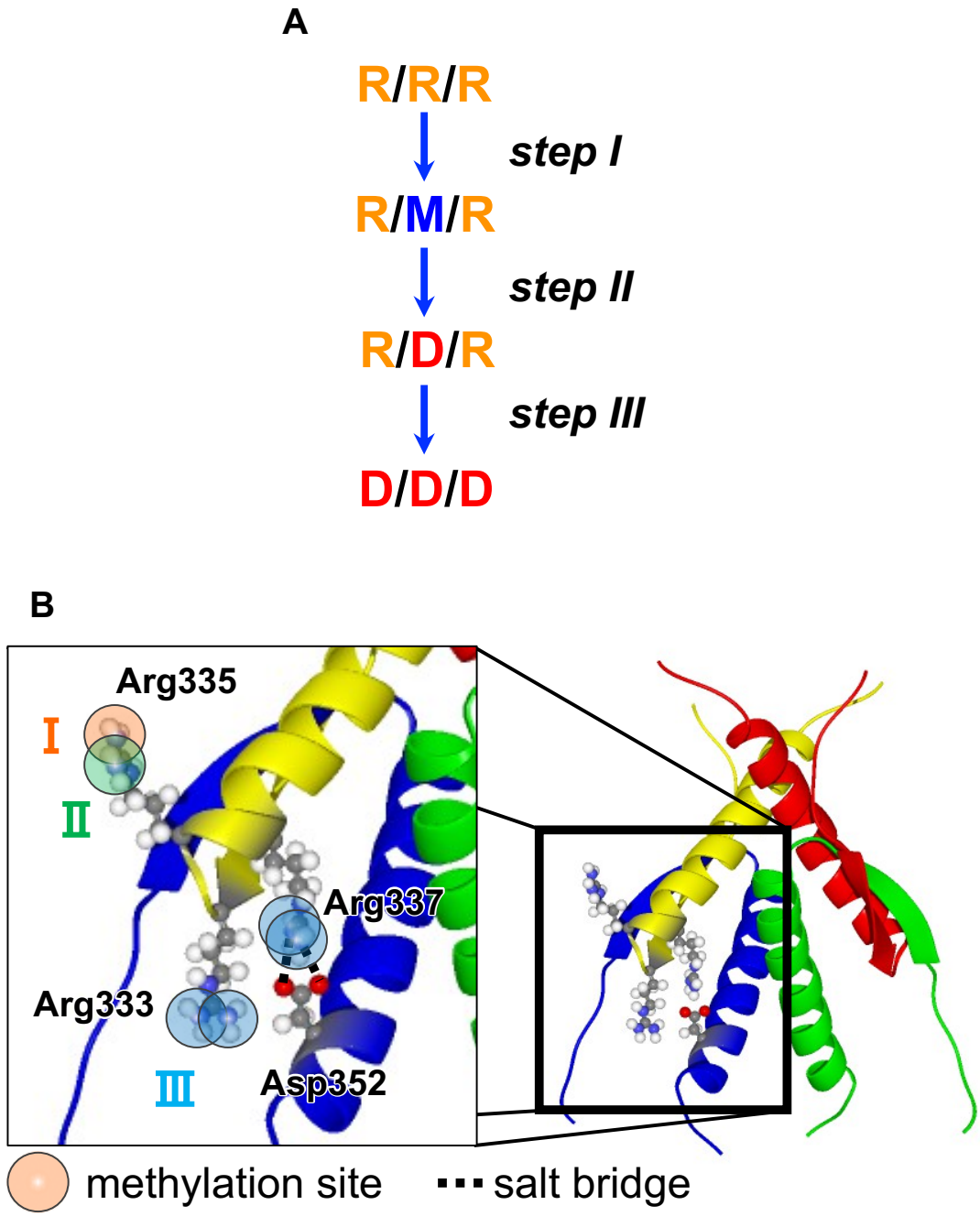

Figure 14. Methylation cascade of p53Tet by PRMT5

A: The methylation cascade occurs in three steps.; B: In the structure of p53Tet (PDB ID: 3SAK), the positively charged side chain of Arg337 from one monomer (Yellow) forms a salt bridge with the negatively charged side chain of Asp352 from an adjacent monomer (Blue).

they play a key role in stabilizing the tetrameric form of the p53 protein. The results with the methylated peptides indicate that either mono- or di-methylation of this residue appears to alter the formation of this salt bridge and thus the stability of the tetramer. Structural studies with the p53Tet peptide methylated at R337 will be needed to provide atomic level detail as to how these PTMs alter the stability of the tetrameric form of the peptide.

The results with the different methylations at the three Arg residues could also provide insights into mutations that occur at these positions in human tumors. In different human tumors, both R335 (R335L, R335G, and R335H) and R337 (R337C, R337H, R337L, and R337P) have been reported to be mutated, but not R333 [71]. Consistent with our results with the methylated peptide, the R337P mutant of p53 only exists in the monomer form. In addition, the thermostability of different R335 and R337 mutated peptides have been examined and they were shown to have T_m values of 46°C, 58°C, and 64°C for R335L, R335G, and R335H, respectively, and T_m values of 22°C, 37°C, and 38°C for R337C, R337H, and R337L, respectively [15]. The stabilities of mutations at R335 are similar to what was observed with the methylated peptides. However, the R337 mutants were less stable than any the methylated peptides. Accordingly, forming a salt bridge via R337 is very important for maintaining the stability of the oligomeric structure and in all of these mutants the ability to form the salt bridge would be lost. Interestingly, within the 124 vertebrate p53 protein sequences, R333 is changed to H, I, K, Q, T, V, and Y in 20 species, whereas R335 is changed to F, H, K, L, Q, and W in 18 species and R337 is changed to K and N in 15 species. Importantly, substitutions of R337 are rare and in general in several cases it is replaced by another amino acid with a positively charged side chain. This strongly suggests that the salt bridge between R337 and D352 is important to maintain the structural stability in other vertebrate species as well [72]. This is consistent with the fact that PRMT5 is expressed from yeast to vertebrates, which suggests that the methylation cascade of p53 occurs in vertebrates as well.

The fact that mutations at R337 destabilize tetramer formation in human cancer and that R337 is highly conserved in the evolution of vertebrates, support the idea that R337 is an important residue for structural stability and regulation of p53 functions. Thus, it appears that the methylation cascade at R333, R335, and R337 is essential for regulating and maintaining p53 transcriptional activity through the destabilization of the p53 tetramer. However, it is not exactly clear why the cascade is initiated by first mono-

methylation and then di-methylation at R335 and whether or not di-methylation at R333 occurs prior to di-methylation at R337. As mentioned above, the side chains of R333 and R335 are on the surface of the structure of the p53Tet and thus exposed to solvent. In contrast, R337 forms a salt bridge with D352, which is orientated towards the interior of the structure and it is less solvent accessible. In these positions, R333 and R335 would be more accessible for methylation by PRMT5. Thus, I hypothesize that R333 and R335 interact with other proteins more easily than R337 does and that a slight structural change caused by the di-methylation of R333 and R335 is required to di-methylate R337. However, our experiments were not able to determine whether di-methylation at R333 occurs before either of the methylation reactions at R337. Moreover, the methylation efficiency of each step was only around 1%, which leads us to speculate that there might be interactions with other regions of p53 required for more efficient methylation by PRMT5 *in vivo*, possibly with the MEP50 protein. Based on our results, I propose a model for the selection of p53 target genes that is mediated through the structural stability of the tetramerization domain and regulated by PRMT5-dependent methylation **(Figure 15)**. To function correctly, p53 must select the right target genes to induce the correct cell fate and either activate or repress transcriptional activity. I suggest that cells take advantage of posttranslational modifications to regulate p53 activity and alter its binding capacity on different p53-regulated response elements. p53 binds with high affinity to the response elements of its target genes that induce cell cycle arrest or DNA repair (K_d = 4.9–12 nM), but with much lower affinity to the response elements of its target genes that induce apoptosis (K_d = 7.1–260 nM) [73]. Several mutants in the tetramerization domain have decreased affinity for p53-response elements and the transcriptional activity of target genes is proportional to the stability of the tetrameric structure. Thus, cell cycle arrest is induced even when p53 tetramerization domain is destabilized (low concentration of active tetramer form), but apoptosis is induced only by stable (high concentration of tetramer form) p53 protein. As we have demonstrated, methylation at Arg residues can reduce the tetramer stability and thus the activity. These results are consistent with the fact that apoptosis can be induced in PRMT5 knockout cells because the non-methylated p53Tet stabilizes the tetrameric form, whereas PRMT5 overexpression does not induce apoptosis but cell cycle arrest because hyper-methylated p53Tet destabilizes the tetrameric form. Therefore, I speculated that p53 selects genes for transcription activation by changing its affinity for

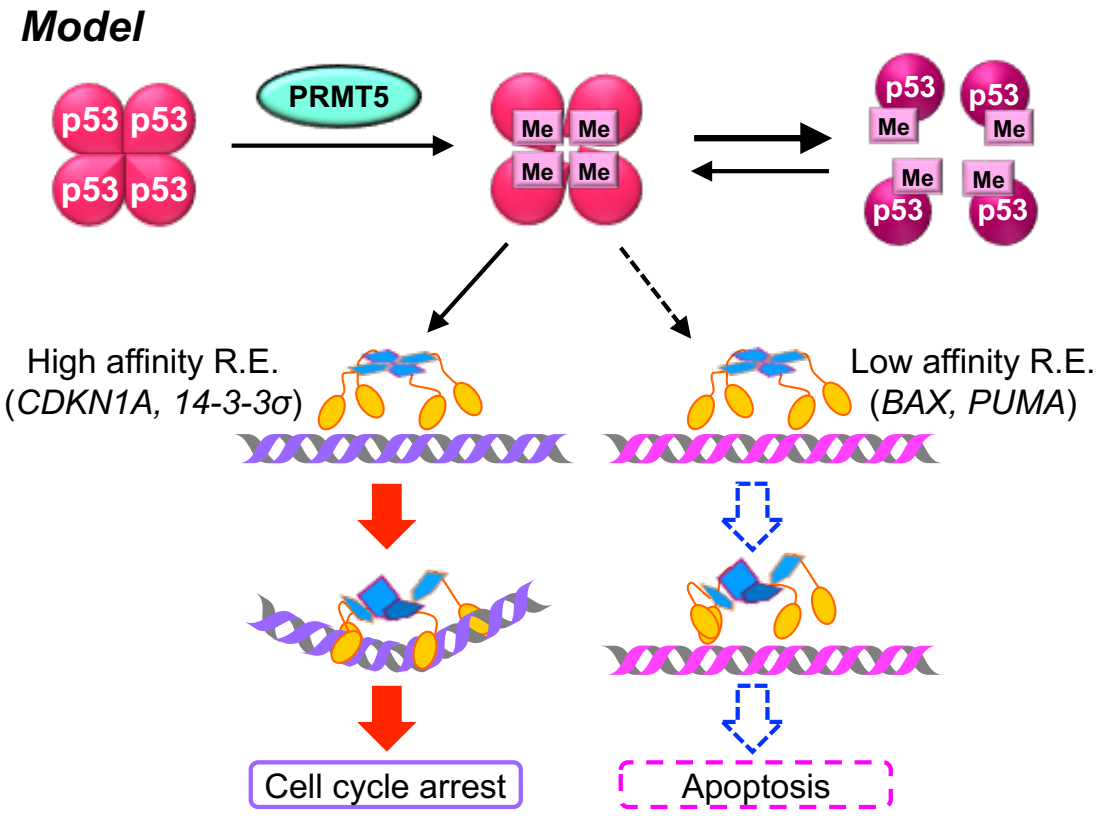

Figure 15. Target gene selection model though modulating the stability of the p53 tetramer

In response to cellular stress, PRMT5 is activated and modifies p53 TD at three different Arg residues (R333, R335 and R337). The methylation of p53 at R337 destabilized the tetrameric form of the protein and alters its capacity to bind to its response elements. (REs). In its methylated form, p53 is able to still activate high affinity REs whereas is not able to activate low affinity REs due to the decreased stability of the tetramer.

target genes, and thereby regulates the cellular response, as the structural stability of p53 tetramer is modulated via methylation by PRMT5.

3. Structural Stability of p53 Tetramerization Domain in Mammals

3.1. Abstract

The p53 protein plays a number of roles in protecting organisms from different genotoxic stresses and this includes DNA damage induced by acetaldehyde, a metabolite of alcohol. To perform its function, p53 must be in its active tetrameric state, which is regulated on its cellular concentration and requires oligomerization through its tetramerization domain (TD). The sequence of the p53 TD is highly conserved in most mammalian species and thus very similar to the sequence found in humans. However, select residues are varied in certain species and this suggests that in these species the stability of the p53 TD may vary and this could have important implications to the function of the p53 protein in that species. To investigate possible differences in the stability of structure of p53 TD from different species, we synthesized a series of 35-residue peptides corresponding to the p53 TD of six different mammals (human, tree shrew, guinea pig, chinese hamster, sheep, and opossum). These sequences were chosen because they have subtle, but interesting sequence variations in comparison to that of the highly studied human p53 TD. The thermostability of the p53 TD peptides (p53Tet) from the five other mammalian species were analyzed using CD spectrometry compared with the human p53Tet. Using a combination of biophysical and modeling studies, I demonstrate that several of these p53Tet have increased thermostability relative to the human peptide and that the secondary structure of the tree shrew and opossum sequence have increased helical content. This was particularly surprising for the tree shrew p53 TD since it shares almost 90% sequence identity with the human p53 TD. Based on modeling and mutagenesis studies, I determine that a glutamine to methionine substitution at position 354 plays a key role in this difference between the human and tree shrew p53 TD. Given the link between stability of the p53 tetramerization domain and its transcriptional activity, the results suggest that this enhanced stability could lead to important consequences at p53-regulated genes in the tree shrew.

3.2. Introduction

The p53-family proteins (p53, p63 and p73) are an evolutionarily conserved group of transcription factors that appeared at the beginning of multicellular life over 1 billion years ago [74]. In humans, the p53 protein functions as a tumor suppressor due to its ability to regulate a number of key cellular functions and mutations in the p53 gene have been directly linked to many different human cancers [33]. The association between p53 mutations and cancers is due to the fact that p53 is a key factor in maintaining genomic integrity by inducing cell cycle arrest and apoptosis in response to cellular stress such as DNA damage. As part of its role as the guardian of the genome, p53 was recently shown to protect cells from DNA damage linked to alcohol metabolism [75]. In these studies, it was reported that the alcohol metabolite acetaldehyde induces DNA damage and that this leads to genome instability in the absence of p53. In addition, it was shown that alcohol induced DNA damage induced p53-dependent apoptosis which prevented malignant transformations caused by genome mutations [76].

To function as a transcriptional regulator, p53 forms a homo-tetrameric structure and the stability of this tetrameric structure is crucial to its transcriptional activity. The tetramer is formed by a short domain located near the C-terminal end of the protein. The structure of the human p53 tetramerization domain (p53Tet; residues 324-356 of human p53) consists of a single β-strand and a single α-helix [13]. To form the tetramer, the β-strand and the α-helix of two monomers come together to form a dimer and the dimers form the tetrameric structure through interactions between the helices of each monomer. Although all p53-family proteins form tetramers, there are structural differences between the tetramerization domain of human p53 in comparison to the tetramerization domain from human p63 and p73. In both p63 and p73, there is a second α-helical region at the C-terminal end of their tetramerization domain that is required for tetramer formation. More recently, this extra helical region was also found to be present in p53 proteins from a subgroup of bony fishes [72].

Most known mammals in existence are viviparous and with only a few exceptions their initial nourishments are provide from their mother’s milk. Presently, the number of species classified as mammals is somewhere between 4,300 and 4,600 and they can be found living in almost all arias on the Earth, including on land, underground, and in aquatic environments. It is believed that Adelobasileus was the original mammal known to exist on earth approximately 225 million years ago. Following a mass extinction

of the dinosaurs approximately 64 million years ago, mammals quickly evolved and became the most prosperous animal species on land. Although the evolution process and classification of mammals are not completely resolved, there are some universal agreements based on phylogenetic studies for this field. It has been established that the divergence from monotreme (oviparous species such as platypus) to Therian (mammals except monotreme) occurred approximately 180 million years ago, and the divergence between marsupials (species growing children in a marsupium such as opossum, kangaroo, and koala) and placentarians (Therian except marsupial) occurred approximately 140 million years ago.

One of the more confusing mammals to classify over the years has been the common tree shrew, which are small mammals that live in tropical rain forests of southeast Asia and they make up the entire classification of Scandentia, Mammalia. This rodent-like animal, which bears physical resemblance to a squirrel, has drawn interest from the scientific research community as a model organism due to fact that they possess a number of characteristics similar to human. The initial interests in the common tree shrew stemmed from the fact that, despite being physically similar to rodents, they share several genetic features in common with primitive primates. Although it is now estimated that they diverged from primates ~90 million years ago, tree shrews are thought to be early precursors for primitive primates that evolved to apes and humans [77]. In addition to this evolutionary link to primates, tree shrews have certain dietary traits in common with humans as they are one of the only other animals that voluntarily consume alcohol on a regular basis [78] as well as foods containing capsaicin [79].

The high consumption of alcohol by tree shrews comes from the fact that they feed on the nectar from the flowers of the Bertam palm tree. This fermented nectar is on average 0.6% alcohol but can reach levels of up to 3.8% and the flowers are a food source during all periods of the year. Based on the average alcohol level in the nectar and the mean feeding time of tree shrews, it is estimated that the typical tree shrew consumes intoxicating levels of alcohol every third evening assuming alcohol metabolic rates similar to humans. Not surprisingly, the alcohol metabolic rates of tree shrews appear to be significantly faster than humans and this maybe be due to the presence of higher levels of the alcohol conjugating enzyme ethyl glucuronide. Given their pension to regularly consume alcohol, the tree shrew is used as a model for studying alcohol induced fatty liver as well as the role of alcohol plays in primate evolution. In addition, it is now known

that the tree shrew can serve as a model for a number of other human diseases including breast cancer and a number of viral infections.

Given the tree shrews high consumption of alcohol and the role of p53 in protecting against acetaldehyde induced DNA damage, I was interested in examining whether or not the p53 protein from the tree shrew possessed any unique properties relative to several other mammalian species including humans that might help it survive high levels of alcohol. In particular, I was curious to determine whether the tetramerization domain of tree shrew p53 had evolved to possess any properties that might help protect it from DNA damage associated with increased levels of acetaldehyde. Using a combination of peptide synthesis, biophysical characterization and modeling, I have compared the stability of the p53Tet from tree shrew, guinea pig, Chinese hamster, sheep, and opossum. Interestingly, I determined that the p53Tet of several of these species is significantly more stable than human p53Tet and that the p53Tet of tree shrew and opossum have significant changes in secondary structure content as determined by circular dichroism (CD) analysis. In addition, I demonstrate that despite sharing extremely high sequence identity, the increased stability for the tree shrew p53 is largely due to a single substitution of a glutamine to methionine at position 354, in their respective sequences. These results suggest that the transcriptional activity of the tree shrew protein may be significantly different at select p53-dependent genes and this may account for some of its unique characteristics including the ability to consume large quantities of alcohol. In future studies, it will be of interest to determine if increases in the stability of their tetramerization domain can be associated to unique traits of different mammals that help they survive in their environmental niche.

3.3. Experimental procedures

3.3.1. Peptide synthesis

Peptides corresponding to the human p53 tetramerization domain (human p53Tet; residues 324-358 of human p53), the human p53Tet(Q354M) variant, the tree shrew p53Tet (residues 324-358 of tree shrew p53), the tree shrew p53Tet(M354Q) variant, the guinea pig p53Tet (residues 321-355 of guinea pig p53), Chinese hamster p53Tet (residues 324-358 of Chinese hamster p53), sheep p53Tet (residues 313-347 of Sheep p53), and opossum p53Tet (residues 269-330 of opossum p53) were synthesized as previously described [80]. The sequence of peptides are shown in **Figure 16**. Peptide concentrations were determined by UV spectroscopy using an extinction coefficient of 1490 M^{-1} cm^{-1} at 280 nm, which corresponds to a single tyrosine present in all sequences.

3.3.2. Circular dichroism (CD) spectrometry

Circular Dichroism (CD) spectra were recorded at 4°C using a J-805s spectropolarimeter (JASCO) in 50 mM phosphate buffer pH 7.5 with 100 mM NaCl at a peptide concentration of 10 μM in a 1 mm quartz cell. Continuous scans were recorded over the region between 195-260 nm at a scan rate of 50 nm/min and a bandwidth of 0.2 nm. The resulting signals from six consecutive CD scans were averaged and normalized for peptide concentration and the number of residues. Peptide denaturation analyses were performed by increasing the temperature from 4°C to 96°C at a constant rate of 1.0°C/min. To monitor the changes in the α-helical content of the peptides, the ellipticity at 222 nm was registered every 0.5°C and the denaturation curves were normalized before analysis [14]. The percentage of secondary structural elements were calculated using the JWSSE-480 program (JASCO) and fit according to the method of Reed [81].

3.3.3. Gel filtration

The oligomeric states of the peptides were determined by gel filtration chromatography. For the analysis, 20 μl of peptide at 100 μM in 50 mM phosphate buffer pH 7.5 and 100 mM NaCl was injected onto a Superdex 75 (GE Healthcare) column. The peptides were eluted at room temperature using a flow rate of 0.1 ml/min with the same buffer and the peptides were monitored by UV detection at 214 nm.

Common Name	p53Tet Sequences	identity	homology
Human	DGEYFTLQIRGRERFEMFRELNEALELKDAQAGKE	-	-
Tree shrew	DEEYFTLQIRGRERFEMLREINEALELKDAMAGKE	88.6%	94.3%
Guinea pig	DAEYFTLKIRGRKNFEILREINEALEFKDAQTEKE	71.4%	91.4%
Chinese hamster	DGEYFTLKIRGHERFKMFQELNEALELKDAQASKG	82.9%	94.3%
Sheep	DGEYFTLQIRGRKRFEMFRELNEALELMDAQAGRE	91.4%	97.1%
Opossum	EGEYFTLQIRGRQRYELLREINEALELKEAHSRKE	71.4%	97.1%

Figure 16. Sequence alignments of six mammalian p53Tet used in the study

Non-core hydrophobic amino acids are in orange, acidic in red, basic in blue and all others in black. The Gly residue in the turn is in green and residues of the hydrophobic core are in light blue. The identity and homology of the different p53 TD sequences are calculated relative to the sequence of the human p53 TD.

3.3.4. Homology modeling

Models of the tree shrew p53 TD structure was generated using both the MODELLER 9.22 software [82] and the SWISS-MODEL tool available through UniProt [83]. For both models, the three-dimensional coordinates of the human p53 TD (PDB: 1AIE) were used as a starting template. When using the MODELLER 9.22 software, the tree shrew p53 TD structure with the lowest DOPE score was chosen for comparison with the structure of human p53 TD.

3.4. Results

3.4.1. Synthesis of p53Tet

A peptide corresponding the tetramerization domain of p53 (p53Tet) from six different mammals (human, tree shrew, guinea pig, Chinese hamster, sheep, and opossum) as well as two variants [human p53Tet(Q354M) and tree shrew p53Tet(M354Q)] were prepared by solid-phase peptides synthesis and purified by reverse phase HPLC on a C8 column. The identity of each peptide was confirmed by mass spectral analysis and the calculated mass and the results of mass spectrometry with each peptide are shown in **Table 4**.

3.4.2. Primary and secondary structure of p53 TD

Given that previous functions studies have established a direct correlation between the stability of the tetramerization domain of p53 and its ability to activate transcription, I was interested in analyzing the structure and the stability of the tetramerization domain of several mammalian p53 proteins including the tree shrew p53. Initially, the oligomeric states of the peptides were compared using gel filtration chromatography. As expected, the human p53Tet and the other mammalian p53Tet peptides were found to be predominantly in the tetrameric form under the experimental conditions used (**Figure 17**; signal at approximately 14 min). However, there was a small fraction of each peptides in the monomeric form (**Figure 17**; peak at approximately 16 min). As a control, the p53Tet(3Ala) peptide which is p53Tet mutant containing three alanine substitutions that exists only as a monomer was evaluate. This peptide gave a single signal at approximately 16 min.

Next, the secondary structure content of the peptides were determined using CD spectroscopy **(Figure 18)**. Although the six curves were very similar **(Figure 18)**, analysis of the secondary structure content indicated that the tree shrew p53Tet had 16.9% (64.2%) and the opossum had 14.7% (62.0%) more helical structure than the human p53Tet (47.3%) under the experimental conditions **(Table 5)**. These differences seen with the tree shrew and opossum are surprising since the tree shrew sequence shares 88.6% sequence identity and 94.3% sequence homology to the human sequence, whereas the opossum shares 71.4% sequence identity and 97.1% sequence homology **(Figure 16)**.

Table 4. Mass spectral analysis of synthetic peptides

No.	Peptides	Calculated ($M+H^+$)	Observed
1	Human	4190.71	4190.50
2	Tree shrew	4231.83	4233.01
3	Guinea pig	4245.81	4245.64
4	Chinese hamster	4100.67	4100.67
5	Sheep	4220.81	4220.53
6	Opossum	4305.87	4305.88
7	Human (Q354M)	4193.78	4193.72
8	Tree shrew (M354Q)	4228.76	4228.76

The MH^+ (average) values were calculated using the protein prospector website at UCSF. The observed MH^+ molecular weights of the peptides were determined using MALDI-TOF MS (linear, positive mode).

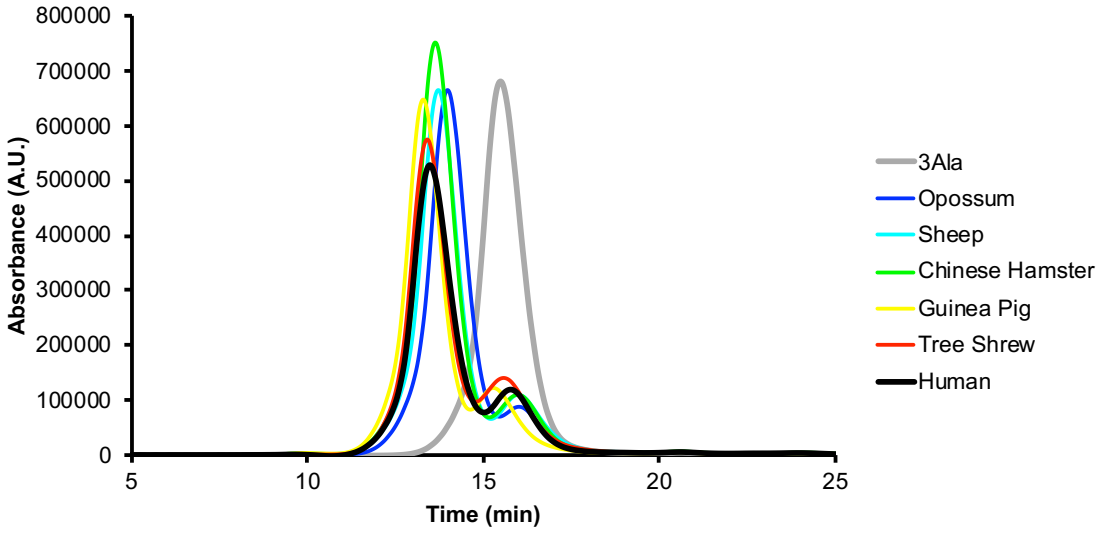

Figure 17. Gel filtration chromatography of mammalian p53Tet

The oligomeric states of the mammalian p53Tet and p53Tet(3Ala) (monomer mutant) were determined by gel filtration chromatography. The more predominant signals that elute at approximately 14 min correspond to the tetrameric forms of the peptide whereas the less predominant signals that elute at approximately 16 minutes correspond to the monomeric form of the peptide. The UV absorbance was monitored at 214 nm. The chromatograms are shown in different colors as indicated above the curves: human (black), tree shrew (red), guinea pig (yellow), chinese hamster (green), sheep (aqua), opossum (blue) and p53Tet(3Ala) (grey).

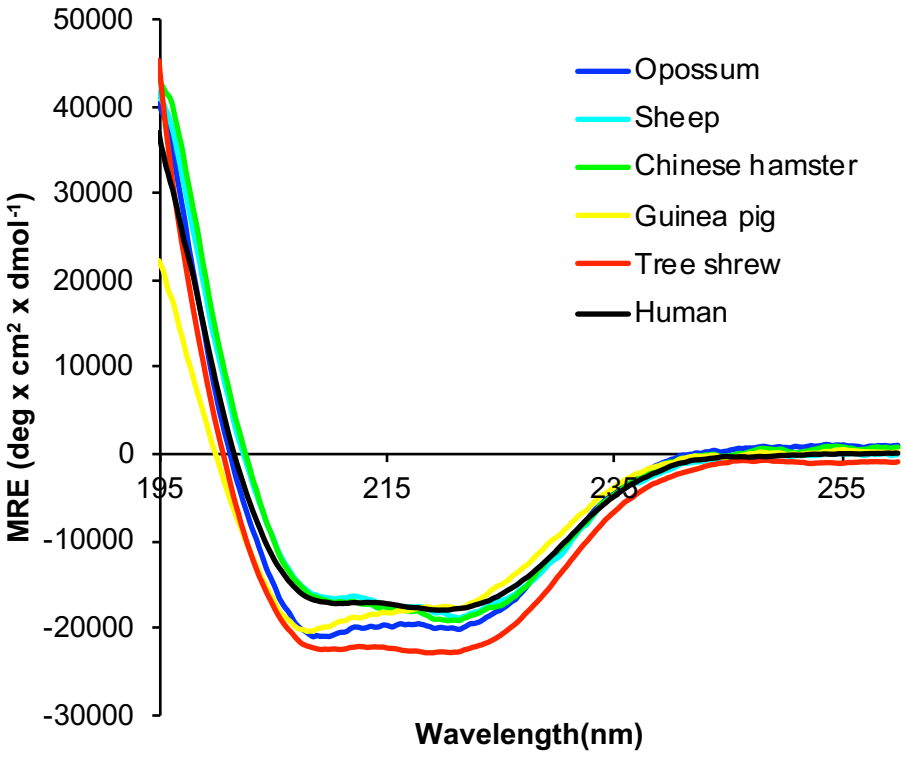

Figure 18. CD spectra of mammalian p53Tet

Comparison of the CD spectra for the different mammalian p53Tet at 4℃. The spectra were recorded between 195 and 260 nm and were used to determine he relative secondary structure elements of the mammalian p53Tet. The spectra are shown in different colors as indicated above the curves: human (black), tree shrew (red), guinea pig (yellow), chinese hamster (green), sheep (aqua) and opossum (blue).

Table 5. Secondary structural elements present in peptides from CD analysis

Peptide	helix (%)	beta (%)	turn (%)	random (%)
calc.	62.9	22.9	2.9	11.4
Human	47.3	34.4	5.6	12.7
Tree shrew	64.2	23.7	0.0	12.1
Guinea pig	47.9	23.8	0.0	28.3
Chinese hamster	50.5	33.8	13.5	2.2
Sheep	47.0	38.8	8.8	5.3
Opossum	62.0	12.7	14.7	10.7

calc.: The contents were calculated based on the structure.

3.4.3. Structural stability of the six mammalian p53Tet

Given the differences in helical content with the tree shrew and opossum despite their high sequence similarity with human p53 TD, the thermostability of the six p53Tet were determined using CD spectrometry. In these experiments, the ellipticity at 222 nm was monitored between 4℃ and 96℃ to generate thermal denaturation curves **(Figure 19)**, which were then used to calculate the T_m, ΔT_m (relative to human p53Tet) and $\Delta G^{37℃}$ of each peptide **(Table 6)**. As is evident from comparing the curve of the human p53Tet to those of the opossum and tree shrew **(Figure 19)**, the tree shrew and opossum p53Tets are considerably more stable than the human p53Tet. In the case of the tree shrew p53Tet, the calculated T_m was 77.1℃ and the $\Delta G^{37℃}$ was 36.4 kcal/mol and for the human p53Tet the T_m was calculated to be 67.8℃ and the $\Delta G^{37℃}$ was 32.4 kcal/mol **(Table 6)**. Thus, the T_m for the tree shrew p53Tet is 9.3℃ higher than for the human p53Tet and there is an increase in the $\Delta\Delta G^{37℃}$ of 4 kcal/mol. Likewise, the calculated T_m for the opossum p53Tet was 78.0℃ and the $\Delta G^{37℃}$ was 36.6 kcal/mol and the T_m for the opossum p53Tet is 10.2℃ higher than for the human p53Tet and there is an increase in the $\Delta\Delta G^{37℃}$ of 4.2 kcal/mol. Taken together, these results demonstrate that the tree shrew and opossum p53Tets are considerably more thermostable than human p53Tet and this could be consistent with these two sequences having higher helical content. However, we also observed significant increases in the thermal stability of the p53Tet from sheep (7.3℃ higher than human p53Tet and a $\Delta\Delta G^{37℃}$ of 1.6 kcal/mol) and guinea pig (6.9℃ higher than human p53Tet and a $\Delta\Delta G^{37℃}$ of 3.0 kcal/mol) despite the fact that their helical content is very similar to that of human p53Tet. Taken together, these results suggest that the full-length p53 from several mammalian species have enhanced thermal stability relative to human p53 despite sharing high sequence identity and this could lead to enhanced transcriptional activity at certain p53-responsive genes in these species.

3.4.4. Modeling of Tree shrew p53 tetrameric structure

Given their difference in helical content and thermostability despite sharing almost 89% sequence identity, I tried to try an explain the differences between tree shrew p53 TD and human p53 TD by generating models of the tree shrew p53 TD to compare with the known structures of the human p53 TD. For this purpose, two models of the tree shrew p53 TD were generated, one model using the MODELLER 9.22 software and a second model using the SWISS-MODEL tool. In both cases, the models of the tree shrew

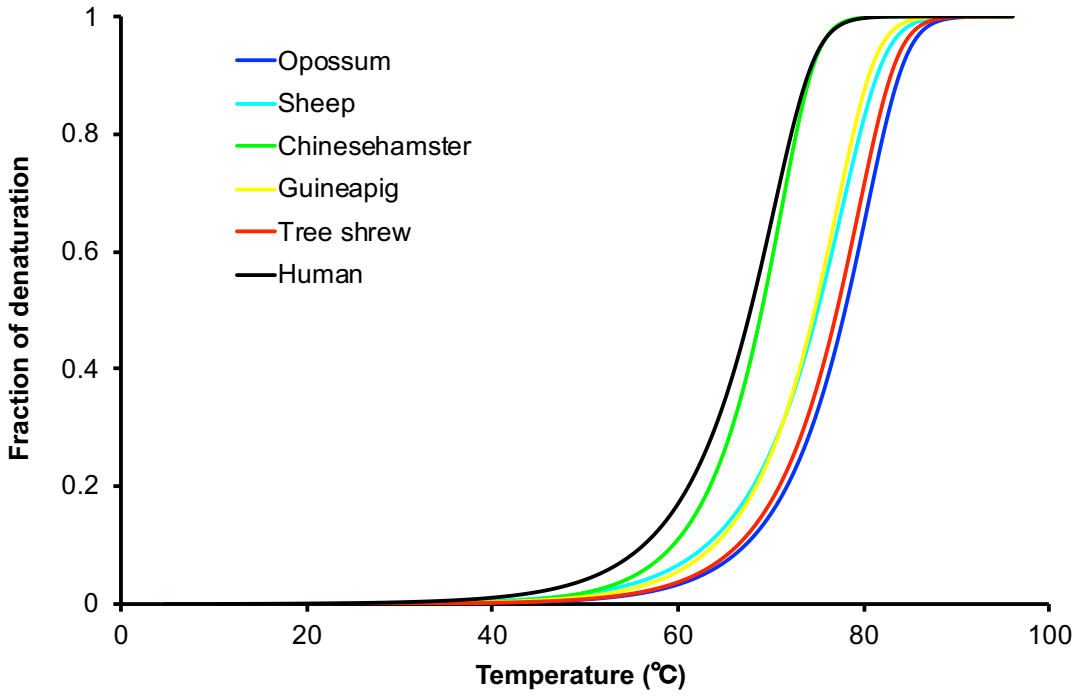

Figure 19. Thermal denaturation curves of the six different mammalian p53Tets

The signal from the six mammalians p53Tets were monitored by CD spectrometry at 222 nm between 4℃ and 96℃. The fraction of denaturation at each temperature was plotted against the temperature to generate the denaturation curves. The value at 222 nm at 4℃ is taken as 0% denaturation. The denaturation curves are shown in different colors as indicated above the curves: human (black), tree shrew (red), guinea pig (yellow), chinese hamster (green), sheep (aqua) and opossum (blue).

Table 6. Thermodynamic parameters of mammalian p53Tet from CD analysis

Peptide	T_m (℃)	ΔT_m (℃)	$\Delta G_u^{37℃}$ (kcal/mol)	$\Delta\Delta G_u^{37℃}$ (kcal/mol)
Human	67.8 ± 0.2	-	32.4	-
Tree shrew	77.1 ± 0.2	9.3	36.4	4.0
Guinea pig	74.7 ± 0.5	6.9	35.4	3.0
Chinese hamster	69.0 ± 0.2	1.2	35.4	3.0
Sheep	75.1 ± 0.4	7.3	34.0	1.6
Opossum	78.0 ± 0.2	10.2	36.6	4.2

T_m and $\Delta G_u^{37℃}$ were calculated by denaturation analysis. The standard errors for fitting are indicated. $\Delta\Delta G_u^{37℃}$ = ($\Delta G_u^{37℃}$ of each species) – ($\Delta G_u^{37℃}$ of human)

p53 TD structure were overall very similar to the structure of the human p53 TD **(Figure 20)** as well as to each other **(Figure 21)**. This similarity is not surprising given that the high sequence identity (88.6%) and even higher sequence homology (94.3%) between the peptides. Given the similarity of the two models, I focused my efforts on the model generated by SWISS-MODEL for more thorough analysis **(Figure 20A)**. Since only four of 35 residues between the two sequences are not identical and only two are not homologous, I focused on the two non-homologous substitutions. These substitutions occur at residue 325 (G to E) and residue 354 (Q to M). From the crystal structure of the human p53 TD, it is clear that substituting a Gly residue in p53 TD to Glu in Tree shrew p53 TD should not significantly alter the stability. This amino acid is located in a disordered region outside of the β-strand. Thus, it is not considered essential for either the formation of human p53 TD or its stability. In contrast, my analysis indicated that replacing Q354 in human p53Tet with the more hydrophobic Met in tree shrew p53Tet has the potential to dramatically stabilize the tetrameric structure. In the model, the side chain of M354 in tree shrew p53 TD is located near the end of the helix and would be in position to form van der Waals contacts with the side chains of L350 and M354 on an adjacent monomer as well as with its own L350 **(Figure 22)**. Together, these residues would form two additional hydrophobic clusters at the tetramer interface and the two clusters would stabilize the 4-helix bundle in the tetrameric structure of the Tree shrew p53 protein.

3.4.5. Stabilization of Tree shrew p53 tetrameric structure by Met

To test the role of position 354 in the stabilization of the p53 tetramerization domains, two variant peptides were prepared. In these peptides, the amino acid in position 354 were swapped between the human and tree shrew peptides. Thus, Q354 in human p53Tet was replaced by a Met residue (human p53Tet(Q354M)) and M354 in tree shrew p53Tet was replaced by a Gln residue (tree shrew p53Tet(M354Q)). The two peptides were synthesized, and their oligomeric state, secondary structure and thermostability evaluated. As with the wild-type sequences, the variant peptides were determined to be predominantly tetrameric by gel filtration chromatography with a small percentage of the monomer **(Figure 23A, B)**. Further analysis by CD spectroscopy provided some interesting results **(Figure 23C, D, Figure 24, and Table 7)**. As predicted, the calculated T_m for human p53Tet(Q354M) variant increased by 6.7°C to 74.5°C and the $\Delta G^{37°C}$

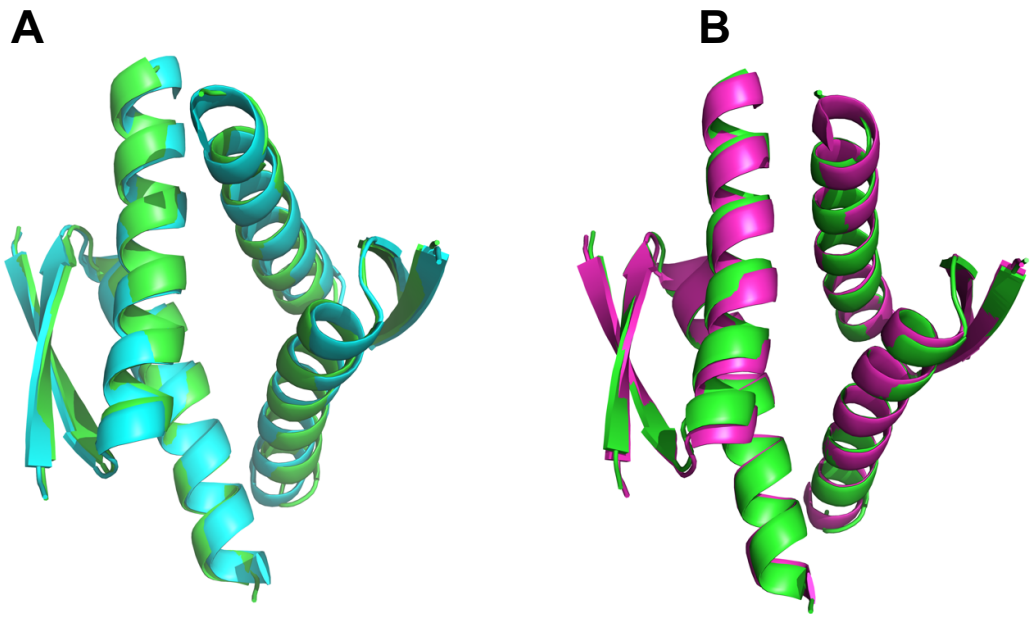

Figure 20. Models of tree shrew p53 TD and comparison with human p53 TD

Models of the tree shrew p53 TD were generated using either the SWISS-MODEL (**A**; aqua) or MODELLER 9.22 (**B**; magenta) software. The structures are shown as cartoons and superimposed to align to the backbone atoms of human p53 TD (**A-B**; green). The human p53 TD cartoon was generated from PDB entry 1AIE.

Figure 21. Models of tree shrew p53 TD structure

Models of the tree shrew p53 TD were generated using either the SWISS-MODEL (aqua structure) or MODELLER 9.22 (magenta structure) software. The resulting structures are represented as cartoons and superimposed to align the backbone atoms.

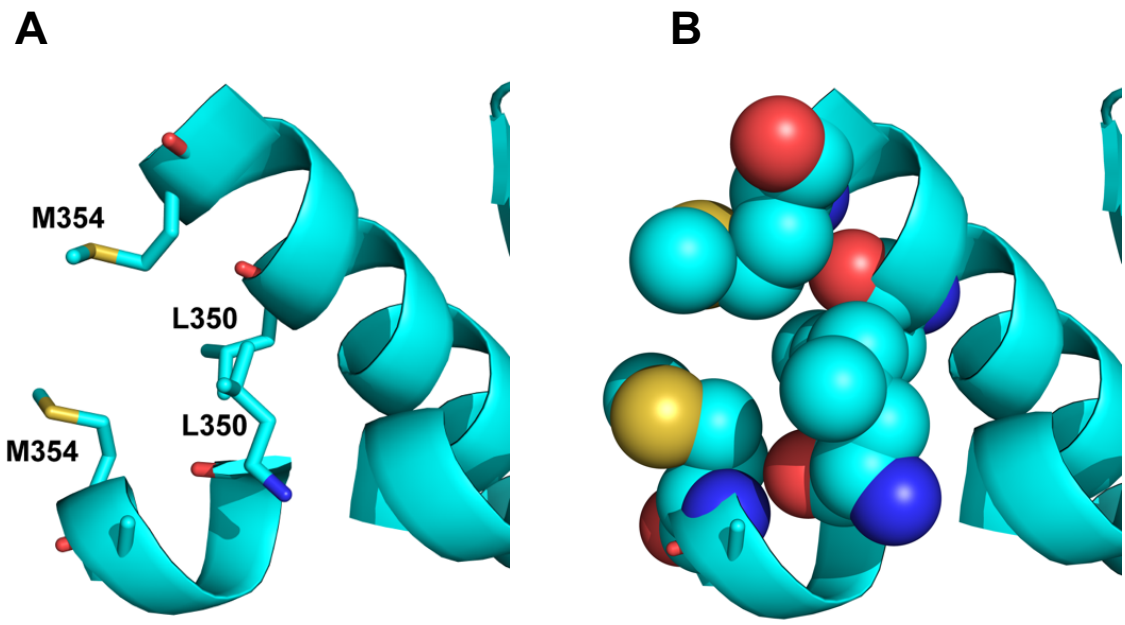

Figure 22. M354 and L350 form a hydrophobic cluster at the tetramer interface in the structure of tree shrew p53 TD

In the SWISS-MODEL generated structure of tree shrew p53 TD, the side chains of Met354 and Leu350 from two monomers are in close proximity at the tetramer interface. The structure of tree shrew p53 TD is zoomed in the region including M354 and L350. The sidechains of the two amino acids are highlighted in stick form (**A**) or as spheres (**B**). The main chains are shown in cartoon form and the colors for the selected atoms are aqua for carbon, red for oxygen, blue for nitrogen and yellow for sulfur.

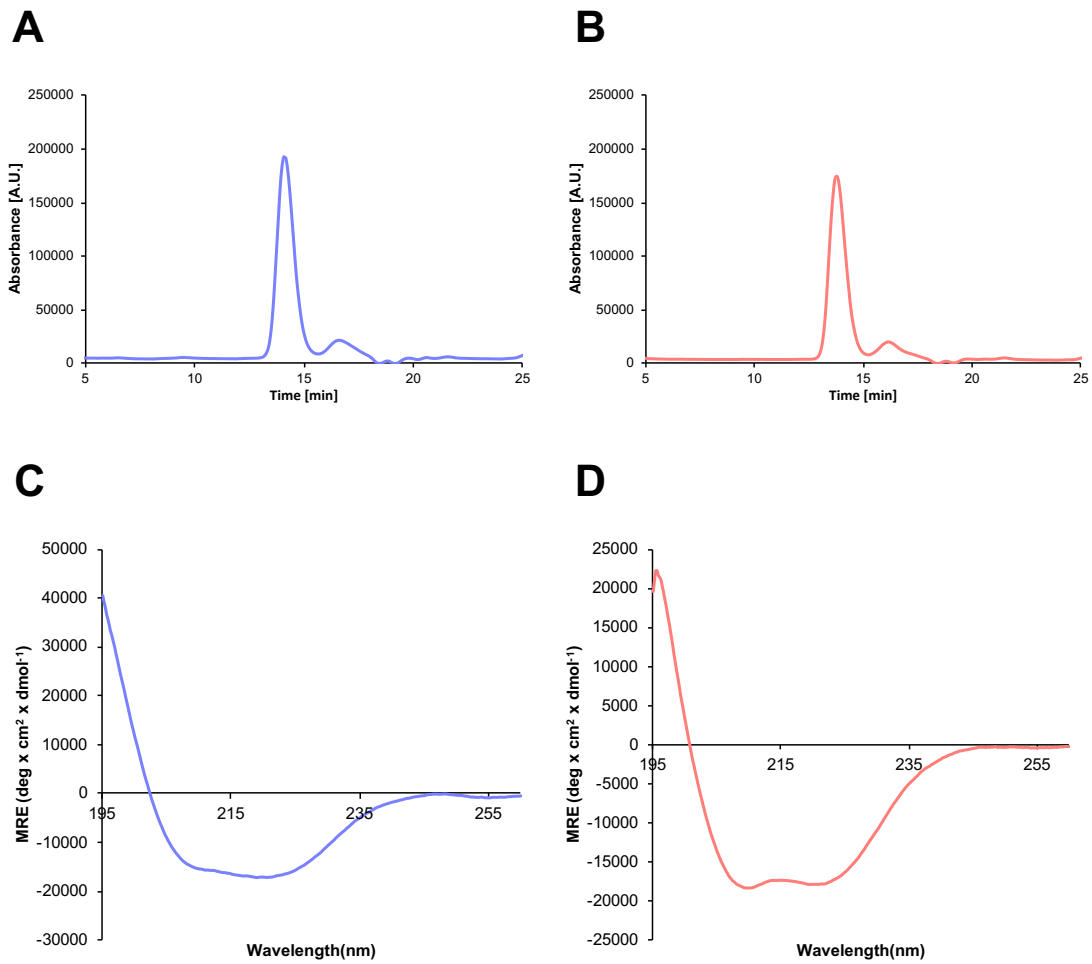

Figure 23. Oligomeric state and secondary structure of human p53Tet(Q354M) and tree shrew p53Tet(M354Q) variants

The oligomeric states of human p53Tet(Q354M) (**A**) and tree shrew p53Tet(M354Q) (**B**) were measured by gel filtration chromatography. The larger signals that elute at roughly 14 min correspond to the tetrameric form of the peptides whereas the smaller signals that elute at approximately 16 minutes correspond to the monomeric form. The UV absorbance was monitored at 214 nm.; The secondary structure of human p53Tet(Q354M) (**C**) and tree shrew p53Tet(M354Q) (**D**) were measured by CD spectroscopy at 4°C.

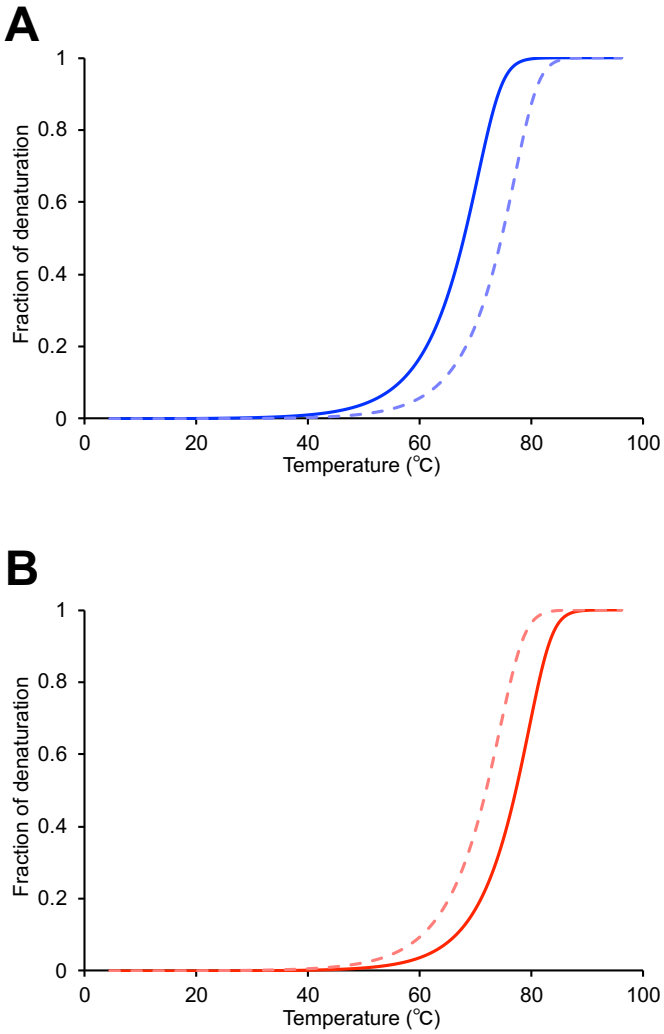

Figure 24. Thermal denaturation curves of human p53Tet(Q354M) and tree shrew p53Tet(M354Q) variants

A) The signal from human p53Tet (blue) and human p53Tet(Q354M) (blue dash) were monitored by CD spectrometry at 222 nm at temperatures ranging from 4°C to 96°C; **B)** The signal from tree shrew p53Tet (red) and tree shrew p53Tet(M354Q) (red dash) were monitored by CD spectrometry at 222 nm at temperatures ranging from 4°C to 96°C. The fraction of denaturation at each temperature was plotted against the temperature to generate the curves. The value at 222 nm at 4°C is taken as 0% denaturation.

Table 7. Thermodynamic parameters of variant peptides from CD analysis

Peptide	T_m (°C)	ΔT_m (°C)	$\Delta G_u^{37°C}$ (kcal/mol)	$\Delta\Delta G_u^{37°C}$ (kcal/mol)
Human	67.8 ± 0.2	-	32.4	-
Human (Q354M)	74.5 ± 0.2	6.7	35.2	2.8
Tree shrew	77.1 ± 0.2	-	36.4	-
Tree shrew (M354Q)	71.8 ± 0.2	-5.3	33.7	-2.7

T_m and $\Delta G_u^{37°C}$ were calculated by denaturation analysis. The standard errors of fittings were indicated. $\Delta\Delta G_u^{37°C}$ = ($\Delta G_u^{37°C}$ of variant) – ($\Delta G_u^{37°C}$ of WT)

increased by 2.8 kcal/mol to 35.2 kcal/mol and the calculated T_m for the tree shrew p53Tet(Q354M) variant decreased by 5.3℃ to 71.8℃ and the $\Delta G^{37℃}$ decreased by 2.7 kcal/mol to 33.7 kcal/mol **(Figure 24 and Table 7)**. However, the two variants both displayed helical content that is more similar to what is observed for the human p53Tet **(Table 8)**. Taken together, these results suggest that the Q354M substitution plays a major role in the enhanced stability, but that the homologous substitutions at position 341 (Phe to Leu) and position 344 (Ile to Leu) must also play a minor role in stabilizing tree shrew p53 TD.

Table 8. Secondary structure present in variant peptides from CD analysis

Peptide	helix (%)	beta (%)	turn (%)	random (%)
calc.	62.9	22.9	2.9	11.4
Human (Q354M)	43.6	39.6	8.2	8.7
Tree shrew (M354Q)	44.3	31.8	0.0	24.0

calc.: The contents were calculated based on the structure.

3.5. Discussion

In this project, I examined the secondary structure and thermal stability of p53Tet from five different mammalian species and compared them to the human p53Tet. These 35 residues peptides were prepared by standard solid-phase synthesis methodology and the five sequences chosen all share high sequence identity (> 70%) with the corresponding sequence from humans. Secondary structure analysis by CD spectroscopy demonstrated that the five p53Tet had similar secondary structure content to the human p53Tet with the exception that the peptides from the tree shrew and opossum presently slightly higher helical content by 16.9% and 12.7%, respectively. In addition, it was revealed that the thermostability of the tetrameric structure was higher than human for the guinea pig (6.9ºC), sheep (7.3ºC), opossum (10.2ºC) and tree shrew (9.3ºC). These differences in secondary structure content and thermal stability were in general surprising for all the p53Tet, but they were particularly surprising for the tree shew p53Tet given that its sequence is so highly similar to the human p53Tet.

Numerous studies have examined the importance of the tetramerization domain present in all members of the p53-family proteins and they have clearly established that this domain is critical to several of their biological functions. These studies have demonstrated that the stability of the tetramerization domain plays an important role in transcriptional activity as well as a key role in the ability of a given protein to form hetero-tetramers with other p53-family members. By using a combination of biophysical and modeling studies, I was able to demonstrate that the tree shrew p53Tet is considerably more thermostable than the corresponding peptide from human p53. This difference occurs despite sharing 88.6% sequence identity and 94.3% sequence homology. In addition, I was able to demonstrate that the substitution of the Met for Gln at position 354 helps impart this significant thermostability to the tree shrew p53Tet in comparison to human p53Tet. Based on modeling studies, the enhanced stability appears to results through the formation of a hydrophobic cluster involving the side chains of M354 and L350 from adjacent monomers, which serves to form additional interactions to stabilize the tetramer. This enhanced stability suggests that the tree shrew p53 protein may have enhanced transcriptional activity at select p53-dependent genes and this enhanced activity could help to explain some of the unusual characteristics of this unique animal such as its resistance to alcohol-induced DNA damage.

The tree shrew p53 TD and the human p53 TD sequences differ by only four

substitutions: G325E, F341L, L344I, and Q354M in human and tree shrew, respectively. Position 325 is located before the start of the β-strand and is considered to be outside of the folded region of the domain. This suggests that the G325E substitution would not play a significant role in enhancing the stability of the domain. The remaining three substitutions occur in the α-helical segment between residues 335 and 356 and are more likely to play a role in the determining the stability difference between the two domains as interactions between the helices of the four monomers are crucial to forming the tetramer. Positions 341 and 344 are located in the center of the helix in human p53 and they clearly play an important role in stabilizing the tetrameric structure **(Figure 25A)**. This is supported by the fact that several mutations have been reported at these positions and in most cases the mutations significantly decrease the stability of the tetrameric form of the protein. For example, either a F341C mutation or a L344R mutation results in a human p53 protein that can adopt a dimeric structure, but fails to form the tetramer [15]. More dramatically, a L344P substitution in the human p53 sequence completely disrupts the helix formation, which prevents formation of the dimer and tetramer [15]. However, the F341L and the L344I substitutions present in the tree shrew p53 TD are homologous replacements and the model of the tree shrew p53 TD suggests that L341 and I344 help stabilize the tetrameric structure of the tree shrew p53 protein **(Figure 25B)**. However, these substitutions may be playing a more significant role in stabilizing the binding interface of the tree shrew tetramerization as the Q354M mutant of the human p53Tet is still slightly less thermal stable than the tree shrew p53Tet.

In contrast to F341 and L344, Q354 is more or less the final residue present in the helix in human p53 TD and it does not appear to play a significant role in stabilizing the tetramer binding interface. This is supported by several reported mutations at this position in human p53. For example, Q354E, Q354K, and Q354R mutants of human p53Tet show similar stability to the wild-type sequence [15]. The side chain of Gln354 is exposed to solvent and mutations to other polar side chain amino acids would not be expected to destabilize the tetrameric structure to any significant degree. However, insertion of the more hydrophobic Met354 appears to create additional contacts with Leu350 and Met354 on an adjacent monomer in my model of the tree shrew p53 TD **(Figure 22)**. These contacts between the methyl groups from Leu and Met residues from adjacent monomers would form van der Waals contact that could stabilize the tetramer by extending the binding interface completely along the four helices. This extended

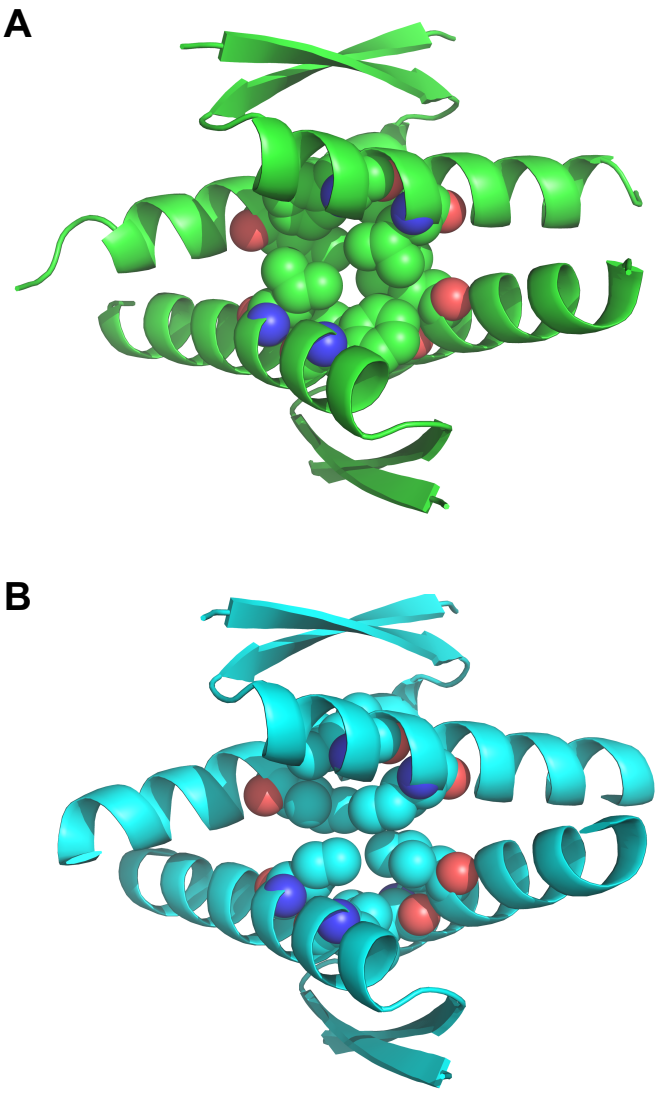

Figure 25. Residues at positions 341 and 344 make important contribution to interactions at the tetramer interface of p53 TD

Cartoon representation of the structure of human p53 TD (**A**; green) and tree shrew p53 TD (**B**; aqua) highlighting the contribution of residues at position 341 and 344 to interactions at the tetramer interface. In the p53 structure (**A**), the residues are F341 and L344, whereas in the tree shrew p53 TD structure (**B**) the residues are L341 and I344. The side chains of residues at position 341 and 344 are drawn as spheres to highlight their contributions. PDB entry AIE1 was used to generate the structure of human p53 TD (**A**) and the model generated by the SWISS-MODEL software was used to generate the structure of tree shrew p53 TD (**B**). The main chains are shown in ribbon form and the colors for the carbon atoms are green (**A**) or aqua (**B**). For the other atoms, the color is red for oxygen and blue for nitrogen in both structures.

interface would be expected to enhance the thermostability and my results support the model.

The increase in the thermostability observed for the tree shrew p53Tet could play an important role in regulating a number of p53-dependent genes *in vivo* and this may help explain several of this animal's unique characteristics. This would of course depend on which p53-related activities were altered. For example, it is known that the copy number of interleukin 6 (IL-6) in tree shrew is elevated [84] and that IL-6 negatively regulates p53 expression [85,86]. Therefore, a more stable p53 may counteract high levels of IL-6. Likewise, high intake of alcohol would be expected to lead to an increase in acetaldehyde induced DNA damage in the tree shrew and enhanced rates of certain cancers. However, enhanced transcriptional activity through a more stable p53 would help to maintain the genomic integrity of the tree shrew despite enhanced acetaldehyde levels. However, more detailed *in vivo* studies are needed to gain insights into how p53 activity in tree shrew is altered by this increased thermostability as well as how this enhanced stability affects key genes regulated by p53. Given that the tree shrew is becoming an important alternative animal model for several human diseases [87–90], it will be crucial to understand the role that this enhanced stability of the p53 protein in tree shrew plays in regulating its functions.

4. Evolution of p53 Tetramerization Domain in Vertebrates

4.1. Abstract

Tumor suppressor protein p53 express from Lamprey, the early vertebrate, to mammals. The phylogenetic analysis showed that p53 tetramerization domains of vertebrates a have longer evolution distance than tetramerization domains of p63 and p73 which form tetramer similar to p53, indicating p53 have positively evolved. Moreover, p53 tetramerization domains more diversified than their DNA binding domains. To reveal the evolution process of p53 TD, I selected 19 species from jaw-less fish, cartilaginous fish, ray-finned fish, lobe-finned fish, amphibia, reptile, bird, and mammal. Although tetramerization domains have a lot of amino acid replacements such as Lamprey, it was revealed that they formed tetramer in all species. I performed structural stability analysis of tetramerization domains and transcriptional activity of chimeric p53 of all species. Lamprey p53 has low structural stability and low activity, and ray-finned fish such as Zebrafish have high activity by stabilization effect via second helix at C-term region. On the other hand, the species in evolution process from Coelacanth to Human gain high stability with just first helix. DNA binding domain directly interact with DNA, meanwhile, evolution of tetramerization domain is able to regulate the p53 activity indirectly, suggesting that tetramerization domain evolve more positively than DNA binding domain. p63 and p73 have mature sequences, because they are important equally for all vertebrates to regulate differentiation epithelial stem-cell and neural stem-cell, respectively. However, p53 which maintains genomic integrity and not a lethal gene, plays a role in evolution process of vertebrates.

4.2. Introduction

The tumor suppressor protein p53 maintains genomic integrity in response to various cellular stresses. Genotoxic stresses such as UV and radiation induce DNA damage which is a cause of tumorigenesis, however, p53 induces cell cycle arrest or apoptosis in damaged cells and prevents cellular tumorigenesis. The tetramerization via the tetramerization domain (TD) is essential for functional expression of p53 protein, and p53 binds to response elements of target genes via the DNA-binding domain and regulates transcription of the genes. The functions of p53 are uniquely defined by the stability of the tetrameric structure. A monomer p53 TD has a β-strand and an α-helix in human p53 tetramer form which stabilized by hydrophobic interactions and salt bridges as a tetramer. Mutations in TD reported in human tumors almost all destabilize the tetrameric structure. Moreover, there are monomer mutants that don't form a tetramer at all and dimer mutants which just form dimers caused by a point mutation. Such a mutant p53 can hardly express the transcriptional activity by the p53 protein. Therefore, the structural stability of p53 tetramer is extremely important for maintaining p53 functions.

The p53 also expresses vertebrates. The ancestral protein of p53/p63/p73 protein family has expressed in sea anemones, invertebrate. The p53 firstly has expressed in lamprey, the early vertebrate, and expresses from fishes to mammals and birds. It is known that animals develop cancer in mammals as well as it is reported that animals living in water such as sharks develop cancer, thus the activity of p53 is important to suppress cellular tumorigenesis as well as human. Also, elephants have a larger copy number of p53 than humans, suggested Peto's paradox that animals with a large body are not liable to cancer (small animals such as mouse develops cancer as well as large animal). In except human, crystal structures of zebrafish p53 TD was reported for a second helix at C-terminal and a shorter first helix than human [72] **(Figure 26)**. However, the p53 TD structures of other species are unknown, and the effect of the second helix in zebrafish p53 TD on the stability and activity as well as the significance of existence are not clear.

For this study, I selected vertebrates of a total of 14 different species from all classes, jaw-less fish, cartilaginous fish, ray-finned fish, lobe-finned fish, amphibia, reptile, mammal, and bird **(Figure 27)**. A lamprey, classified as jawless fish, is a primitive vertebrate that does not have a jaw and paired fins. For cartilaginous fish, I chose ghost shark (classified as Holocephali) and Japanese bullhead shark (classified as Elasmobranchii). Holocephali has only one pair of gill slits, but Elasmobranchii has five

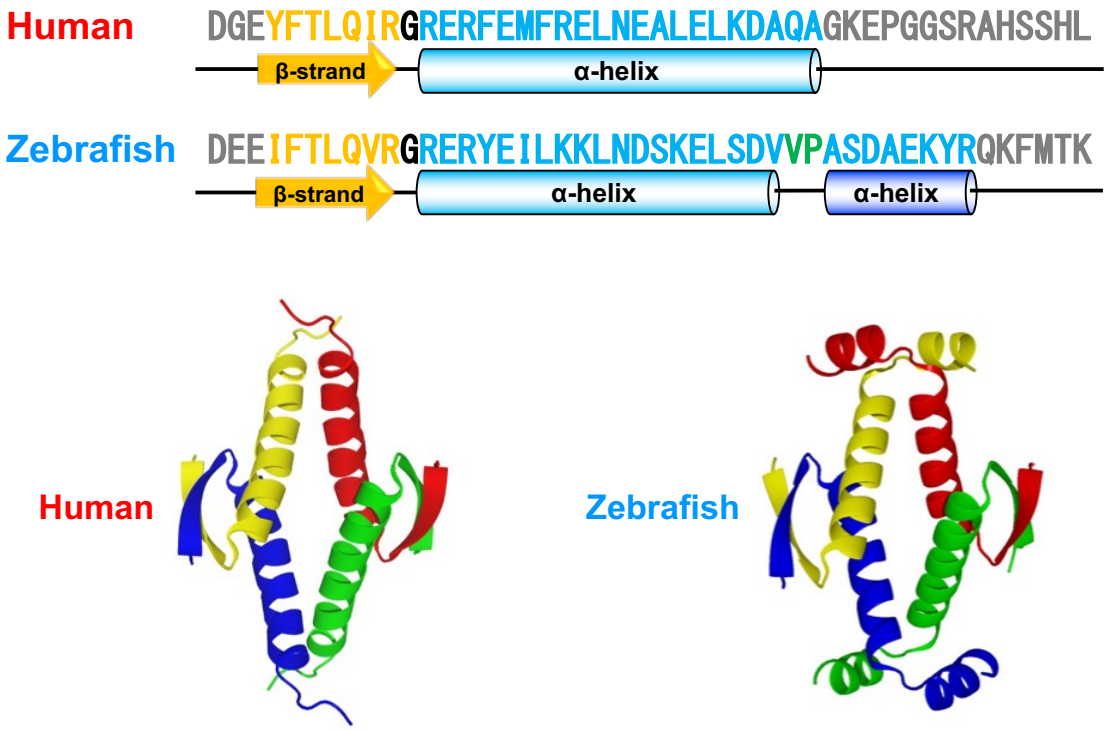

Figure 26. Structures of Human and Zebrafish p53 tetramerization domain

Zebrafish p53 TD has a second helix at C-terminus. PDB ID: Human, 3SAK; Zebrafish, 4D1M

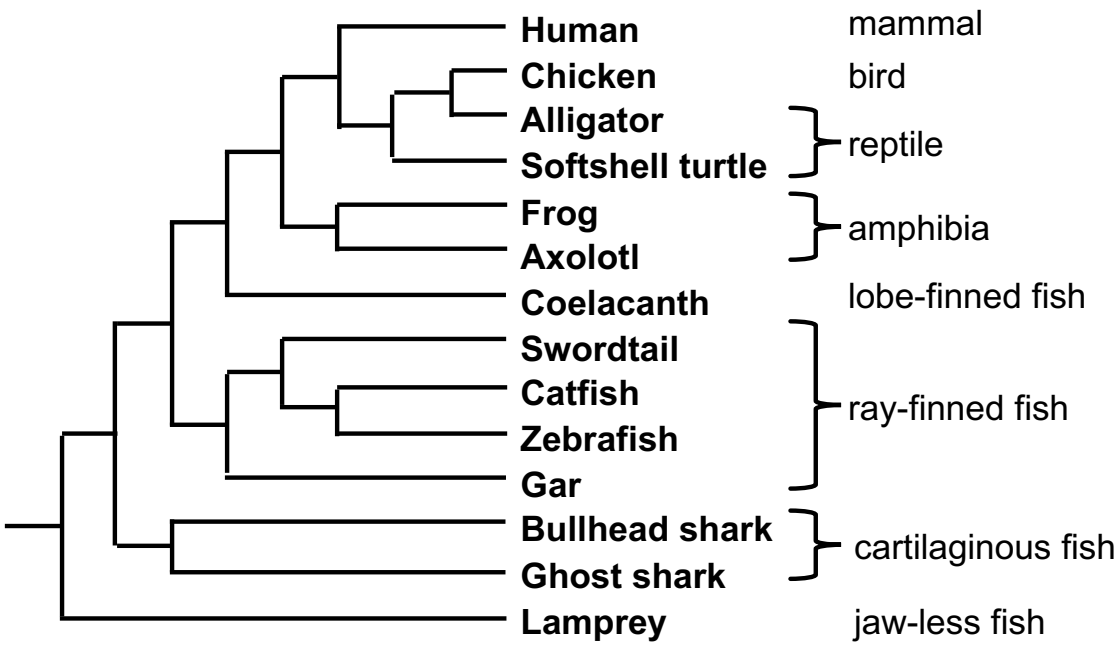

Figure 27. Classification of 14 species selected for this study

14 mammals were selected for this study.

to seven pairs. For ray-finned fish, I chose spotted gar (classified as Garpikes), zebrafish (classified as Carp), catfish (classified as Catfishes), and swordtail (classified as Cyprinodontiformes). In the ray-finned fish, it is thought that there was a whole-genome duplication in the fish, which diverged more than the Garpikes. A zebrafish and catfish are also classified as Ostariophysi and prosper mainly in freshwater areas. A swordtail was classified as Acanthopterygii and prospers mainly in the seawater area. It is thought that the coelacanth of the lobe-finned fish is an ancestor of the Tetrapoda and that its lobefins became the limbs. For amphibia, I selected frog (African clawed frog; classified as Anura) and axolotl (classified in Caudata). African clawed frogs are widely used as laboratory animals and are a tetraploid creature by the crossing of its ancestors. An axolotl usually becomes neoteny when leaving the larval form. For reptilian, I chose alligator (classified as crocodile) and softshell turtle (classified as Testudinata). A softshell turtle is fitted for underwater life. An alligator is a group of animals occupying the top of the ecological pyramid in the ecosystem of freshwater. For birds, I chose chicken, as it is the only species that p53 was reported in. For mammalian, I chose a human.

The tetrameric structures of p53 are different between human and zebrafish, suggesting that the p53 tetramerization domain has evolved. For vertebrates which have changed the live environment from water to land, it is interesting to understand the evolution of p53, which is important for damage response. Speaking of study about protein evolution, generally, researchers perform phylogenetic analysis, however, in this study, I comprehensively analyzed the structure, thermostability of the structure, and the activity not only phylogenetic analysis for whole vertebrates. Interestingly, I determined that the second helix of zebrafish stabilized the tetrameric structure by the analysis using p53 tetramerization domain peptides (p53Tet) and increased the transcriptional activity of chimeric p53. Additionally, I determined that coelacanth p53 TD didn't form a second helix by X-ray crystallography. Moreover, I expected to have or not having second helices for the other species by using the results of thermostability and transcriptional activity. It was revealed that the structure and the stability of the p53 tetramerization domain had changed, and p53 functions had changed by these results, suggesting that each species has p53 adopted in each live environment. In future studies, crystallography of the lamprey p53 tetrameric structure will be performed, and also the significance of the second helix is analyzing from hetero oligomer formation with p63 and p73.

4.3. Experimental procedures

4.3.1. Peptide synthesis

The peptides corresponding to the Human p53 tetramerization domain (Human p53Tet; residues 324-358 and 324-369 of Human p53), Chicken p53 tetramerization domain (residues 307-341 and 307-352 of Chicken p53), Alligator p53 tetramerization domain (residues 310-344 and 310-355 of Alligator p53), Softshell turtle p53 tetramerization domain (residues 319-353 and 319-364 of Softshell turtle p53), Frog p53 tetramerization domain (residues 297-331 and 297-342 of Frog p53), Axolotl p53 tetramerization domain (residues 317-351 and 317-362 of Axolotl p53), Coelacanth p53 tetramerization domain (residues 332-366 and 332-376 of Coelacanth p53), Swordtail p53 tetramerization domain (residues 287-321 and 287-332 of Swordtail p53), Catfish p53 tetramerization domain (residues 302-336 and 302-347 of Catfish p53), Zebrafish p53 tetramerization domain (residues 300-334 and 300-345 of Zebrafish p53), Gar p53 tetramerization domain (residues 316-350 and 316-361 of Gar p53), Japanese bullhead shark p53 tetramerization domain (residues ?-? and ?-? of Japanese bullhead shark p53), Ghost shark p53 tetramerization domain (residues 313-347 and 313-358 of Ghost shark p53), and Lamprey p53 tetramerization domain (residues 354-388 and 354-399 of Lamprey p53),were synthesized as previously described [80]. The sequence of peptides is shown in **Table 9**. Peptide concentrations were determined using an extinction coefficient, ε_{280} = 1490 M^{-1} cm^{-1}, which corresponds to a single tyrosine.

4.3.2. Circular dichroism (CD) spectrometry

Circular Dichroism (CD) spectra were recorded at 4℃ using a J-805s spectropolarimeter (JASCO) in 50 mM phosphate buffer (pH7.5) with 100 mM NaCl at a peptide concentration of 10 μM in a 1 mm quartz cell. Continuous scans were recorded over the region between 195-260 nm at a scan rate of 50 nm/min and a bandwidth of 0.2 nm. The resulting signals from six consecutive CD scans were averaged and normalized for peptide concentration and the number of residues.

4.3.3. Denaturing analysis by CD spectrometry

Peptide denaturation analyses were performed by increasing the temperature from 4℃ to 96℃ at a constant rate of 1.0℃/min after measuring CD spectrum. To monitor the changes in the α-helical content of the peptides, the ellipticity at 222 nm was

Table 9. Sequences of vertebrate p53 tetramerization domain

Common Name	p53 Sequences
Human	DGEYFTLQIRGRERFEMFRELNEALELKDAQAGKEPGGSRAHSSHL
Tree shrew	DEEYFTLQIRGRERFEMLREINEALELKDAMAGKESAGSRAHSSHL
Guinea pig	DAEYFTLKIRGRKNFEILREINEALEFKDAQTEKEPGESRPHSSYP
Chinese hamster	DGEYFTLKIRGHERFKMFQELNEALELKDAQASKGSEDNGAHSSYL
Sheep	DGEYFTLQIRGRKRFEMFRELNEALELMDAQAGREPGESRAHSSHL
Opossum	EGEYFTLQIRGRQRYELLREINEALELKEAHSRKEPEGSRPHRSQL
Chicken	DNEIFYLQVRGRRRYEMLKEINEALQLAEGGSAPRPSKGRRVKVEG
Alligator	STEIFTLQIRGHERYEMFKKLNEGLEALDGQEARAEDPGIRSPKPL
Softshell turtle	DKEVFCLEVHGRENYEMLKKINNALEVAAARPQGELETQRNPKAWL
Frog	DEEIFTLRIKGRSRYEMIKKLNDALELQESLDQQKVTIKCRKCRDE
Axolotl	EEETFTLQIHGRERYEMFKKLNEALELKDMIPQTDLEKIKQQKSQK
Coelacanth	EEELYSLQVRGRERYEMFKKLNNALELQDSVSAAETEKHKTKPSKN
Swordtail	DKEIYTLSIRGRNRYLWFKSLNDGLELMDKTGPKIKQEIPAPSSGK
Catfish	DDEIYTLQVRGKERYEFLKKINDGLELSDVVPPADQEKYRQKLLSK
Zebrafish	DEEIFTLQVRGRERYEILKKLNDSLELSDVVPASDAEKYRQKFMTK
Gar	EEEIFTLQVRGRERFEMLKKINESLELKDLVPVADLEKYRQKLHTR
Japanese bullhead shark	DDKVFTLQIRGRERYELMKKLNESLEIWDLIPSEVIEDYKLKHQVK
Ghost shark	DTEVFTLQVTGRERYETLKQINESLEVQELVPASVVQACRQQHKLR
Lamprey	KEELFLIPVRGRENYELLLHLKESLEMKQLVPQQAMETYRQQQLHQ

hydrophobic amino acids, orange; acidic, red; basic, blue; proline, green; others, black

Gly of turn, green; hydrophobic core, light blue; highly conserved region on second helix, orange

registered every 0.5℃ and the denaturation curves were normalized before analysis [14].

4.3.4. Gel filtration

The oligomeric states of the peptides were determined by gel filtration chromatography. For the analysis, 20 μl of peptide at 100 μM in 50 mM phosphate buffer pH 7.5 and 100 mM NaCl was injected onto a Superdex 75 (GE Healthcare) column. The peptides were eluted at room temperature using a flow rate of 0.1 ml/min with the same buffer and the peptides were monitored by UV detection at 214 nm.

4.3.5. Plasmid for transcriptional activity

p53RE-mCherry(NLS)-hCMV(2)-Venus-p53 plasmid constructed by Dr. Imagawa from our laboratory was used for transcriptional activity. Venus fusion p53 protein was expressed by hCMV(2) promotor, and tetramer formed p53 bound to p53 response element derived from *CDKN1A* (p21) and induced expression of mCherry(NLS) **(Figure 28)**. In this study, I used chimeric p53 which is TD of Human p53 protein replaced by TD of each species constructed by two primers.

4.3.6. Transcriptional activity analysis

H1299 (American Type Culture Collection) cells of 10% in ϕ10 cm dish 100% confluent were seeded in a ϕ35 mm plastic dish (Falcon). RPMI-1640 (SIGMA), 10% FBS (Thermo Fisher Scientific), and Penicillin-Streptomycin (Gibco) was used for normal culture. After 12 h, cells were washed by 1.5 ml PBS three times. 100 μl Opti-MEM (Thermo Fisher Scientific), 2.4 μg plasmid, and 6 μl Lipofectamine 2000 (Thermo Fisher Scientific) were mixed and incubated for 20 min at room temperature. 700 μl Opti-MEM was added to the mixture (transfection mixture). The transfection mixture was added to the cells dish and incubated for 1 h, at 37℃, 5% CO_2. After that, the transfection mixture was removed, and the cells were cultured in 1.5 ml the medium for the normal culture at 37℃, 5% CO_2. After 11 h, the cells were washed by 900 μl PBS three times and fixed by 900 μl 10% formalin neutral buffer solution (Wako) for 10 min at room temperature on a wave shaker. The formalin solution was removed, and the cells were incubated in 900 μl 0.2% Triton-X-100/PBS for 5 min at room temperature on the wave shaker and removed. The cells were washed by 900 μl PBS three times and incubated in 1 ml 0.1% DAPI/PBS for 15 min at room temperature on the wave shaker to stain nuclei

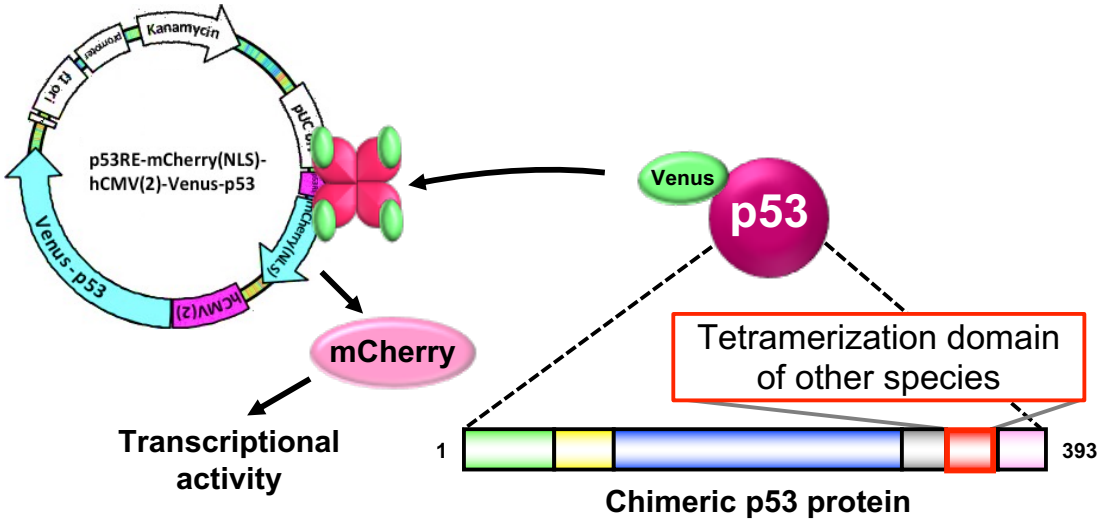

Figure 28. Transcriptional activity of chimeric p53

Chimeric p53 protein is replaced tetramerization domain derived other species. H1299 cells was transfected by the plasmid encoded Venus-chimeric p53 and mCherry-NLS. Venus-p53 is expressed by hCMV promoter and forms tetramer in the cells. The tetramer formed p53 binds to a response element derived p21 and activates transcription of mCherry-NLS. p53 expression level was measured by Venus intensity, and the transcriptional activity was quantified by mCherry intensity.

and removed. The cells were washed by 900 μl PBS two times, and 1 ml PBS was added to the dish. The cells were observed its fluorescence by fluorescence microscope (BIOREVO BZ-9000, Keyence). Each exposure time and fluorescence mirror unit were 2.0 s, YFP-BP for Venus; 1.0 s, TRITC for mCherry; 1/5 s, DAPI for DAPI. Objective lens was Nicon Plan Fluor 10x/0.30. Image Analysis and Data Analysis developed by Dr. Imagawa from our laboratory were used for the image analysis.

4.3.7. Crystallography of p53Tet

・Construction of the protein expression vector

pET-TEV vector was used for express His-GST-(TEV site)-Coelacanth p53Tet-long(333-376).The cDNA encoding Coelacanth p53Tet-long(333-376) was ordered in pUC57-KANA vector. For Coelacanth p53Tet-short(333-366), a stop codon was induced to Coelacanth p53Tet-long(333-376) by the quick change method using two primers including a stop codon.

・Expression and purification of peptides

The Coelacanth p53Tet-long and -short peptides were expressed in *E. coli* BL21(DE3). BL21(DE3) transformed by the plasmid were initially grown for overnight (16 h) in 2 L of LB in the presence of ampicillin (100 mg/L) at 37℃, and this culture was used for inoculation of 8 L of LB, with ampicillin and IPTG (125 mg/L). The resulting culture was grown for 4 h at 30℃. The cells were harvested and suspended in lysis buffer. The suspended cells were lysed using a French press and centrifuged at 105,000*g* for 30 min at 4℃. The resulting supernatant was incubated with GS resin for GST-tag affinity purification. The GST-tag was cut by TEV protease on the resin overnight at room temperature. The resulting supernatant was applied to an ion exchange column. The fractions containing GS-p53Tet were pooled for purification by gel filtration using a SuperoseTM 12 (GE healthcare) column equilibrated with 20 mM Tris, pH7.5, 1 mM DTT.

・Crystallization conditions

Crystals of GS-Coelacanth p53Tet-long were grown by the vapor diffusion method at 20℃ using either 1:1 or 2:1 mixtures of peptide solution (4.0 mg/ml) and precipitant buffer. The precipitant buffer was 20% PEG 3350 with 0.2 M NH_4NO_3. Before the samples were flash frozen, 24% ethylene glycol was added as a cryoprotectant. Crystals of the GS-coelacanth p53Tet-short were grown by the vapor diffusion method at

23℃ using either 1:1 or 2:1 mixtures of peptide solution (4.9 mg/ml) and precipitant buffer. The precipitant buffer was 24% PEG 4000 with 0.2 M $(NH_4)_2SO_4$. Before the samples were flash frozen, 15% glycerol and 16% ethylene glycol were added as a cryoprotectant.

・X-ray data collection and processing and structure determination

Diffraction data were collected from single crystals using a beamline of the Canadian Light Source (CLS) (Saskatoon, Canada). All data sets were processed with HKL2000. The initial phases for determining the Coelacanth p53 tetrameric structures were obtained by molecular replacement using the structure of Human p53 TD as a search template. Phases were improved by iterative cycles of model building with Coot [91], and refinement was performed with PHENIX [92]. The figures were visualized using PyMOL.

4.4. Results

4.4.1. Synthesis of p53Tet

I synthesized p53Tet-long (with second helix region) and -short (without second helix region) of 14 vertebrates, Human, Chicken, Alligator, Softshell turtle, Frog, Axolotl, Coelacanth, Swordtail, Catfish, Zebrafish, Gar, Japanese bullhead shark, Ghost shark, and Lamprey. The molecular weights of each peptide were measured by MALDI-TOF MS.

4.4.2. Phylogenetic analysis of vertebrate p53

The evolutional rates of the p53/p63/p73 DBD and TD were calculated by Mr. Kudoh from our laboratory using the sequences of 45 species **(Figure 29)**. The sequences were aligned by MAFFT (v7.310) and trimmed using MEGA 6.06. p63 and p73 have a small evolution rate containing mature domains, whereas p53 has a higher evolution rate than p63 and p73, indicating that p53 has evolved more positively. The evolution rate of the p53 TD was higher than that of its DBD, resulting in are diverse TDs. Therefore, the TD sequence has evolved along with vertebrate evolution, suggesting a selective pressure for vertebrate evolution. The phylogenic tree of p53 TD is shown in **Figure 30**. Mammals such as humans are closely packed with short branches (upper tree), whereas the early vertebrate, Lamprey, has a long branch, indicating that Lamprey has a different sequence from other species. Ray-finned fishes are closely packed at the bottom of the tree. **Table 10** shows the sequences of the p53 TD including the C-terminal region. The Gly that has been suggested to form the turn is conserved in all vertebrates. The region from the N-terminus to the center of the sequence has highly conserved residues among mammals and other species, whereas 15 residues at the C-terminal region are highly conserved in mammals but are completely different in the other species. Thus, I determined that the sequences of the C-terminal region, in particular, have positively evolved. Remarkably, the position of the Pro that is a helix breaker is different among mammal and the other species.

4.4.3. Secondary structure and oligomeric state of p53Tet

To determine the oligomeric state and the secondary structure of vertebrate p53 TD, I performed gel filtration and CD spectrometry. The gel filtration analysis of short peptides which were without second helix detected the main peaks of all species at around

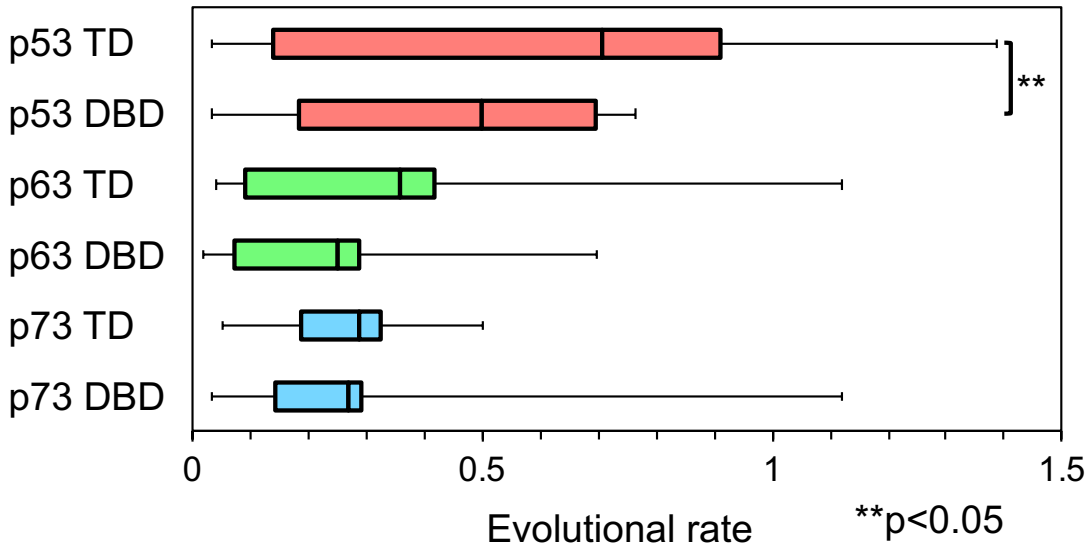

Figure 29. Evolutional rate of tetramerization domain and DNA binding domain in vertebrate p53/p63/p73

Evolution rates of p53/p63/p73 TD and DBD were calculated using 45 species sequences which available all sequences.

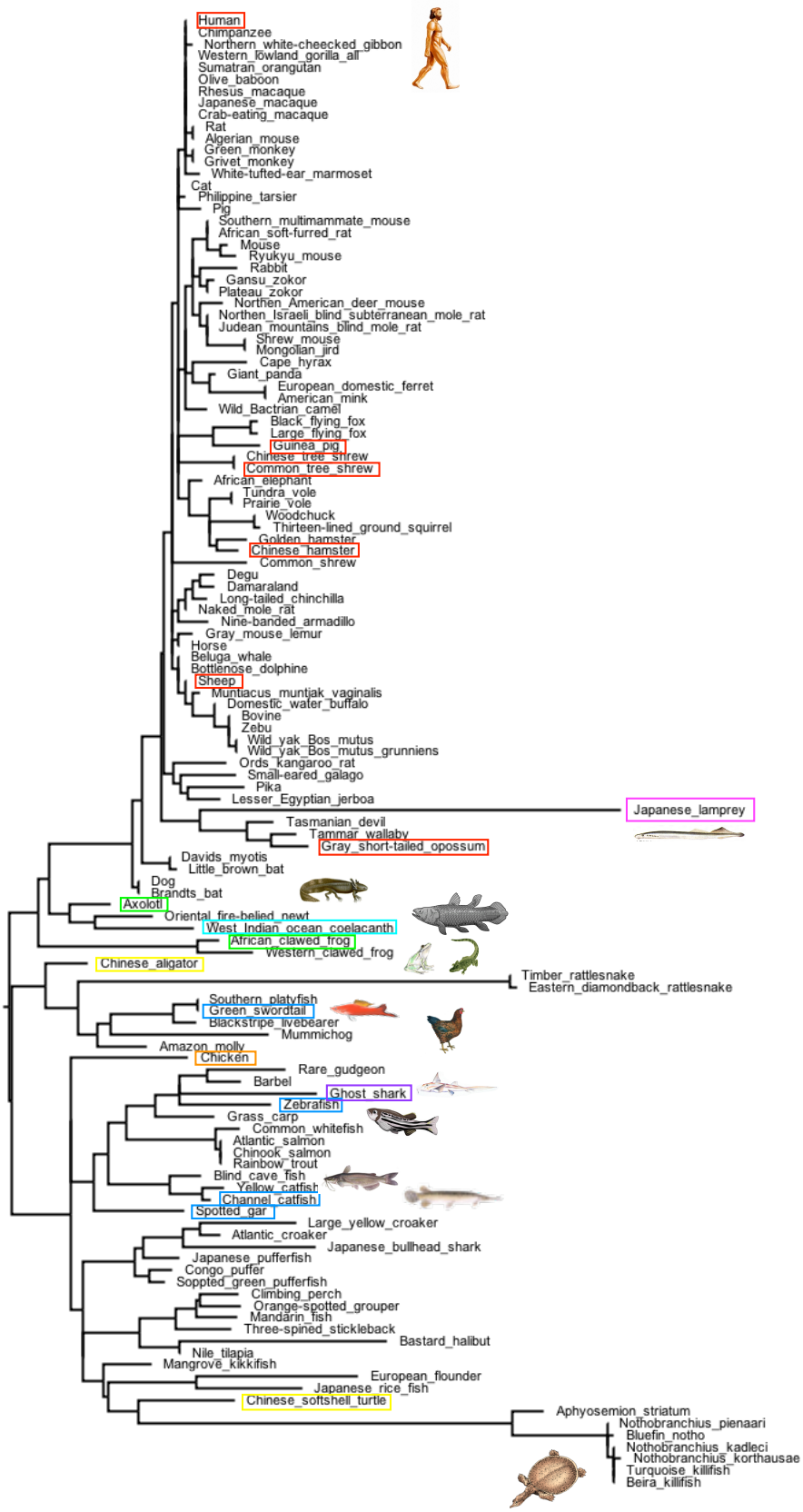

Figure 30. Phylogenetic tree of p53 tetramerization domain in vertebrates

Table 10. Sequences of vertebrates p53 TD

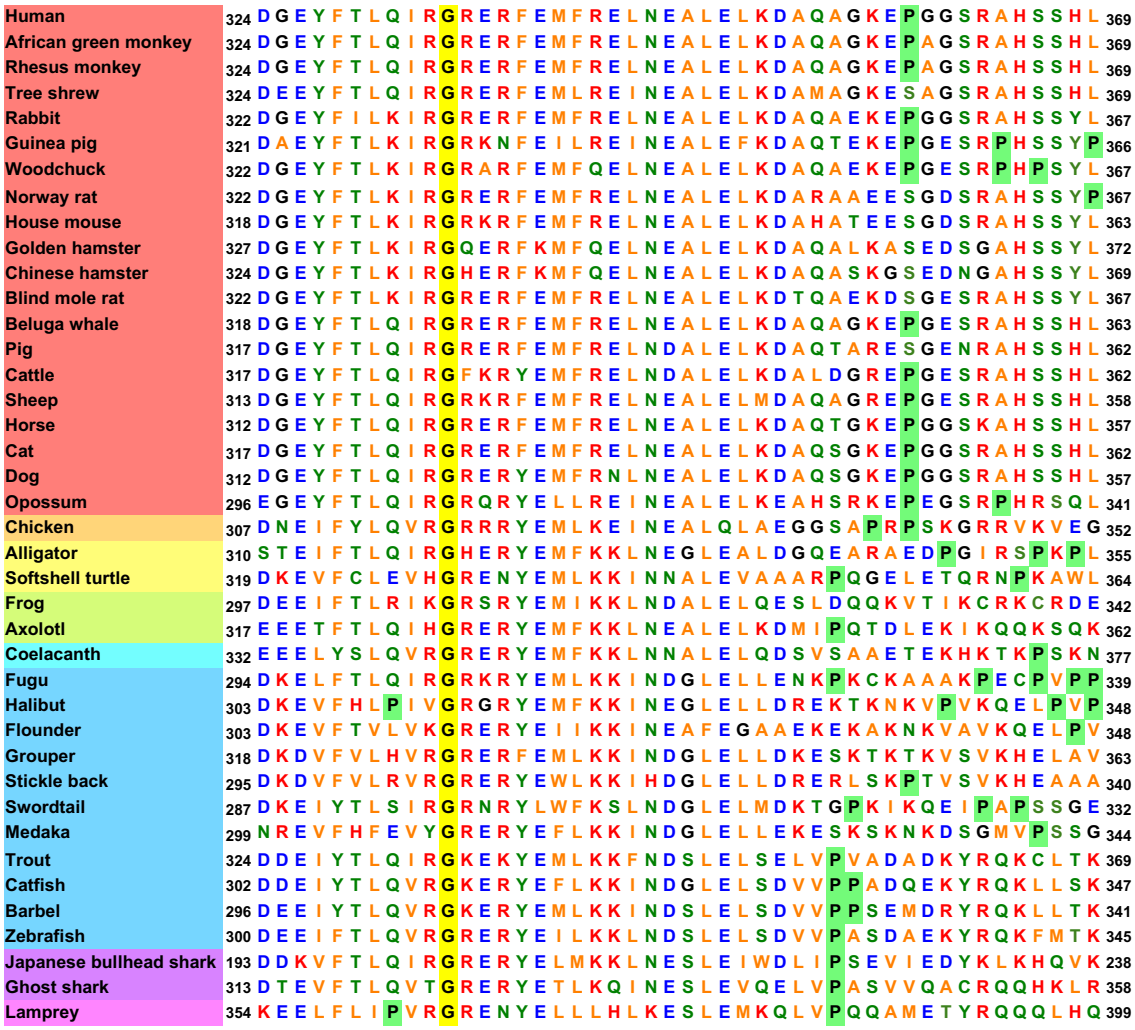

hydrophobic amino acids, orange; acidic, blue; basic, red; Gly, black; others, green

Gly of turn, yellow; Proline, light green

14 min like Human, indicated forming tetramer **(Figure 31)**. Chicken p53Tet-short was detected after 3Ala, monomer mutant, suggesting the peptide strongly interacted with the column. The CD spectra of the Zebrafish p53Tet-short and -long were measured, and the different spectra (long – short) are shown in **Figure 32**. The structure of the long type had more helices than the short type, confirming that the Zebrafish p53 TD formed a new helix (second helix) at the C-terminal region. I also measured the CD spectra of the p53Tet-short and -long of the other fishes (Lamprey, Catfish, and Coelacanth), amphibian (Axolotl), and reptile (Softshell turtle), to analyze the secondary structure of second helix region **(Figure 33)**. I found that both the long type and short type formed a helical structure, although it was mutated in many residues like Lamprey. In Softshell turtle, the long type had a more random coil structure than the short type, indicating that the second helix region was not a helix but a flexible structure, i.e., the Softshell turtle p53 TD did not have a second helix. In Axolotl, the long type had more of a helix structure than the short type, suggesting the possibility of forming a second helix. In Coelacanth, the long type and short type had almost the same spectra, so I was not able to decide whether a second helix was formed or not. In Catfish, the different spectra were the same as the Zebrafish, and the identity of the second helix region with that of Zebrafish was high, indicating that Catfish formed a second helix. In Lamprey, the long type slightly increased the helical structure compared with the short type, suggesting that the second helix region may partially form a helix.

4.4.4. Structural stability of p53Tet

To analyze the structural stability of the p53 TD in vertebrates, I performed thermostability measurements of the short and long peptides using CD spectrometry **(Figure 34, 35)**. The denaturation curves from tetramer to monomer were fit, and thermodynamic parameters were calculated **(Table 11, 12)**. The stabilities of the p53 tetrameric structures in vertebrates were significantly different, however, the width of the stability was shorter than it was in the point mutants reported in humans. Of the point mutants, the most stable mutant was T329I with T_m = 73°C, and the least stable mutant was R337C with T_m = 22°C. Moreover, there were monomer mutants and dimer mutants. The TD of all vertebrates formed tetramers, although Lamprey had 32 residues out of 46 replaced, compared with humans. The most stable species was Chicken-short with T_m = 73°C, and the least stable species was Ghost shark-long with T_m = 40°C (because Ghost

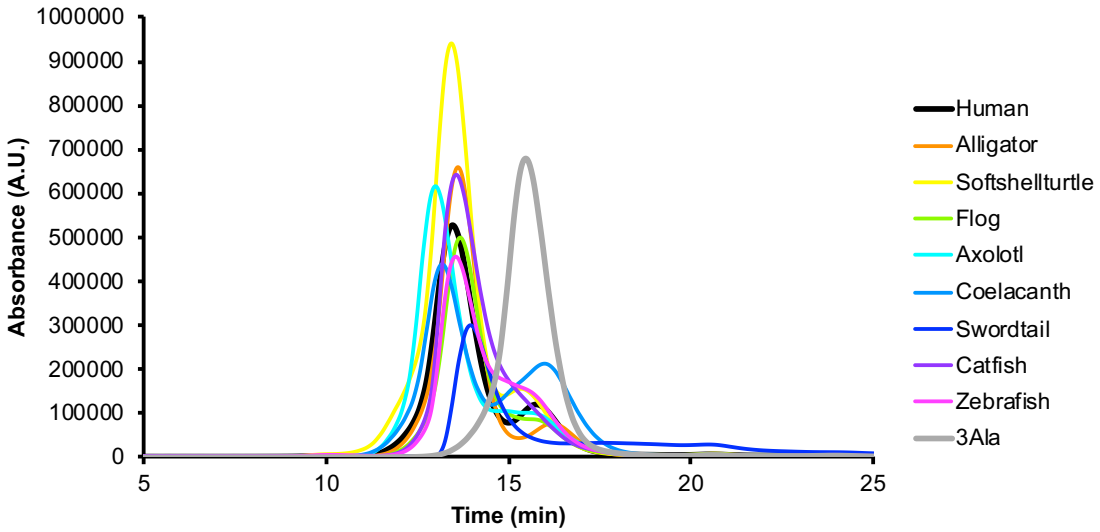

Figure 31. Gel filtration of vertebrates p53Tet-short

The oligomeric states of the vertebrates p53Tet and 3Ala (monomer mutant) were measured by gel filtration chromatography. The larger peaks that elute at roughly 14 min correspond to the tetramer whereas the smaller peaks at roughly 16 minutes correspond to the monomer. The UV absorbance was monitored at 214 nm.

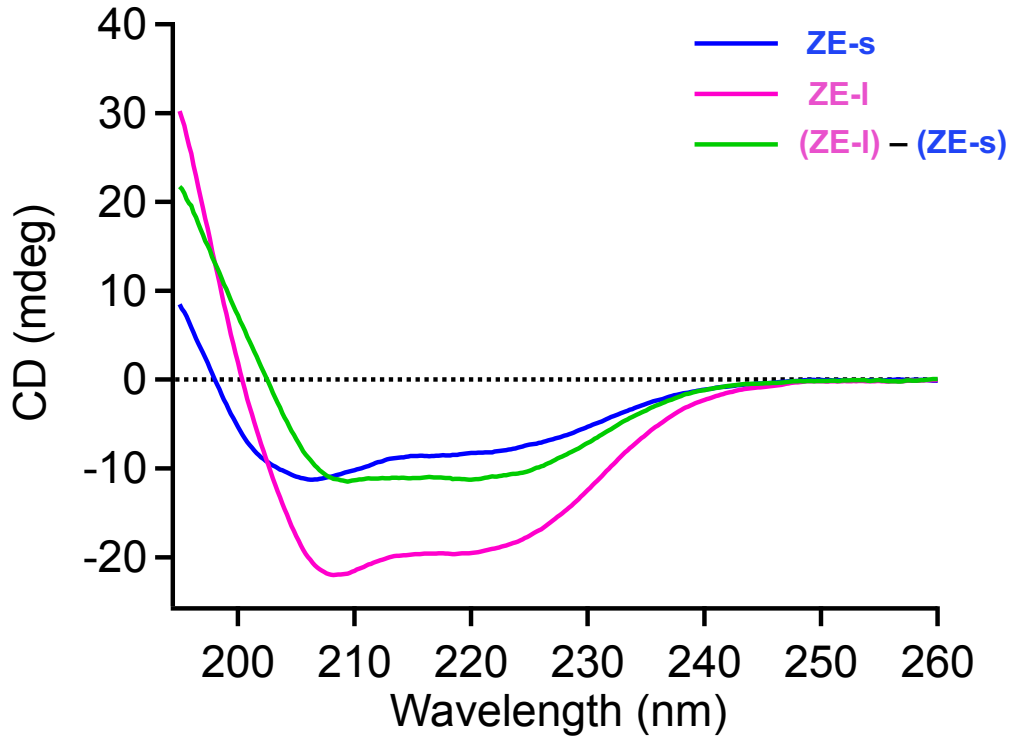

Figure 32. CD spectra of Zebrafish p53Tet-short and -long

The secondary structure of the Zebrafish p53Tet-short and long were measured by CD spectrometry at 4℃.

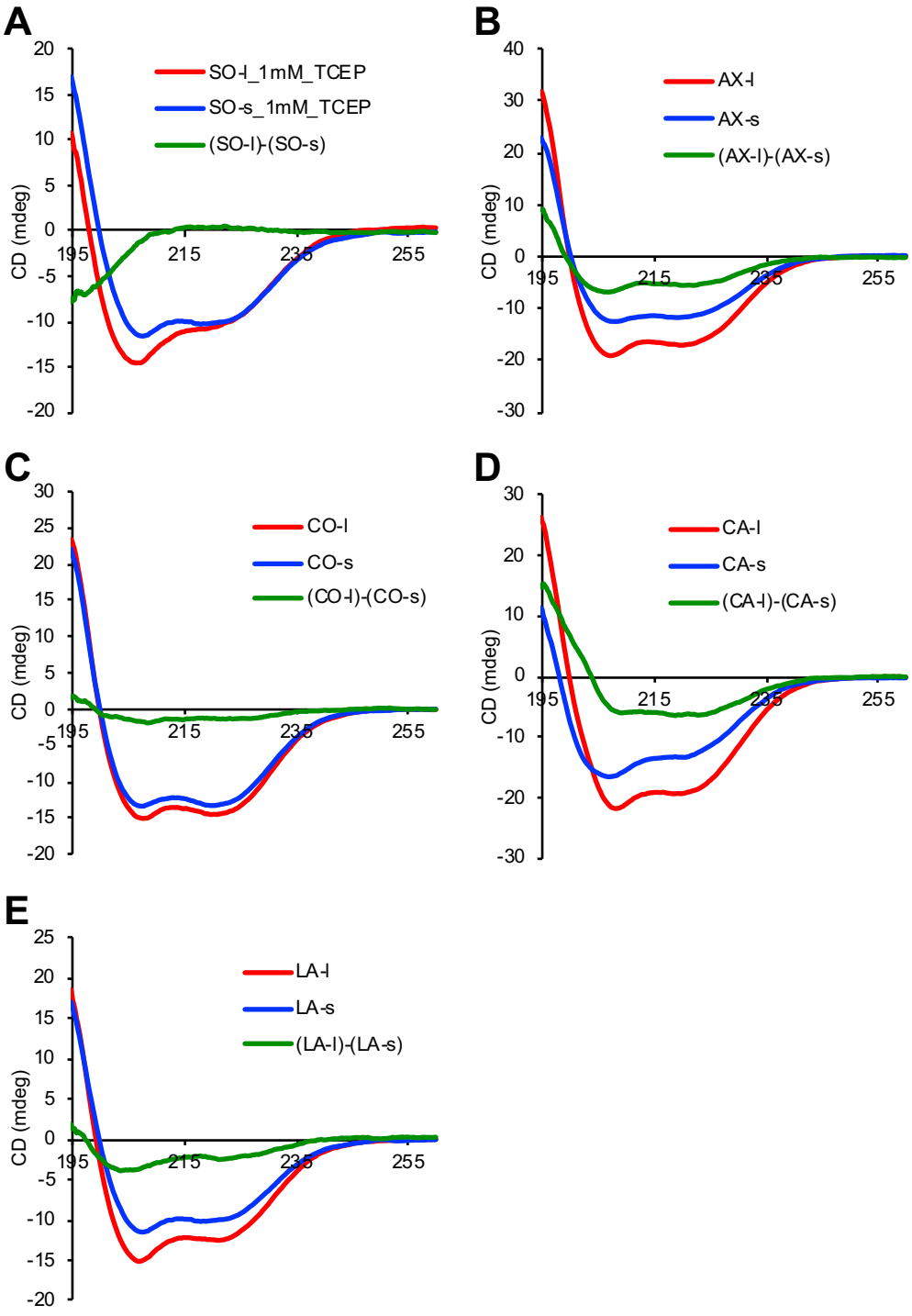

Figure 33. CD spectra of vertebrates p53Tet-long and -short

The secondary structure of the vertebrates p53Tet were measured by CD spectrometry at 4°C.

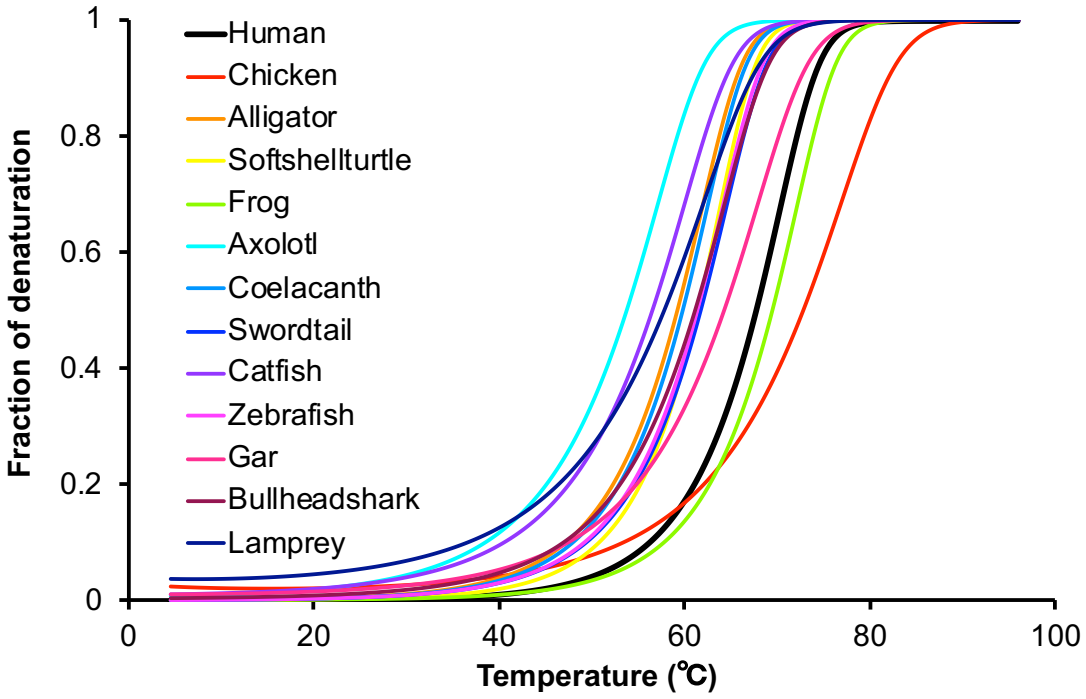

Figure 34. Thermal denaturation curves of vertebrates p53Tet-short

The signal from the vertebrates p53Tet-short were monitored by CD spectrometry at 222 nm between 4℃ and 96℃. The fraction of denaturation at each temperature was plotted to generate the denaturation curves. The value at 222 nm at 4℃ is taken as 0% denaturation.

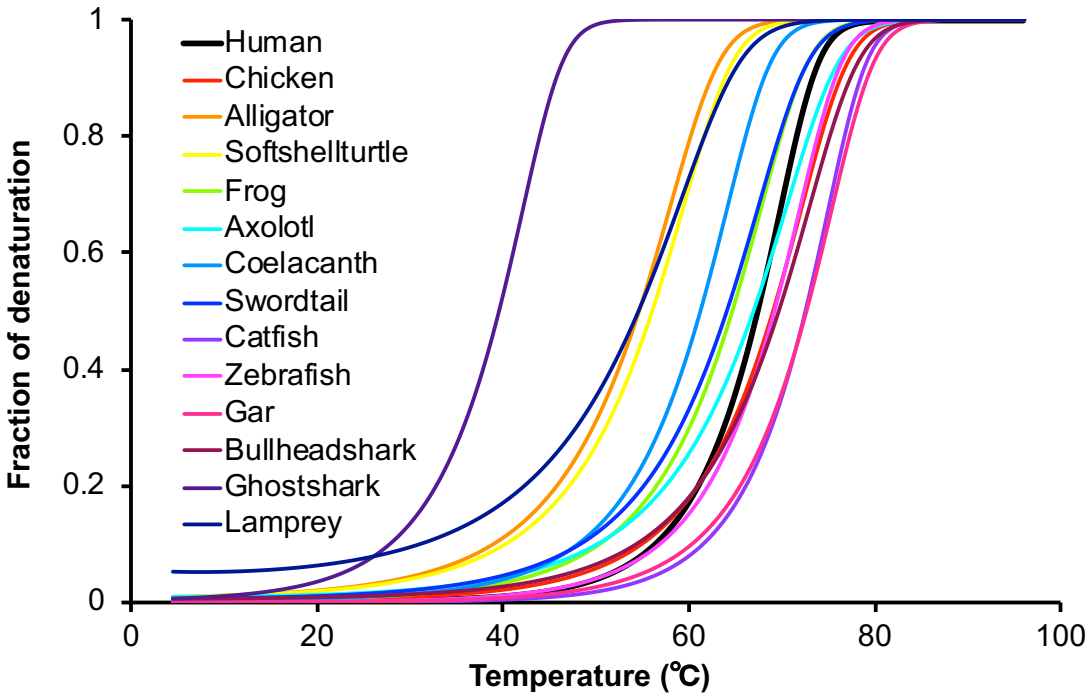

Figure 35. Thermal denaturation curves of vertebrates p53Tet-long

The signal from the vertebrates p53Tet-long were monitored by CD spectrometry at 222 nm between 4℃ and 96℃. The fraction of denaturation at each temperature was plotted to generate the denaturation curves. The value at 222 nm at 4℃ is taken as 0% denaturation.

Table 11. Thermodynamic parameters of tetramerization domain peptides from CD analysis

Peptide	T_m (°C)	ΔT_m (°C)	$\Delta G_u^{37°C}$ (kcal/mol)	$\Delta\Delta G_u^{37°C}$ (kcal/mol)
Human-short	67.8 ± 0.2	-	32.4	-
Human-long	67.4 ± 0.4	-0.4	32.9	0.5
Chicken-short	72.8 ± 0.4	5.0	28.5	-3.9
Chicken-long	69.0 ± 0.4	1.2	30.6	-1.8
Alligator-short	59.2 ± 0.2	-8.6	29.3	-3.1
Alligator-long	54.6 ± 0.2	-13.2	26.5	-5.9
Softshell turtle-short	61.4 ± 0.2	-6.4	31.2	-1.2
Softshell turtle-long	56.0 ± 0.2	-11.8	26.8	-5.6
Frog-short	69.3 ± 0.6	1.5	30.7	-1.7
Frog-long	64.6 ± 0.4	-3.2	29.5	-2.9
Axolotl-short	53.7 ± 0.2	-14.1	26.4	-6.0
Axolotl-long	66.9 ± 0.4	-0.9	28.7	-3.7
Coelacanth-short	59.8 ± 0.5	-8.0	29.6	-2.8
Coelacanth-long	61.2 ± 0.4	-6.6	29.3	-3.1
Swordtail-short	61.7 ± 0.4	-6.1	29.9	-2.5
Swordtail-long	64.0 ± 0.4	-3.8	28.6	-3.8
Catfish-short	56.5 ± 0.4	-11.3	26.9	-5.5
Catfish-long	72.5 ± 0.2	4.7	34.5	2.1
Zebrafish-short	61.3 ± 0.4	-6.5	29.9	-2.5
Zebrafish-long	69.1 ± 0.2	1.3	32.0	-0.4
Gar-short	64.2 ± 0.4	-3.6	28.2	-4.2
Gar-long	72.6 ± 0.4	4.8	33.0	0.6
Japanese bullhead shark-short	61.1 ± 0.6	-6.7	28.7	-3.7
Japanese bullhead shark-long	69.6 ± 0.4	1.8	30.1	-2.3
Ghost shark-short	-	-	-	-
Ghost shark-long	39.6 ± 0.4	-28.2	22.7	-9.7
Lamprey-short	57.8 ± 0.8	-10.0	26.0	-6.4
Lamprey-long	54.6 ± 0.9	-13.2	25.2	-7.2

T_m and $\Delta G_u^{37°C}$ were calculated by denaturation analysis. The standard errors of fittings were indicated. $\Delta\Delta G_u^{37°C}$ = ($\Delta G_u^{37°C}$ of each species) – ($\Delta G_u^{37°C}$ of Human-short)

Table 12. Thermodynamic parameters of tetramerization domain peptides from CD analysis

Peptide	T_m (°C)	ΔT_m (°C)	$\Delta G_u^{37°C}$ (kcal/mol)	$\Delta\Delta G_u^{37°C}$ (kcal/mol)
Human-short	67.8 ± 0.2	-	32.4	-
Human-long	67.4 ± 0.4	-0.4	32.9	0.5
Chicken-short	72.8 ± 0.4	-	28.5	-
Chicken-long	69.0 ± 0.4	-3.8	30.6	2.1
Alligator-short	59.2 ± 0.2	-	29.3	-
Alligator-long	54.6 ± 0.2	-4.6	26.5	-2.8
Softshell turtle-short	61.4 ± 0.2	-	31.2	-
Softshell turtle-long	56.0 ± 0.2	-5.4	26.8	-4.4
Frog-short	69.3 ± 0.6	-	30.7	-
Frog-long	64.6 ± 0.4	-4.7	29.5	-1.2
Axolotl-short	53.7 ± 0.2	-	26.4	-
Axolotl-long	66.9 ± 0.4	13.2	28.7	2.3
Coelacanth-short	59.8 ± 0.5	-	29.6	-
Coelacanth-long	61.2 ± 0.4	1.4	29.3	-0.3
Swordtail-short	61.7 ± 0.4	-	29.9	-
Swordtail-long	64.0 ± 0.4	2.3	28.6	-1.3
Catfish-short	56.5 ± 0.4	-	26.9	-
Catfish-long	72.5 ± 0.2	16.0	34.5	7.6
Zebrafish-short	61.3 ± 0.4	-	29.9	-
Zebrafish-long	69.1 ± 0.2	7.8	32.0	2.1
Gar-short	64.2 ± 0.4	-	28.2	-
Gar-long	72.6 ± 0.4	8.4	33.0	4.8
Japanese bullhead shark-short	61.1 ± 0.6	-	28.7	-
Japanese bullhead shark-long	69.6 ± 0.4	8.5	30.1	1.4
Ghost shark-short	-	-	-	-
Ghost shark-long	39.6 ± 0.4	-	22.7	-
Lamprey-short	57.8 ± 0.8	-	26.0	-
Lamprey-long	54.6 ± 0.9	-3.2	25.2	-0.8

T_m and $\Delta G_u^{37°C}$ were calculated by denaturation analysis. The standard errors of fittings were indicated. $\Delta\Delta G_u^{37°C}$ = ($\Delta G_u^{37°C}$ of long) – ($\Delta G_u^{37°C}$ of short)

shark-short did not show a tetramer-like CD spectrum, the result of its thermostability analysis was excluded). However, because the long type showed a tetramer-like CD spectrum, I determined that the Ghost shark TD formed tetramers. In Zebrafish, which is already known to form a second helix, the short type had low stability, and the long type showed 8°C higher stability than the short type **(Figure 36)**. Therefore, I concluded that the second helix strongly contributes to the stabilization of the tetrameric structure. Similarly, Japanese bullhead shark, Gar, and Catfish containing the long type were strongly stabilized compared with the short type, suggesting the second helix has a stabilization effect. In Ghost shark, I could not compare the long type with the short type, however I think the second helix region contributed to structure stabilization, because the long type was able to form tetramers (less stability). In Lamprey, both the short and long types had low stability, and the second helix region did not stabilize the structure. Swordtail and Coelacanth also did not show differences between the long type and short type, i.e., no stabilization effect via the second helix region. The Swordtail p53 TD has Pro residues breaking the helix at the second helix region, and it was estimated that it does not have a second helix on the basis of the sequence. Amphibian (Axolotl and Frog) and reptile (Softshell turtle and Alligator) showed medium stability for the long type and short type **(Figure 37)**. In Axolotl, the long type was more stable than the short type, showing a stabilization effect of the second helix region. In Frog, the short type was more stable than the long type, indicating that the second helix region destabilized the oligomeric structure. In Softshell turtle and Alligator, the long type was also less stable than short type, i.e., the second helix region did not contribute to structure stabilization, suggesting a second helix was not formed. The human sequence did not form a second helix, and the long type and short type were not different. In chicken, the long type had a lower T_m than the short type, but the long type had a higher ΔG_u than the short type. It was because the chicken short type had high T_m, however the transition from tetramer to monomer was very slow.

4.4.5. Transcriptional activity of chimeric p53

To analyze the effect of the p53 TD structural stability on transcriptional activity, I analyzed the transcriptional activity of a chimeric p53 composed of human p53 protein containing the TD of other species. The transcriptional activity of the chimeric p53 in H1299 cells was quantified by fluorescent microscopy. Three types of chimeric p53 were

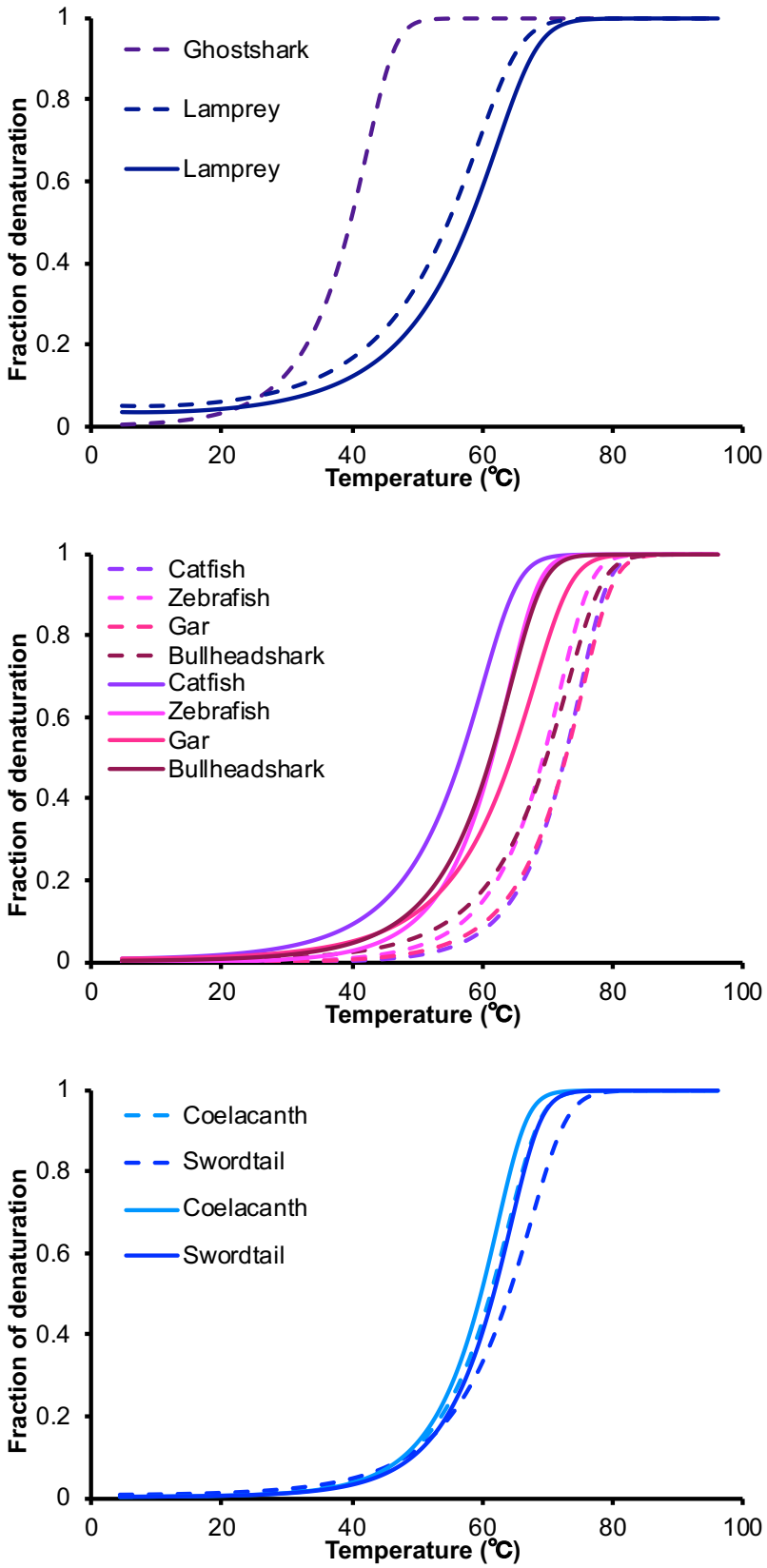

Figure 36. Thermal denaturation curves of fish p53Tet-long and -short long, broken line; short, solid line

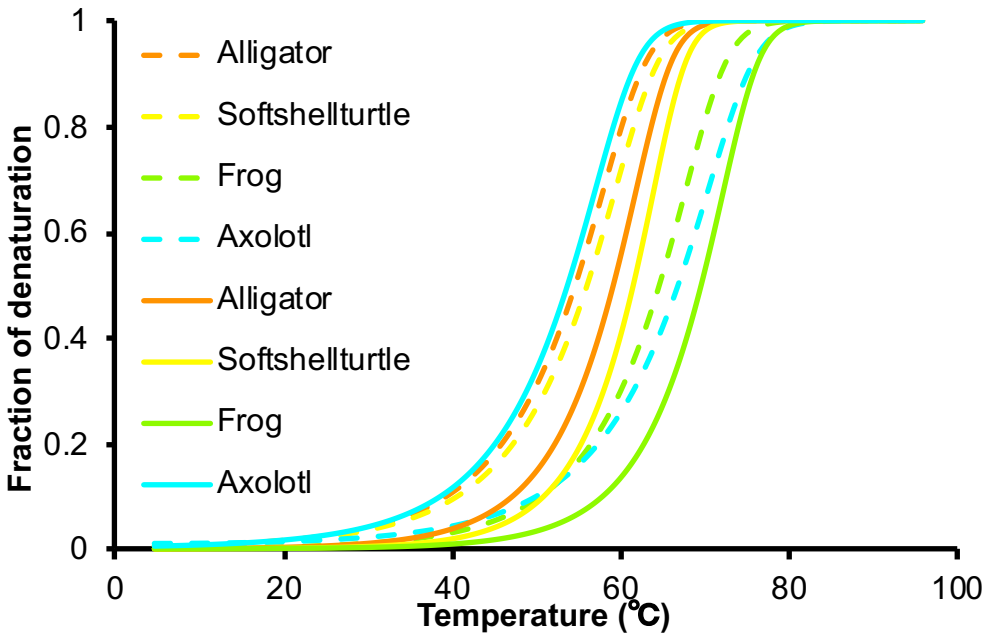

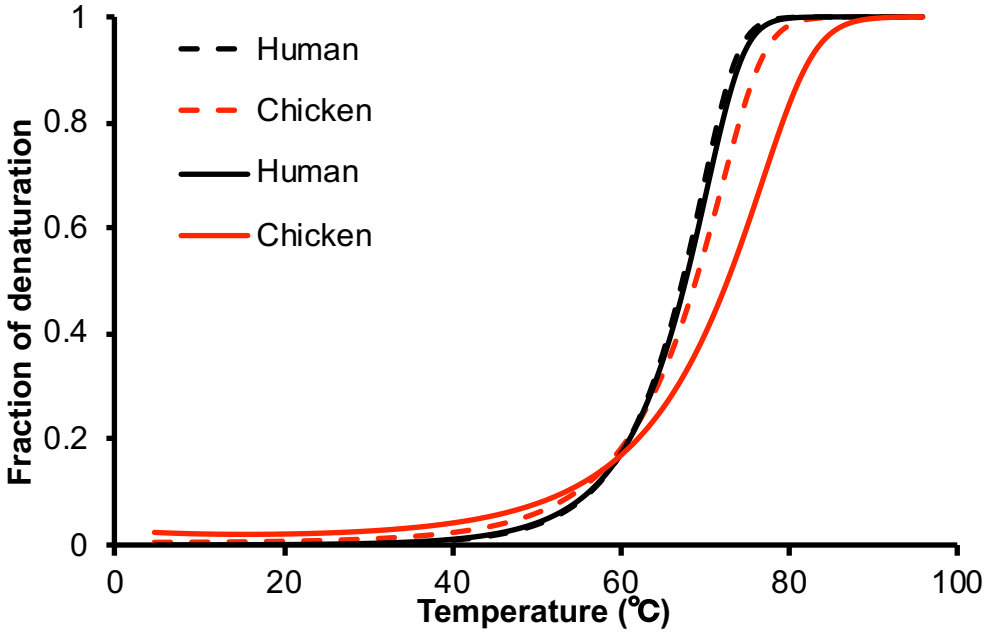

Figure 37. Thermal denaturation curves of Tetrapoda p53Tet-long and -short
long, broken line; short, solid line

constructed: short: the short type sequence was replaced; long: the long type sequence was inserted; long_ΔC: the C-terminus (BD) was deleted from the long type. The long type was replaced with 46 residues of the TD to 35 residues WT sequence, which overlapped with the sequence of the second helix region. In the long_ ΔC, the overlap was deleted; this form enhanced the effect of the C-terminal region of the TD on transcriptional activity. The transcriptional activity of each species and type was calculated as a percentage of the Human-short (WT) activity **(Table 13)**. The five mammals used in chapter three were analyzed on short type. Because the structural stability of the mammals was higher than that of the human protein, I estimated that the transcriptional activity will be higher. However, it did not exceed 100% of the human activity under these experimental conditions **(Figure 38)**. The results of the Zebrafish containing a second helix and the other fishes suggested that the second helix had only 50% transcriptional activity relative to the human short type. The activity of the Ghost shark short type was 10% of the WT activity, which was the lowest activity. Comparing the transcriptional activity of the long type and short type of Chicken, Alligator, Softshell turtle, Frog, Axolotl, Coelacanth, and Swordtail revealed that the activity was almost the same or slightly lower in the short type **(Figure 39)**. However, in Zebrafish with a second helix, the transcriptional activity of the long type was notably higher than that of the short type through the stabilization effect of the second helix. In Ghost shark, the long type transcriptional activity was 43%, and that of the short type was 10%. The stabilization effect of the second helix region was much high in Ghost shark. In Lamprey, the transcriptional activity was similar between the short and long types, both were around 40% of WT. Long_ΔC had higher transcriptional activity than WT, e.g., the human-long_ΔC activity was 145% of WT **(Figure 40)**. Thus, I concluded that the BD negatively regulated transcriptional activity. The Ghost shark and Lamprey activity was about 65% of WT, which was lower than the other species, and similar to the other fishes, Amphibia, and reptile.

4.4.6. Crystal structure of p53 tetramerization domain

Coelacanth, which is the species just before going up to land from water, is an important creature for understanding the evolution process of vertebrates. To determine the tetrameric structure of Coelacanth p53, I performed X-ray crystallography of Coelacanth p53Tet-short and -long. I obtained both crystals and analyzed the tetrameric

Table 13. Transcriptional activity of chimeric p53

Species	short		long		long_ΔC	
	% of Human	S.D.	% of Human	S.D.	% of Human	S.D.
Human	100	0.0	-	-	145	10.0
Tree shrew	99.3	7.0	-	-	-	-
Guinea pig	97.3	6.2	-	-	-	-
Chinese hamster	94.9	0.4	-	-	-	-
Sheep	95.8	3.9	-	-	-	-
Opossum	96.1	6.4	-	-	-	-
Chicken	78.7	2.0	68.2	4.5	107	4.5
Alligator	87.9	3.0	92.2	6.8	153	0.8
Softshell turtle	91.3	6.1	79.5	3.8	135	11.3
Frog	82.8	8.8	74.5	6.5	138	6.4
Axolotl	89.4	9.0	78.4	2.4	137	12.6
Coelacanth	93.2	6.3	78.3	3.0	142	14.9
Swordtail	75.4	8.4	76.5	3.6	131	6.1
Catfish	49.6	4.0	101.5	3.7	180	27.5
Zebrafish	57.1	4.2	85.2	2.1	150	23.9
Gar	47.7	3.0	86.4	3.2	138	7.6
Japanese bullhead shark	75.1	1.7	91.8	4.2	125	5.5
Ghost shark	10.6	0.6	42.7	3.3	65.6	3.1
Lamprey	41.3	1.7	43.6	1.5	63.0	2.9

The transcriptional activities were calculated using mCherry intensity and normalized by Human-short (WT).

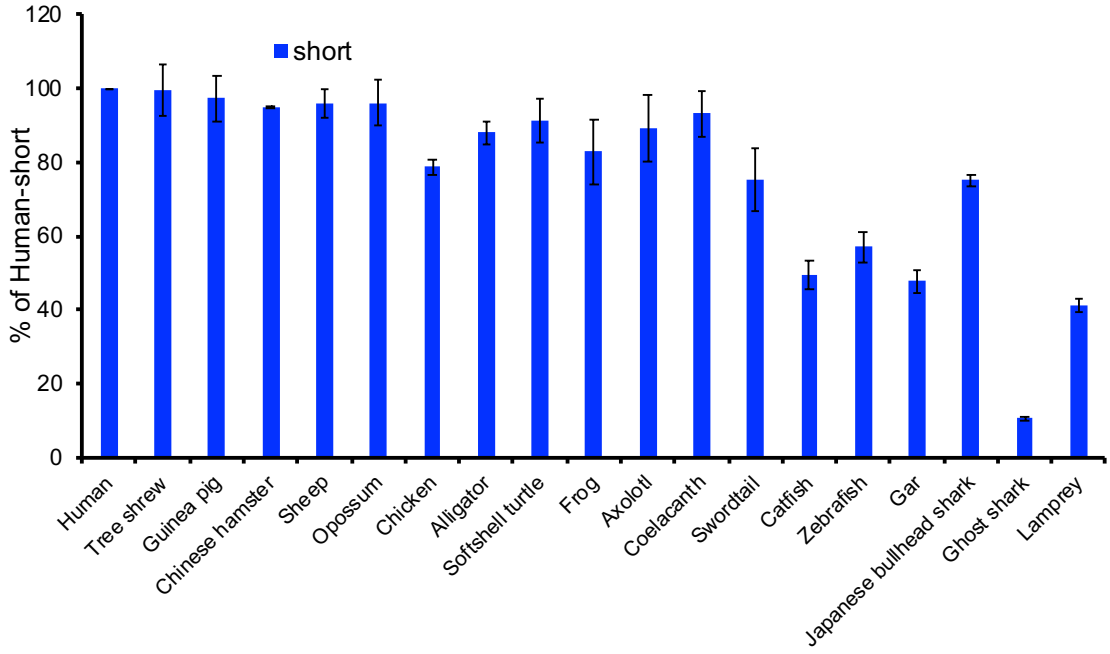

Figure 38. Transcriptional activity of chimeric p53-short

The transcriptional activities of each species are shown in a bar graph.

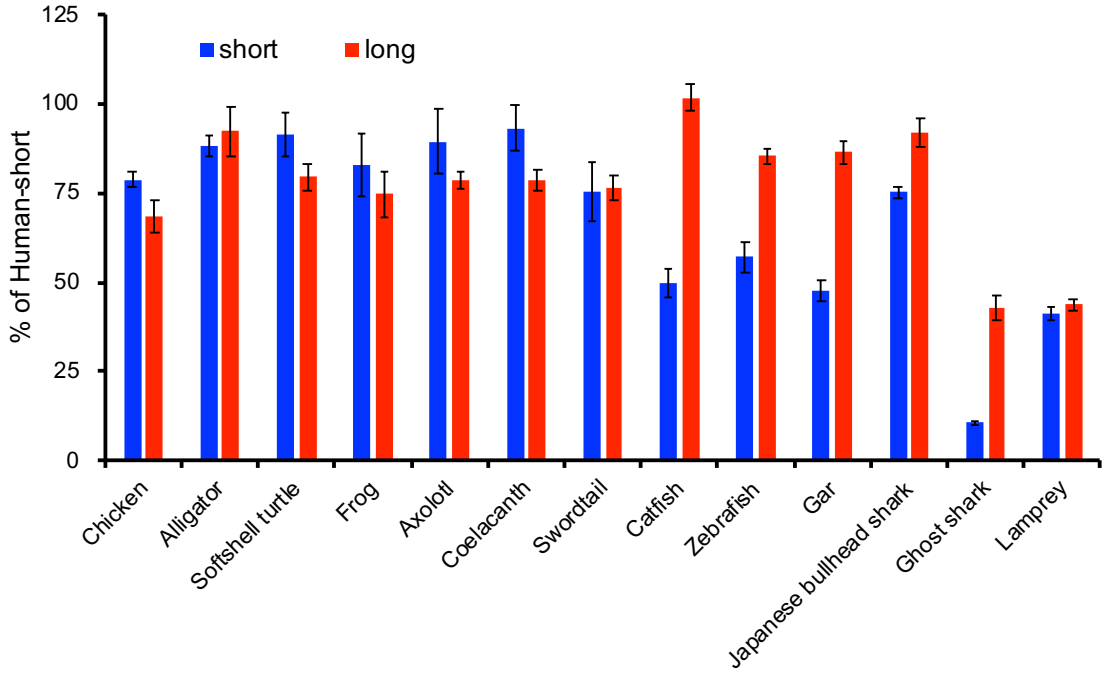

Figure 39. Transcriptional activity of chimeric p53-short and -long

The transcriptional activities of each species are shown in a bar graph. short, blue; long, red

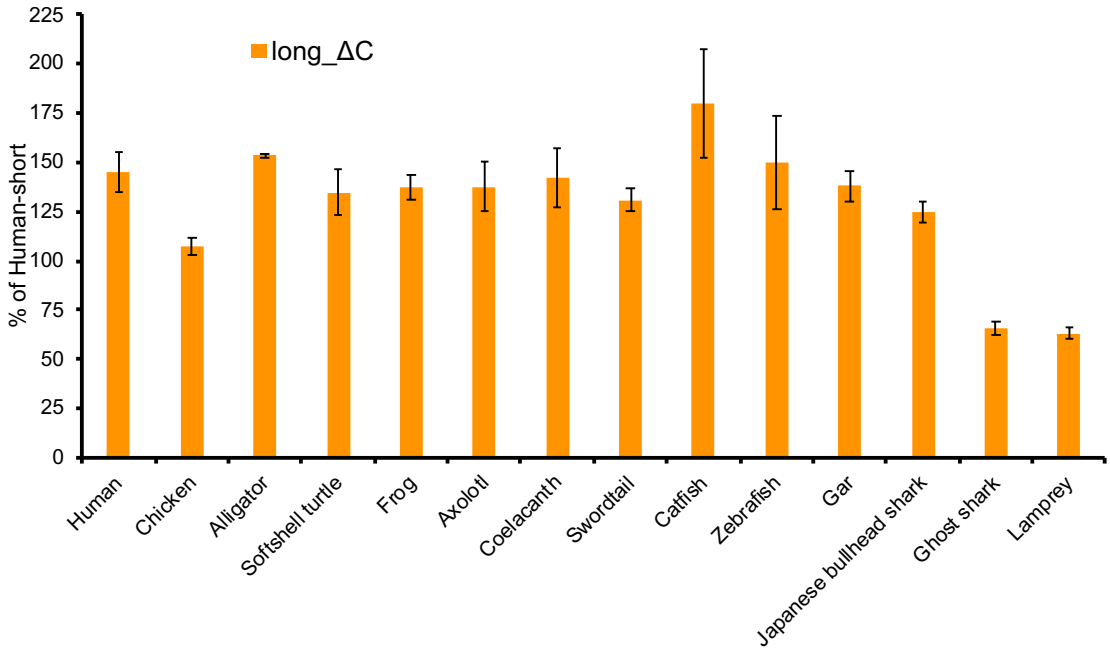

Figure 40. Transcriptional activity of chimeric p53 long_ΔC

The transcriptional activities of each species are shown in a bar graph.

structures **(Table 14)**. The resolution of both structures was 1.8 Å. The structures were symmetrical tetramers with a β-strand, turn, and α-helix. Like in human, the Coelacanth p53 TD did not have a second helix **(Figure 41, 42)**. Compared with the human tetrameric structure of p53 TD, Coelacanth p53Tet-short overlapped with the human structure, however, Coelacanth p53Tet-long had a longer (a roll) α-helix than the human-short **(Figure 43)**.

Table 14. Data collection and refinement statistics of crystallography

Data set	GS-Coelacanth p53Tet-long	GS-Coelacanth p53Tet-short
Data Collection		
Wavelength (Å)	1.033 Å	1.03 Å
Space group	$P6_522$	$P6_522$
Unit-cell parameter (Å)	a=34.97, b=34.97, c=240.92 α=90, β=90, γ=120	a=34.73, b=34.73, c=240.61 α=90, β=90, γ=120
Resolution (Å)	30.28-1.75 (1.81-1.75)	30.07-1.82 (1.89-1.82)
Total reflections	161577	121626
No. of unique reflections	9425	8515
Multiplicity	17.1	14.3
Completeness (%)	95.62 (66.26)	98.06 (91.56)
R_{merge}	0.064 (0.51)	0.135 (1.21)
I/σ (I)	23.10 (3.27)	13.59 (1.27)
Refinement Statistics		
Resolution (Å) R_{work}/R_{free} (%)	30.28-1.75 27.53/30.72	30.07-1.82 32.52/32.84
Number of atoms (excluding hydrogens) Protein Water	 562 25	 534 6
B-factors (Å^2) Protein Water	 57.59 54.14	 78.76 61.90
RMSDs Bond lengths (Å) Bond angles (°)	 0.004 0.74	 0.012 1.36
Ramachandran Favored (%) Outliers (%)	 100 0	 95 1.7

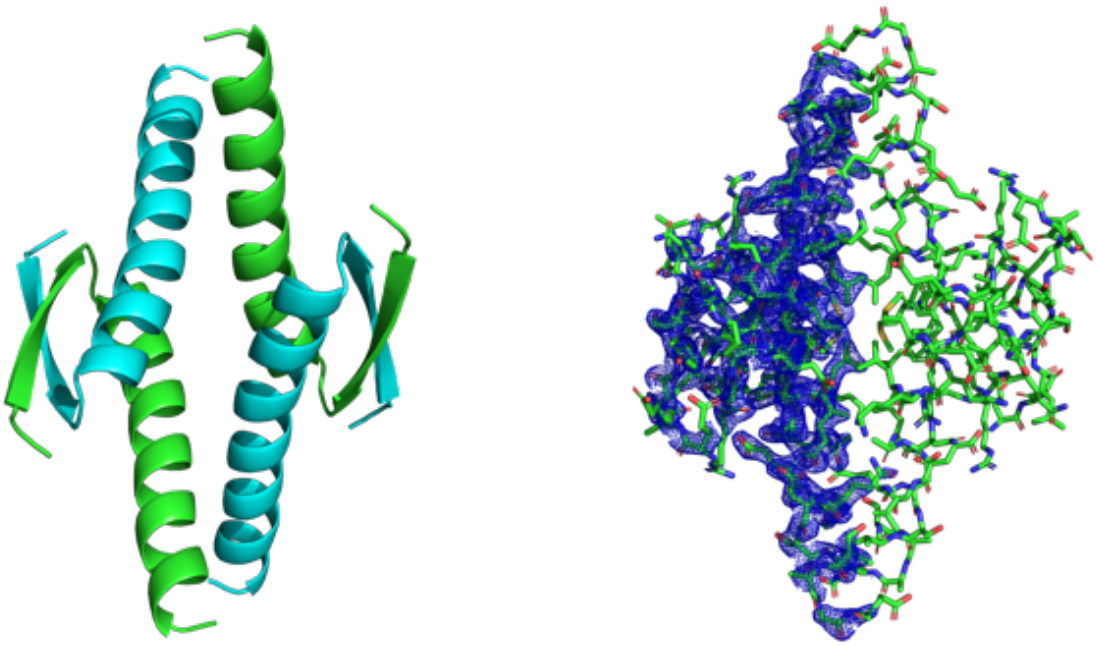

Figure 41. Crystal structure of GS-Coelacanth p53Tet-long

left, ribbon model of tetramer; right, stick model of tetramer (carbon, green; nitrogen, blue; oxygen, red; sulfur, yellow; electron density, blue mesh)

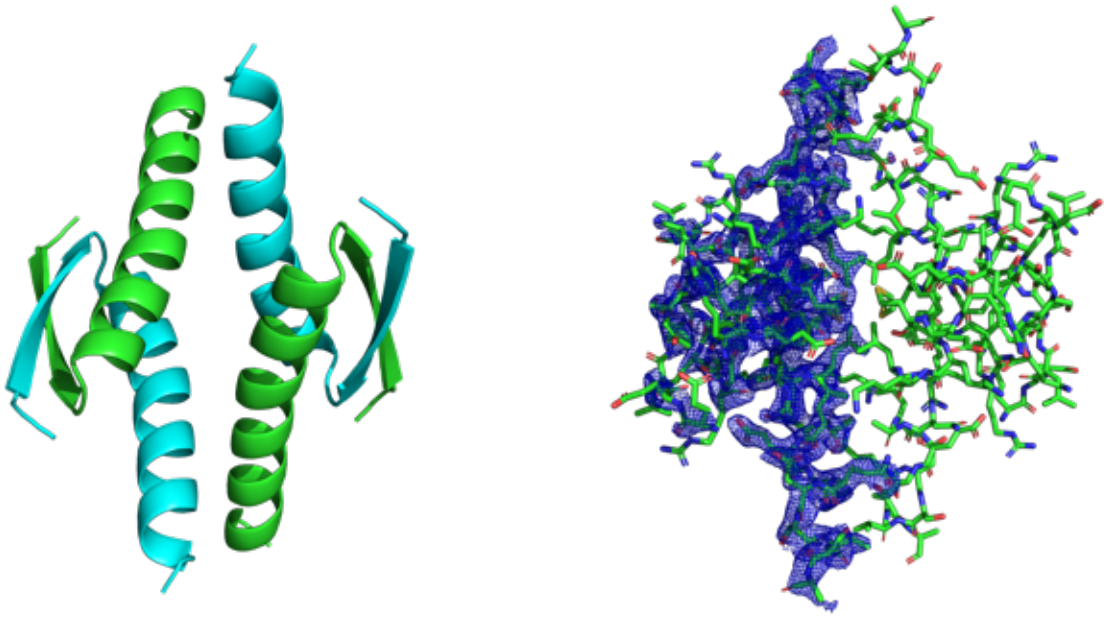

Figure 42. Crystal structure of GS-Coelacanth p53Tet-short
left, ribbon model of tetramer; right, stick model of tetramer (carbon, green; nitrogen, blue; oxygen, red; sulfur, yellow; electron density, blue mesh)

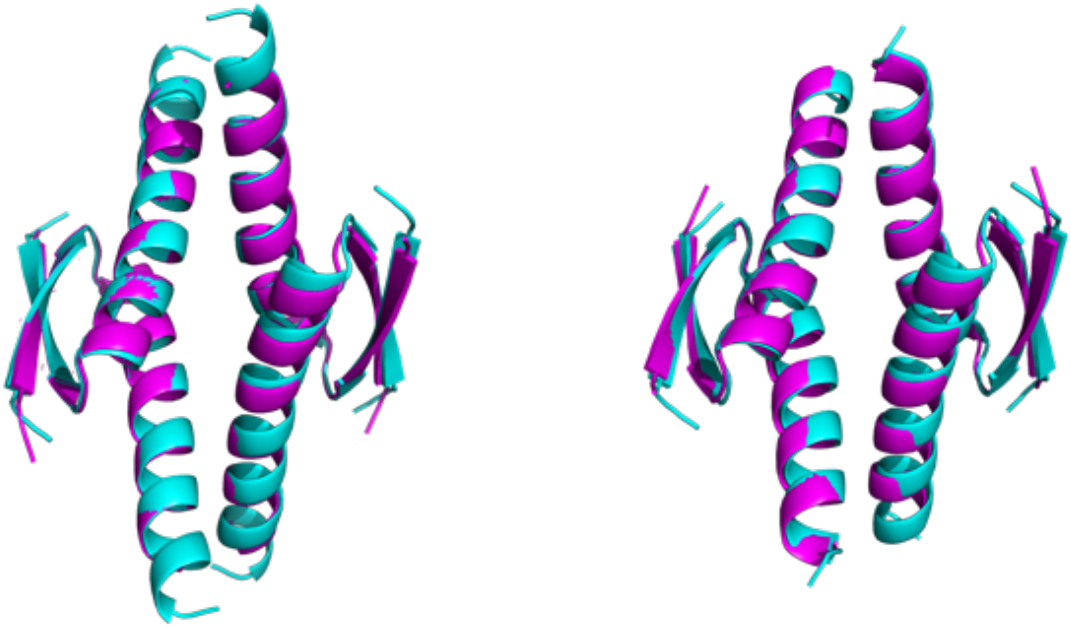

Figure 43. The structures of GS-Coelacanth p53Tet-long and -short with GS-Human p53Tet-short

left, Coelacanth p53Tet-long (cyan) with Human p53Tet-short (magenta); right, Coelacanth p53Tet-short (cyan) with Human p53Tet-short (magenta)

4.5. Discussion

In this study, to clarify the structure and the stability of p53 tetramerization domain, and the activity of p53 protein in the evolution of vertebrates, I performed thermostability analysis of p53 tetramerization domain peptide (p53Tet), X-ray crystallography, and transcriptional activity of chimeric p53 targeted 14 species of vertebrates I chose. The tetramerization domain of zebrafish forms the second helix at C-terminal, by comparing the thermostability between p53Tet short type not including second helix region and p53Tet long type including second helix region, the long type was more stabilized (7.8°C) than short type. Therefore, it was revealed that the second helix can extremely stabilize the tetrameric structure. Whereas, the coelacanth p53Tet had no difference between long type and short type. To determine the structure of coelacanth p53 TD, I performed X-ray crystallography, determined that coelacanth does not form the second helix. From the results of the thermostability analysis for p53Tet short type of all species and the transcriptional activity analysis of chimeric p53 protein, it was determined that the stability of the tetrameric structure positively related with the transcriptional activity **(Figure 44)**. The mammalian p53Tets were more stable than human p53Tet, however, the transcriptional activities of mammalian chimeric p53 proteins were not higher than human p53 protein in this experimental condition **(Figure 45)**. The stability and the transcriptional activity of lamprey and ghost shark were low, and coelacanth was middle, and mammals had high stability.

So far, the structure of p53 TD of human and zebrafish are reported. It was known that human p53 TD does not form the second helix, and zebrafish p53 TD forms a shorter first helix than human and the second helix. This time, I revealed anew that coelacanth p53 TD does not form the second helix. Moreover, **Table 15** shows the effect of the second helix region on structural stability and transcriptional activity compared with the long type and short type. The second helix region of human p53 TD which does not form the second helix did not make change the structural stability, as well as the second helix region of coelacanth p53 TD which does not form the second helix did not make change the structural stability and decreased the transcriptional activity. On the other hand, the second helix region of zebrafish which forms the second helix stabilized the structural stability and increased the transcriptional activity. From these results, it was expected that if the second helix region of the species increases the structural stability and transcriptional activity, the species forms the second helix, whereas, if the second helix

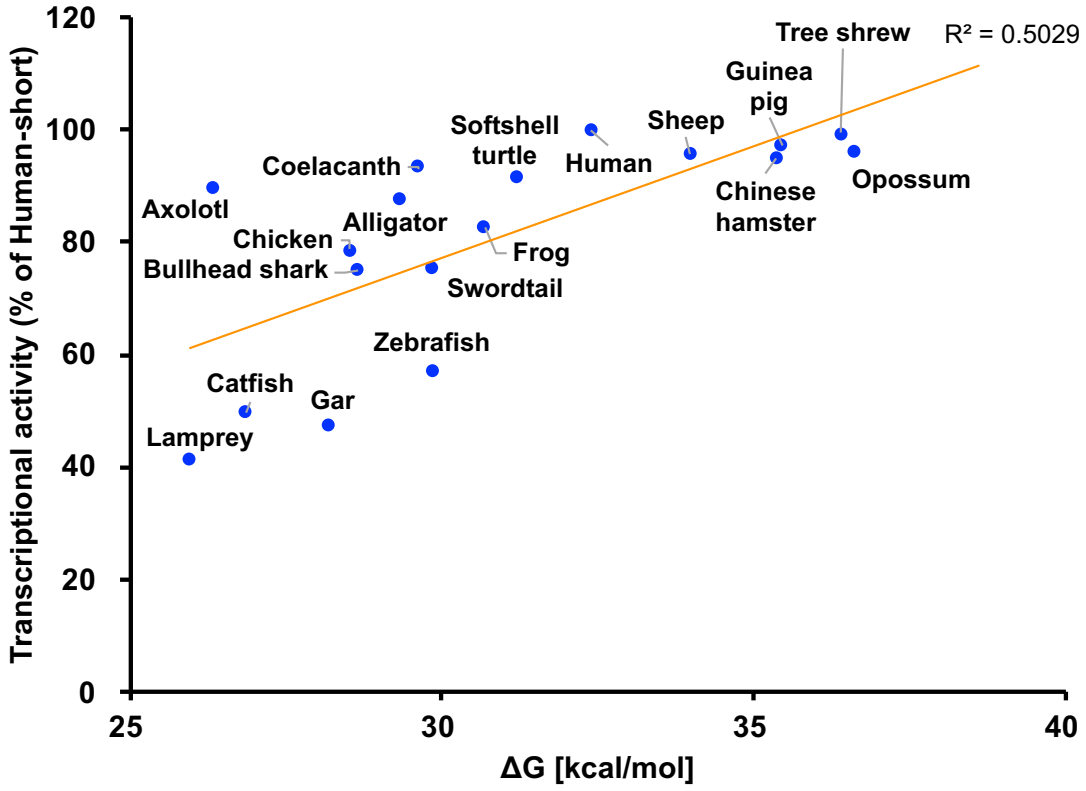

Figure 44. Correlation between the structural stability and the transcriptional activity (short)

The structural stability and the transcriptional activity of each species are plotted on the graph. approximately straight line, orange

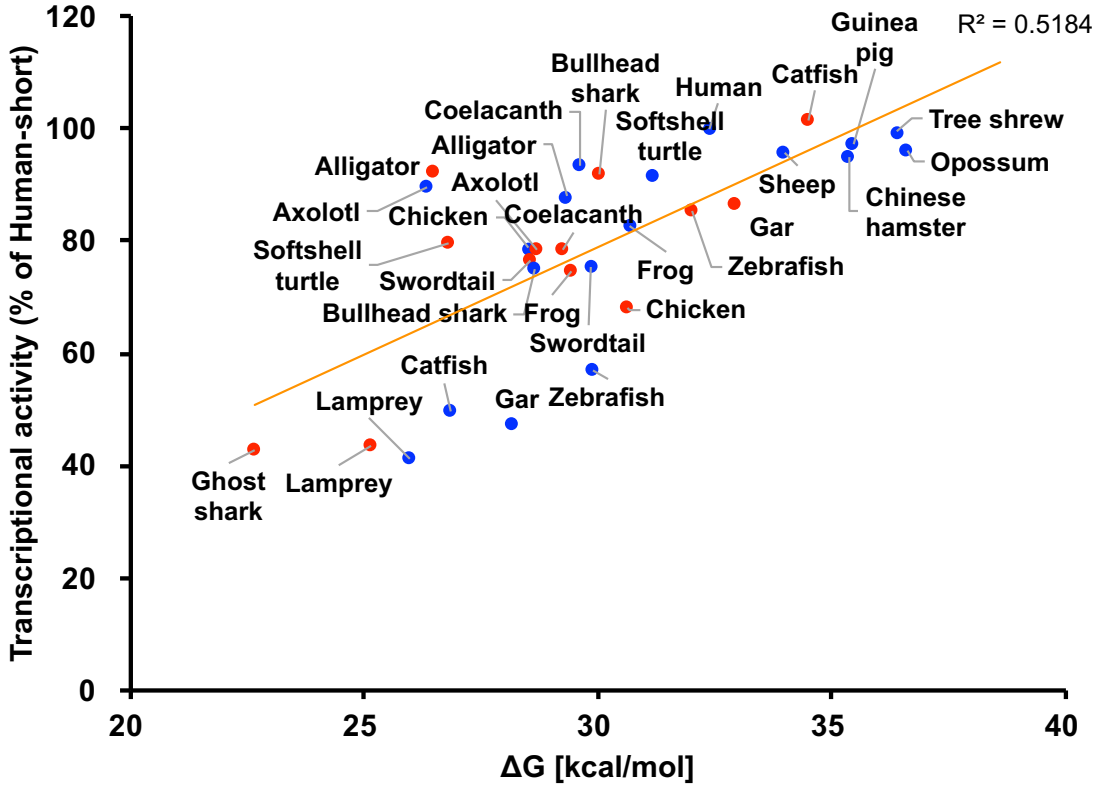

Figure 45. Correlation between the structural stability and the transcriptional activity (short and long)

The structural stability and the transcriptional activity of each species are plotted on the graph. short, blue dot; long, red dot; approximately straight line, orange

Table 15. The effect of second helix region on the structural stability and the transcriptional activity

Species	Structural stability	Transcriptional activity	Second helix
Human	unchanged	-	No
Chicken	unchanged	down	No
Alligator	down	unchanged	No
Softshell turtle	down	down	No
Frog	down	down	No
Axolotl	up	down	?
Coelacanth	unchanged	down	No
Swordtail	unchanged	unchanged	No
Catfish	up	up	Yes
Zebrafish	up	up	Yes
Gar	up	up	Yes
Japanese bullhead shark	up	up	Yes
Ghost shark	(up)	up	?
Lamprey	down	unchanged	?

Having p53 of each species second helix or not was estimated by the effect of second helix region on structural stability and transcriptional activity. It is reported that Human p53 TD doesn't have a second helix, and Zebrafish p53 TD has a second helix. In my structural study, Coelacanth p53 TD doesn't have a second helix.

region of the other species does not make a change or decreases them, the other species do not form the second helix. Thus, by the results of the structural stability and the transcriptional activity, for the species with structure unknown, it was expected that chicken, alligator, softshell turtle, frog, coelacanth, and swordtail did not form the second helix, however, catfish, gar, and Japanese bullhead shark formed the second helix. The second helix region of axolotl increased structural stability but decreased the transcriptional activity. The ghost shark p53Tet short type could not measure the thermostability, and the transcriptional activity of it was very low (10%), suggesting that it does not form a tetramer. However, ghost shark p53Tet long type could measure the thermostability, and the transcriptional activity was 43%, indicating that the long type was much stable than a short type. Therefore, it was determined that the effect of the second helix region of ghost shark on structural stabilization was drastically strong. The sequence of lamprey second helix region is similar to the species forming the second helix, however, by the results of thermostability and transcriptional activity, the second helix region of lamprey did not contribute to changing the structural stability and the transcriptional activity. For these species, further study of crystallography is required. Furthermore, on the sequence and tetrameric structure of the tetramerization domain, the position of Pro which is helix breaker is important for the length of the helix. The position of Pro in human p53 TD is C-terminus of the first helix, and Pro in coelacanth p53 TD is C-terminal region than human and beyond the structure. Also, zebrafish have a Pro between the first helix and second helix. Interestingly, swordtail is classified as Teleostei same as catfish and zebrafish, however, the sequence of swordtail second helix region is different to catfish and zebrafish, it has Pro, suggesting that swordtail does not form the second helix.

It was revealed that the structural stability of the p53 tetramerization domain and along the transcriptional activity of p53 protein have varied in the evolution process of vertebrates by this study **(Figure 46)**. Lamprey, the early vertebrate has low stability and low transcriptional activity, and then, fishes have high transcriptional activity by the effect of the second helix on the stability. On the other hand, the other species evolved to go to land from coelacanth to humans without second helix but gained high stability by first helix elongation.

The vertebrates have dramatically changed the live environment from water to land. Animals are exposure higher UV and oxygen caused genotoxic stress on land than

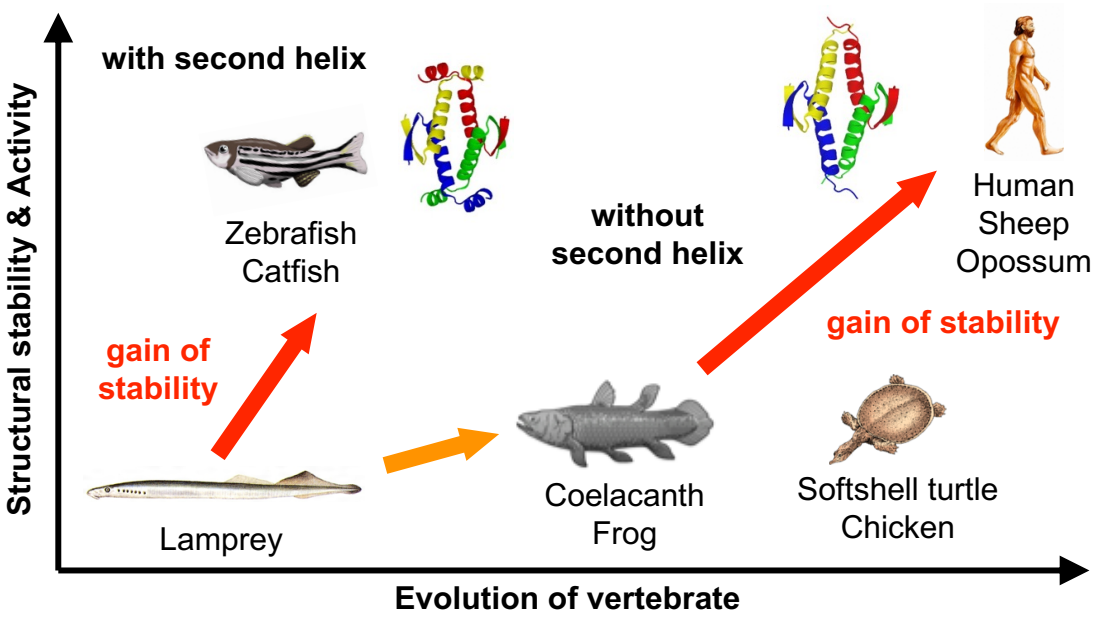

Figure 46. The evolution of vertebrate with the p53 structural stability and the p53 activity According to my results, Lamprey p53 has low stability and activity. The fish such as Zebrafish gains high stability and activity via second helix. Whereas, the species from Coelacanth to mammals such as Human gain high stability and activity without second helix.

in water, and high UV and high oxygen concentration caused DNA damage, finally occurred tumorigenesis. p53 with stable tetrameric structure and high transcriptional activity has a high response to DNA damage, it may more prevent tumorigenesis. Therefore, the species having such a p53 may have the advantage to go to land **(Figure 47)**. And also, swordtail does not form the second helix, but zebrafish and catfish form the second helix, interestingly, the fishes classified as Euteleostei such as swordtail mainly prosper in seawater, whereas, the other fishes classified as Ostarioclupeomorpha such as zebrafish and catfish mainly prosper in freshwater. It is known to less UV in seawater than in freshwater, which may help the prosperity of fishes without second helix such as swordtail in seawater. Because the role of p53 in cells is maintaining genomic integrity, p53 does not allow mutation, which is a trigger of evolution, suggesting that the species having stable p53 hardly evolve. The vertebrates may have diversity because the early vertebrate such as lamprey has less stable p53.

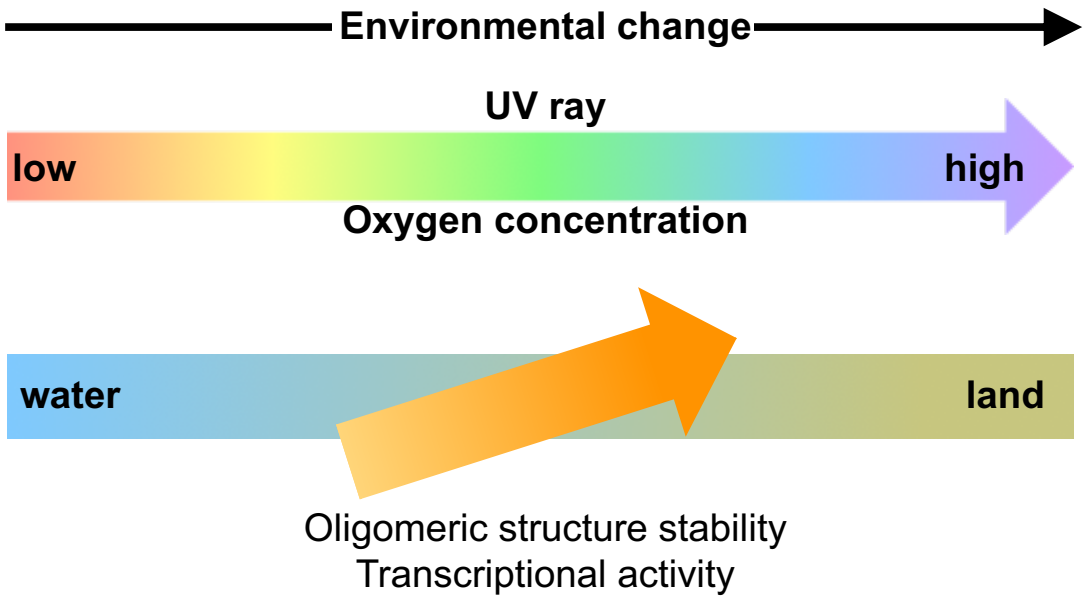

Figure 47. The evolution of p53 in vertebrates

Vertebrates have changed the live environment from water to land. For this reason, increasing the UV ray and the oxygen concentration are demerits on maintaining genomic integrity for vertebrates living in land. It is suggested that gain of high stability and activity p53 is advantage for surviving on the land.

5. Conclusion

It is very important to clear the stability adjustment mechanism of the p53 tetrameric structure for thinking about the regulatory mechanism of functions in the cell. In this study, I cleared that structural stability was regulated by the methylation of the p53 tetramerization domain and proposed the target gene choice control model that used a difference of the affinity with the responsive element. Furthermore, as well as phylogenic tree analysis for the protein which expressed in the whole vertebrate, I performed structural stability and functional analysis for the first time. It was suggested that the vertebrate lived in the environment that adapted to the stability of the p53 tetramerization domain, and p53 played an extremely important role in an evolution process.

Posttranslational modifications are important for exact functional regulation of p53, but it is not completely clear which posttranslational modifications are applied to one p53 protein at the same time, and whether it becomes a heterotetramer or homotetramer. Regarding the methylation of the p53 TD, it is extremely interesting it becomes a tetramer which pattern a methylation state with functions and which posttranslational modifications in other domains occur at that time. To elucidate the regulation mechanism, further research using *in vivo* assays and MS analysis is required.

Coelacanth p53 TD had around one role longer α-helix in comparison with the structure of Human p53 TD. However, as for the structural stability, Human was more stable than Coelacanth, and Human was higher in the transcription activity, too. In Tree shrew p53 TD, the tetrameric structure was stable by a stabilization effect of M354 of the C-terminus. Therefore, in the species which does not have the second helix, the stabilization of the C-terminal region of p53 TD is important to the structural stability of the whole p53 TD but may not be necessarily connected for structure stabilization even if it forms α-helix. In other words, elucidation of the structural stability requires both structure analysis and stability analysis.

The p53/p63/p73 family is expressed in the whole vertebrate. Only p53, which suppresses cellular tumorigenesis, underwent sequence changes positively and has evolved. Furthermore, it is thought that it played an important role in the vertebrate evolution that greatly changed with the living environment changes. In particular, it is very interesting that the stability of the tetrameric domain changed, rather than the DBD of p53. Elucidation of the novel p53 regulatory mechanism requires analysis of the evolution of the posttranslational modifications and the coevolution with posttranslational

modification enzymes including PRMT5 and the interaction factors that are involved in functional control of p53.

As mentioned above, the knowledge of the stability and the regulatory mechanism through posttranslational modification cascades and the evolution of the protein function of the p53 tetrameric structure revealed by this study may be expanded to other oligomer formation proteins and protein-protein interactions.

6. References

[1] M.L. Agarwal, W.R. Taylor, M. V. Chernov, O.B. Chernova, G.R. Stark, The p53 network, J. Biol. Chem. 273 (1998) 1–4. doi:10.1074/jbc.273.1.1.

[2] A.J. Giaccia, M.B. Kastan, The complexity of p53 modulation: Emerging patterns from divergent signals, Genes Dev. 12 (1998) 2973–2983. doi:10.1101/gad.12.19.2973.

[3] D.P. Lane, p53, guardian of the genome, Nature. 358 (1992) 15–16. doi:10.1038/358015a0.

[4] C. Kandoth, M.D. McLellan, F. Vandin, K. Ye, B. Niu, C. Lu, M. Xie, Q. Zhang, J.F. McMichael, M.A. Wyczalkowski, M.D.M. Leiserson, C.A. Miller, J.S. Welch, M.J. Walter, M.C. Wendl, T.J. Ley, R.K. Wilson, B.J. Raphael, L. Ding, Mutational landscape and significance across 12 major cancer types, Nature. 502 (2013) 333–339. doi:10.1038/nature12634.

[5] T. Riley, E. Sontag, P. Chen, A. Levine, Transcriptional control of human p53-regulated genes, Nat. Rev. Mol. Cell Biol. 9 (2008) 402–412. doi:10.1038/nrm2395.

[6] M. Mihara, S. Erster, A. Zaika, O. Petrenko, T. Chittenden, P. Pancoska, U.M. Moll, p53 Has a Direct Apoptogenic Role At the Mitochondria, Mol. Cell. 11 (2003) 577–590. doi:10.1016/S1097-2765(03)00050-9.

[7] H.I. Suzuki, K. Yamagata, K. Sugimoto, T. Iwamoto, S. Kato, K. Miyazono, Modulation of microRNA processing by p53., Nature. 460 (2009) 529–533. doi:10.1038/nature08199.

[8] T.P. Zanto, K. Hennigan, M. Östberg, W.C. Clapp, A. Gazzaley, NIH Public Access, 46 (2011) 564–574. doi:10.1016/j.cortex.2009.08.003.Predictive.

[9] N. Dumaz, D. W.Meek, Serine15 phosphorylation stimulates p53 transactivation but does not directly influence interaction with HDM2, EMBO J. 18 (1999) 7002–7010. doi:10.1093/emboj/18.24.7002.

[10] H. Zheng, H. You, X.Z. Zhou, S.A. Murray, T. Uchida, G. Wulf, L. Gu, X. Tang, K.P. Lu, Z.-X.J. Xiao, The prolyl isomerase Pin1 is a regulator of p53 in genotoxic response, Nature. 419 (2002) 849–853. doi:10.1038/nature01116.

[11] W.S. El-Deiry, S.E. Kern, J.A. Pietenpol, K.W. Kinzler, B. Vogelstein, Definition of a consensus binding site for p53, Nat. Genet. 1 (1992) 45–49. doi:10.1038/ng0492-45.

[12] R.L. Weinberg, S.M.V. Freund, D.B. Veprintsev, M. Bycroft, A.R. Fersht, Regulation of DNA binding of p53 by its C-terminal domain, J. Mol. Biol. 342 (2004) 801–811. doi:10.1016/j.jmb.2004.07.042.

[13] G.M. Clore, J. Ernst, R. Clubb, J.G. Omichinski, W.M.P. Kennedy, K. Sakaguchi, E. Appella, A.M. Gronenborn, Refined solution structure of the oligomerization domain of the tumour suppressor p53, Nat. Struct. Biol. 2 (1995) 321–333. doi:10.1038/nsb0495-321.

[14] M.G. Mateu, A.R. Fersht, Nine hydrophobic side chains are key determinants of the thermodynamic stability and oligomerization status of tumour suppressor p53 tetramerization domain., EMBO J. 17 (1998) 2748–2758. doi:10.1093/emboj/17.10.2748.

[15] R. Kamada, T. Nomura, C.W. Anderson, K. Sakaguchi, Cancer-associated p53 tetramerization domain mutants: quantitative analysis reveals a low threshold for tumor suppressor inactivation., J. Biol. Chem. 286 (2011) 252–258. doi:10.1074/jbc.M110.174698.

[16] T. Imagawa, T. Terai, Y. Yamada, R. Kamada, K. Sakaguchi, Evaluation of transcriptional activity of p53 in individual living mammalian cells, Anal. Biochem. 387 (2009) 249–256. doi:10.1016/j.ab.2009.01.030.

[17] C.A. Pise-Masison, M. Radonovich, J.N. Brady, K. Sakaguchi, E. Appella, Phosphorylation of p53: A novel pathway for p53 inactivation in human t- cell lymphotropic virus type 1-transformed cells, J. Virol. 72 (1998) 6348–6355.

[18] C. Prives, Signaling to p53: Breaking the MDM2-p53 circuit, Cell. 95 (1998) 5–8. doi:10.1016/S0092-8674(00)81774-2.

[19] P.H. Kussie, S. Gorina, V. Marechal, B. Elenbaas, J. Moreau, A.J. Levine, N.P. Pavletich, Structure of the MDM2 Oncoprotein Bound to the p53 Tumor Suppressor Transactivation Domain, Science. 274 (1996) 948 LP – 953. doi:10.1126/science.274.5289.948.

[20] M.H.G. Kubbutat, S.N. Jones, K.H. Vousden, Regulation of p53 stability by Mdm2, Nature. 387 (1997) 299–303. doi:10.1038/387299a0.

[21] Y. Haupt, R. Maya, A. Kazaz, M. Oren, Mdm2 promotes the rapid degradation of p53, Nature. 387 (1997) 296–299. doi:10.1038/387296a0.

[22] S.P. Lees-Miller, K. Sakaguchi, S.J. Ullrich, E. Appella, C.W. Anderson, Human DNA-activated protein kinase phosphorylates serines 15 and 37 in the amino-

terminal transactivation domain of human p53., Mol. Cell. Biol. 12 (1992) 5041–5049. doi:10.1128/mcb.12.11.5041.

[23] S.-Y. Shieh, M. Ikeda, Y. Taya, C. Prives, DNA Damage-Induced Phosphorylation of p53 Alleviates Inhibition by MDM2 phosphorylated at sites within its N-terminal and C-termi-nal regions, and several protein kinases have been shown to phosphorylate p53 in vitro. One such kinase, Cell. 91 (1997) 325–334. https://ac.els-cdn.com/S009286740080416X/1-s2.0-S009286740080416X-main.pdf?_tid=0b42c174-a2e1-4e81-a0f9-c0ca13246064&acdnat=1549364836_61cda07298ee5cf39800c3c3f4891928.

[24] J.D. Siliciano, C.E. Canman, Y. Taya, K. Sakaguchi, E. Appella, M.B. Kastan, DNA damage induces phosphorylation of the amino terminus of p53, Genes Dev. 11 (1997) 3471–3481. doi:10.1101/gad.11.24.3471.

[25] M. Fiscella, H. Zhang, S. Fan, K. Sakaguchi, S. Shen, W.E. Mercer, G.F. Vande Woude, P.M. O'Connor, E. Appella, Wip1, a novel human protein phosphatase that is induced in response to ionizing radiation in a p53-dependent manner, Proc. Natl. Acad. Sci. U. S. A. 94 (1997) 6048–6053. doi:10.1073/pnas.94.12.6048.

[26] K. Sakaguchi, J.E. Herrera, S. Saito, T. Miki, M. Bustin, A. Vassilev, C.W. Anderson, E. Appella, DNA damage activates p53 through a phosphorylation-acetylation cascade, Genes Dev. 12 (1998) 2831–2841. doi:10.1101/gad.12.18.2831.

[27] Y. Itahana, H. Ke, Y. Zhang, p53 oligomerization is essential for its C-terminal lysine acetylation, J. Biol. Chem. 284 (2009) 5158–5164. doi:10.1074/jbc.M805696200.

[28] K. Sakaguchi, H. Sakamoto, M.S. Lewis, C.W. Anderson, J.W. Erickson, E. Appella, D. Xie, Phosphorylation of serine 392 stabilizes the tetramer formation of tumor suppressor protein p53., Biochemistry. 36 (1997) 10117–10124. doi:10.1021/bi970759w.

[29] M. Jansson, S.T. Durant, E.-C. Cho, S. Sheahan, M. Edelmann, B. Kessler, N.B. La Thangue, Arginine methylation regulates the p53 response., Nat. Cell Biol. 10 (2008) 1431–1439. doi:10.1038/ncb1802.

[30] G. Chillemi, S. Kehrloesser, F. Bernassola, A. Desideri, Structural Evolution and Dynamics of the p53 Proteins, Cold Spring Harb. Perspect. Med. (2016) 1–16. doi:10.1101/cshperspect.a028308.

[31] V.A. Belyi, P. Ak, E. Markert, H. Wang, W. Hu, A. Puzio-Kuter, A.J. Levine, The Origins and Evolution of the p53 Family of Genes, Cold Spring Harb. Perspect. Biol. 2 (2010) a001198–a001198. doi:10.1101/cshperspect.a001198.

[32] A.J. Levine, J. Momand, C.A. Finlay, The p53 tumour suppressor gene, Nature. 351 (1991) 453–456. doi:10.1038/351453a0.

[33] R. Kamada, Y. Toguchi, T. Nomura, T. Imagawa, K. Sakaguchi, Tetramer formation of tumor suppressor protein p53: Structure, function, and applications., Biopolymers. 106 (2016) 598–612. doi:10.1002/bip.22772.

[34] K. Suzuki, H. Matsubara, Recent advances in p53 research and cancer treatment., J. Biomed. Biotechnol. 2011 (2011) 1–7. doi:10.1155/2011/978312.

[35] Q. Hao, W. Cho, Battle Against Cancer: An Everlasting Saga of p53, Int. J. Mol. Sci. 15 (2014) 22109–22127. doi:10.3390/ijms151222109.

[36] A.C. Joerger, A.R. Fersht, Structural Biology of the Tumor Suppressor p53, Annu. Rev. Biochem. 77 (2008) 557–582. doi:10.1146/annurev.biochem.77.060806.091238.

[37] P. Chène, The role of tetramerization in p53 function, Oncogene. 20 (2001) 2611–2617. doi:10.1038/sj.onc.1204373.

[38] H. Sakamoto, M.S. Lewis, H. Kodama, E. Appella, K. Sakaguchi, Specific sequences from the carboxyl terminus of human p53 gene product form anti-parallel tetramers in solution., Proc. Natl. Acad. Sci. U. S. A. 91 (1994) 8974–8978. http://www.pubmedcentral.nih.gov/articlerender.fcgi?artid=44729&tool=pmcentrez&rendertype=abstract (accessed March 3, 2015).

[39] R.T. Clubb, J.G. Omichinski, K. Sakaguchi, E. Appella, A.M. Gronenborn, G.M. Clore, Backbone dynamics of the oligomerization domain of p53 determined from 15N NMR relaxation measurements., Protein Sci. 4 (1995) 855–862. doi:10.1002/pro.5560040505.

[40] E. Appella, C.W. Anderson, Post-translational modifications and activation of p53 by genotoxic stresses, Eur. J. Biochem. 268 (2001) 2764–2772. doi:10.1046/j.1432-1327.2001.02225.x.

[41] T.-A. Nguyen, D. Menendez, M. a Resnick, C.W. Anderson, Mutant TP53 posttranslational modifications: challenges and opportunities., Hum. Mutat. 35 (2014) 738–755. doi:10.1002/humu.22506.

[42] S.L. Berger, Out of the jaws of death: PRMT5 steers p53., Nat. Cell Biol. 10 (2008) 1389–1390. doi:10.1038/ncb1208-1389.

[43] C. Dai, W. Gu, p53 post-translational modification: Deregulated in tumorigenesis, Trends Mol. Med. 16 (2010) 528–536. doi:10.1016/j.molmed.2010.09.002.

[44] M.T. Bedford, S. Richard, Arginine methylation: An emerging regulator of protein function, Mol. Cell. 18 (2005) 263–272. doi:10.1016/j.molcel.2005.04.003.

[45] T.L. Branscombe, A. Frankel, J.H. Lee, J.R. Cook, Z. Yang, S. Pestka, S. Clarke, PRMT5 (Janus kinase-binding protein 1) catalyzes the formation of symmetric dimethylarginine residues in proteins., J. Biol. Chem. 276 (2001) 32971–32976. doi:10.1074/jbc.M105412200.

[46] M. van Haren, L.Q. van Ufford, E.E. Moret, N.I. Martin, Synthesis and evaluation of protein arginine N-methyltransferase inhibitors designed to simultaneously occupy both substrate binding sites., Org. Biomol. Chem. 13 (2015) 549–560. doi:10.1039/c4ob01734j.

[47] M.C. Ho, C. Wilczek, J.B. Bonanno, L. Xing, J. Seznec, T. Matsui, L.G. Carter, T. Onikubo, P.R. Kumar, M.K. Chan, M. Brenowitz, R.H. Cheng, U. Reimer, S.C. Almo, D. Shechter, Structure of the Arginine Methyltransferase PRMT5-MEP50 Reveals a Mechanism for Substrate Specificity, PLoS One. 8 (2013) 1–16. doi:10.1371/journal.pone.0057008.

[48] P. Thandapani, T.R. O'Connor, T.L. Bailey, S. Richard, Defining the RGG/RG Motif, Mol. Cell. 50 (2013) 613–623. doi:10.1016/j.molcel.2013.05.021.

[49] K. Ancelin, U.C. Lange, P. Hajkova, R. Schneider, A.J. Bannister, T. Kouzarides, M.A. Surani, Blimp1 associates with Prmt5 and directs histone arginine methylation in mouse germ cells, Nat. Cell Biol. 8 (2006) 623–630. doi:10.1038/ncb1413.

[50] Y. Feng, J. Wang, S. Asher, L. Hoang, C. Guardiani, I. Ivanov, Y.G. Zheng, Histone H4 acetylation differentially modulates arginine methylation by an in cis mechanism, J. Biol. Chem. 286 (2011) 20323–20334. doi:10.1074/jbc.M110.207258.

[51] E.S. Burgos, C. Wilczek, T. Onikubo, J.B. Bonanno, J. Jansong, U. Reime, D. Shechter, Histone H2A and H4 N-terminal tails are positioned by the MEP50

WD repeat protein for efficient methylation by the PRMT5 arginine methyltransferase, J. Biol. Chem. 290 (2015) 9674–9689. doi:10.1074/jbc.M115.636894.

[52] Q. Zhao, G. Rank, Y.T. Tan, H. Li, R.L. Moritz, R.J. Simpson, L. Cerruti, D.J. Curtis, D.J. Patel, C.D. Allis, J.M. Cunningham, S.M. Jane, PRMT5-mediated methylation of histone H4R3 recruits DNMT3A, coupling histone and DNA methylation in gene silencing, Nat. Struct. Mol. Biol. 16 (2009) 304–311. doi:10.1038/nsmb.1568.

[53] N. Stopa, J.E. Krebs, D. Shechter, The PRMT5 arginine methyltransferase: many roles in development, cancer and beyond., Cell. Mol. Life Sci. 72 (2015) 2041–2059. doi:10.1007/s00018-015-1847-9.

[54] K. Saha, G. Adhikary, R.L. Eckert, MEP50/PRMT5 Reduces Gene Expression by Histone Arginine Methylation and this is Reversed by PKCδ/p38δ Signaling., J. Invest. Dermatol. 136 (2015) 214–224. doi:10.1038/jid.2015.400.

[55] W.W. Tee, M. Pardo, T.W. Theunissen, L. Yu, J.S. Choudhary, P. Hajkova, M.A. Surani, Prmt5 is essential for early mouse development and acts in the cytoplasm to maintain ES cell pluripotency, Genes Dev. 24 (2010) 2772–2777. doi:10.1101/gad.606110.

[56] S. Pal, R.A. Baiocchi, J.C. Byrd, M.R. Grever, S.T. Jacob, S. Sif, Low levels of miR-92b/96 induce PRMT5 translation and H3R8/H4R3 methylation in mantle cell lymphoma., EMBO J. 26 (2007) 3558–3569. doi:10.1038/sj.emboj.7601794.

[57] Y. Li, J.A. Diehl, PRMT5-dependent p53 escape in tumorigenesis., Oncoscience. 2 (2015) 700–702. doi:10.18632/oncoscience.222.

[58] P. Aggarwal, L.P. Vaites, J.K. Kim, H. Mellert, B. Gurung, H. Nakagawa, M. Herlyn, X. Hua, A.K. Rustgi, S.B. McMahon, J.A. Diehl, Nuclear cyclin D1/CDK4 kinase regulates CUL4 expression and triggers neoplastic growth via activation of the PRMT5 methyltransferase, Cancer Cell. 18 (2010) 329–340. doi:10.1016/j.ccr.2010.08.012.

[59] K.J. Mavrakis, E. Robert McDonald, M.R. Schlabach, E. Billy, G.R. Hoffman, A. DeWeck, D.A. Ruddy, K. Venkatesan, J. Yu, G. McAllister, M. Stump, R. DeBeaumont, S. Ho, Y. Yue, Y. Liu, Y. Yan-Neale, G. Yang, F. Lin, H. Yin, H. Gao, D. Randal Kipp, S. Zhao, J.T. McNamara, E.R. Sprague, B. Zheng, Y. Lin, Y.S. Cho, J. Gu, K. Crawford, D. Ciccone, A.C. Vitari, A. Lai, V. Capka, K.

Hurov, J.A. Porter, J. Tallarico, C. Mickanin, E. Lees, R. Pagliarini, N. Keen, T. Schmelzle, F. Hofmann, F. Stegmeier, W.R. Sellers, Disordered methionine metabolism in MTAP/CDKN2A-deleted cancers leads to dependence on PRMT5, Science. 351 (2016) 1208–1213. doi:10.1126/science.aad5944.

[60] X. Bao, S. Zhao, T. Liu, Y. Liu, Y. Liu, X. Yang, Overexpression of PRMT5 Promotes Tumor Cell Growth and Is Associated with Poor Disease Prognosis in Epithelial Ovarian Cancer, J. Histochem. Cytochem. 61 (2013) 206–217. doi:10.1369/0022155413475452.

[61] A. Scoumanne, J. Zhang, X. Chen, PRMT5 is required for cell-cycle progression and p53 tumor suppressor function, Nucleic Acids Res. 37 (2009) 4965–4976. doi:10.1093/nar/gkp516.

[62] E.R. Kastenhuber, S.W. Lowe, Putting p53 in Context, Cell. 170 (2017) 1062–1078. doi:10.1016/j.cell.2017.08.028.

[63] S.M. Carr, A. Poppy Roworth, C. Chan, N.B. La Thangue, Post-translational control of transcription factors: Methylation ranks highly, FEBS J. 282 (2015) 4450–4465. doi:10.1111/febs.13524.

[64] G. Nagamatsu, T. Kosaka, M. Kawasumi, T. Kinoshita, K. Takubo, H. Akiyama, T. Sudo, T. Kobayashi, M. Oya, T. Suda, A germ cell-specific gene, Prmt5, works in somatic cell reprogramming, J. Biol. Chem. 286 (2011) 10641–10648. doi:10.1074/jbc.M110.216390.

[65] S.T. Durant, E.C. Cho, N.B. La Thangue, p53 methylation—the Arg-ument is clear, Cell Cycle. 8 (2009) 801–802. doi:10.4161/cc.8.6.7850.

[66] A. Scoumanne, X. Chen, Protein methylation: A new mechanism of p53 tumor suppressor regulation, Histol. Histopathol. 23 (2008) 1143–1149. doi:10.1016/j.surg.2006.10.010.Use.

[67] Z. Chu, B. Niu, H. Zhu, X. He, C. Bai, G. Li, J. Hua, PRMT5 enhances generation of induced pluripotent stem cells from dairy goat embryonic fibroblasts via down-regulation of p53., Cell Prolif. 48 (2015) 29–38. doi:10.1111/cpr.12150.

[68] M. Qi, E.A. Elion, MAP kinase pathways, J. Cell Sci. 118 (2005) 3569–3572. doi:10.1242/jcs.02470.

[69] A. Oeckinghaus, M.S. Hayden, S. Ghosh, Crosstalk in NF-κB signaling pathways, Nat. Immunol. 12 (2011) 695–708. doi:10.1038/ni.2065.

[70] K. Sakaguchi, S. Saito, Y. Higashimoto, S. Roy, C.W. Anderson, E. Appella, Damage-mediated phosphorylation of human p53 threonine 18 through a cascade mediated by a casein 1-like kinase. Effect on MDM2 binding, J. Biol. Chem. 275 (2000) 9278–9283. doi:10.1074/jbc.275.13.9278.

[71] L. Bouaoun, D. Sonkin, M. Ardin, M. Hollstein, G. Byrnes, J. Zavadil, M. Olivier, TP53 Variations in Human Cancers: New Lessons from the IARC TP53 Database and Genomics Data, Hum. Mutat. 37 (2016) 865–876. doi:10.1002/humu.23035.

[72] A.C. Joerger, R. Wilcken, A. Andreeva, Tracing the evolution of the p53 tetramerization domain, Structure. 22 (2014) 1301–1310. doi:10.1016/j.str.2014.07.010.

[73] R.L. Weinberg, D.B. Veprintsev, M. Bycroft, A.R. Fersht, Comparative binding of p53 to its promoter and DNA recognition elements, J. Mol. Biol. 348 (2005) 589–596. doi:10.1016/j.jmb.2005.03.014.

[74] V. Dötsch, F. Bernassola, D. Coutandin, E. Candi, G. Melino, p63 and p73, the ancestors of p53., Cold Spring Harb. Perspect. Biol. 2 (2010) a004887. doi:10.1101/cshperspect.a004887.

[75] J.I. Garaycoechea, G.P. Crossan, F. Langevin, L. Mulderrig, S. Louzada, F. Yang, G. Guilbaud, N. Park, S. Roerink, S. Nik-Zainal, M.R. Stratton, K.J. Patel, Alcohol and endogenous aldehydes damage chromosomes and mutate stem cells, Nature. 553 (2018) 171–177. doi:10.1038/nature25154.

[76] S.A. Ahrendt, J.T. Chow, S.C. Yang, L. Wu, M.J. Zhang, J. Jen, D. Sidransky, Alcohol consumption and cigarette smoking increase the frequency of p53 mutations in non-small cell lung cancer, Cancer Res. 60 (2000) 3155–3159.

[77] V. Kumar, B.M. Hallström, A. Janke, Coalescent-Based Genome Analyses Resolve the Early Branches of the Euarchontoglires, PLoS One. 8 (2013) e60019. doi:10.1371/journal.pone.0060019.

[78] F. Wiens, A. Zitzmann, M.-A. Lachance, M. Yegles, F. Pragst, F.M. Wurst, D. von Holst, S.L. Guan, R. Spanagel, Chronic intake of fermented floral nectar by wild treeshrews, Proc. Natl. Acad. Sci. 105 (2008) 10426–10431. doi:10.1073/pnas.0801628105.

[79] Y. Han, B. Li, T.T. Yin, C. Xu, R. Ombati, L. Luo, Y. Xia, L. Xu, J. Zheng, Y. Zhang, F. Yang, G.D. Wang, S. Yang, R. Lai, Molecular mechanism of the tree

shrew's insensitivity to spiciness, PLoS Biol. 16 (2018) 1–17. doi:10.1371/journal.pbio.2004921.

[80] T. Sakaguchi, J.I.B. Janairo, M. Lussier-Price, J. Wada, J.G. Omichinski, K. Sakaguchi, Oligomerization enhances the binding affinity of a silver biomineralization peptide and catalyzes nanostructure formation, Sci. Rep. 7 (2017) 1400. doi:10.1038/s41598-017-01442-8.

[81] J. Reed, T.A. Reed, A set of constructed type spectra for the practical estimation of peptide secondary structure from circular dichroism, Anal. Biochem. 254 (1997) 36–40. doi:10.1006/abio.1997.2355.

[82] A. Šali, T.L. Blundell, Comparative Protein Modelling by Satisfaction of Spatial Restraints, J. Mol. Biol. 234 (1993) 779–815. doi:10.1006/jmbi.1993.1626.

[83] Y. V. Wang, M. Wade, E. Wong, Y.C. Li, L.W. Rodewald, G.M. Wahl, Quantitative analyses reveal the importance of regulated Hdmx degradation for P53 activation, Proc. Natl. Acad. Sci. U. S. A. 104 (2007) 12365–12370. doi:10.1073/pnas.0701497104.

[84] A.F. Caulin, T.A. Graham, L.S. Wang, C.C. Maley, Solutions to peto's paradox revealed by mathematical modelling and cross-species cancer gene analysis, Philos. Trans. R. Soc. B Biol. Sci. 370 (2015). doi:10.1098/rstb.2014.0222.

[85] L. Margulies, P. Sehgal, Modulation of the human interleukin-6 promoter (IL-6) and transcription factor C/EBPβ (NF-IL6) activity by p53 species, J. Biol. Chem. 268 (1993) 15096–15100.

[86] E. Brighenti, C. Calabrese, G. Liguori, F.A. Giannone, D. Trerè, L. Montanaro, M. Derenzini, Interleukin 6 downregulates p53 expression and activity by stimulating ribosome biogenesis: a new pathway connecting inflammation to cancer, Oncogene. 33 (2014) 4396–4406. doi:10.1038/onc.2014.1.

[87] U.S. Park, J.J. Su, K.C. Ban, L. Qin, E.H. Lee, Y.I. Lee, Mutations in the p53 tumor suppressor gene in tree shrew hepatocellular carcinoma associated with hepatitis B virus infection and intake of aflatoxin B1, Gene. 251 (2000) 73–80. doi:10.1016/S0378-1119(00)00183-9.

[88] J. Cao, E.-B. Yang, J.-J. Su, Y. Li, P. Chow, The tree shrews: Adjuncts and alternatives to primates as models for biomedical research, J. Med. Primatol. 32 (2003) 123–130. doi:10.1034/j.1600-0684.2003.00022.x.

[89] J.J. Su, K.C. Ban, Y. Li, L.L. Qin, H.Y. Wang, C. Yang, C. Ou, X.X. Duan, Y.L.

Lee, R.Q. Yang, Alteration of p53 and p21 during hepatocarcinogenesis in tree shrews, World J. Gastroenterol. 10 (2004) 3559–3563. doi:10.3748/wjg.v10.i24.3559.

[90] L. Ye, M. He, Y. Huang, G. Zhao, Y. Lei, Y. Zhou, X. Chen, Tree shrew as a new animal model for the study of lung cancer, Oncol. Lett. 11 (2016) 2091–2095. doi:10.3892/ol.2016.4156.

[91] P. Emsley, K. Cowtan, Coot: Model-building tools for molecular graphics, Acta Crystallogr. Sect. D Biol. Crystallogr. 60 (2004) 2126–2132. doi:10.1107/S0907444904019158.

[92] P.D. Adams, P. V. Afonine, G. Bunkóczi, V.B. Chen, I.W. Davis, N. Echols, J.J. Headd, L.W. Hung, G.J. Kapral, R.W. Grosse-Kunstleve, A.J. McCoy, N.W. Moriarty, R. Oeffner, R.J. Read, D.C. Richardson, J.S. Richardson, T.C. Terwilliger, P.H. Zwart, PHENIX: A comprehensive Python-based system for macromolecular structure solution, Acta Crystallogr. Sect. D Biol. Crystallogr. 66 (2010) 213–221. doi:10.1107/S0907444909052925.

7. Acknowledgement

I would like to express the deepest appreciation to my supervisors, Professor Kazuyasu Sakaguchi, and Professor James G. Omichinski (Université de Montréal). Professor Kazuyasu Sakaguchi told me all things of life, science, and research. Professor James G. Omichinski supported my life and study in Montreal. Without their kind help, this thesis would not have been possible.

I would like to thank my thesis committee: Professor Yota Murakami, Professor Stephen Michnick (Université de Montréal), Professor Toru Dairi, Professor Koichiro Ishimori, and Professor Hiroshi Sakamoto for their constructive suggestions from novel perspective.

I am also grateful to immediate superior, Dr. Junya Wada who showed me a base of all studies: experimental methods, showing results, and how to discuss, for his kindly support.

I would like to express sincere thanks to Dr. Haytham Wahba (Université de Montréal) and Mr. Mathieu Lussier-Price (Université de Montréal) for their essential support in a lot of experiment and great experience working hard together.

I would particularly like to thank former Assistant Professor Toshiaki Imagawa for technical supports for lots of experiment and critical suggestion, Ms. Michiko Taniguchi for her warm care.

I would like to thank the Japan Society for the Promotion of Science for making my Ph.D. study possible through financial support.

I would like to thank my colleagues and family: parents, younger sister for psychological supports.